

I. Meyer-Schuster rearrangement

II. Synthesis of potential FtsZ inhibitors

Master's thesis

Kaisa Horkka

Laboratory of Organic chemistry

Department of Chemistry

University of Helsinki

May 2016

Tiedekunta/Osasto Fakultet/Sektion – Faculty Matemaattis-luonnontieteellinen		Laitos/Institution – Department Kemian laitos	
Tekijä/Författare – Author Kaisa Horkka			
Työn nimi / Arbetets titel – Title I. Meyer-Schuster rearrangement II. Synthesis of potential FtsZ inhibitors			
Oppiaine /Läroämne – Subject Orgaaninen kemia			
Työn laji/Arbetets art – Level Pro gradu	Aika/Datum – Month and year Toukokuu 2016	Sivumäärä/ Sidoantal – Number of pages 91 sivua + 25 liitesivua	
Tiivistelmä/Referat – Abstract I. Meyer-Schuster rearrangement  Meyer-Schuster rearrangement is an atom economical reaction, in which $\alpha,\beta$ -unsaturated carbonyl compounds are formed from propargylic alcohols and their derivatives by formal migration of the carbonyl group. Brønsted acids have been used traditionally as stoichiometric catalysts, but more recently, several Lewis acids both salts and metal complexes, have become popular due to their selectivity and mild conditions applied. Also oxo-metal complexes are often used despite the high reaction temperature needed.  In this thesis, various manners and catalysts for the Meyer-Schuster rearrangement are reviewed. Reactivity of different substrates and practicality of several types of catalysts are evaluated. In addition, different reaction mechanisms are discussed, as they are highly substrate and catalyst-dependent. Propargylic alcohols have two functional groups, in which the catalysts can coordinate according to their characteristics. Especially gold compounds, which are soft Lewis acids, have gained interest due to their specific coordination ability.  II. Synthesis of potential FtsZ inhibitors  FtsZ, which is a bacterial homologue for tubulin, is essential in the cell division. It polymerizes into a dynamic ring structure, which constricts to separate the new daughter cells. Being FtsZ protein-directing compounds, 3-methoxybenzamide derivatives have been noticed to inhibit growth of certain bacteria.  In this work, a set of molecules was synthesized based on PC190723, which is a 3-methoxybenzamide derivative. In order to study interactions between the protein and the inhibitors, fluorescent groups were attached. Polymer sedimentation tests and fluorescence spectroscopy were used to study shortly the biological behavior of the products. It was discovered that one of the products is a polymer-stabilizing and thus, FtsZ activity inhibiting compound.			
Avainsanat – Nyckelord – Keywords Meyer-Schuster, rearrangement, propargylic alcohol, enone, enal, FtsZ, antibacterial			
Säilytyspaikka – Förvaringställe – Where deposited Helsingin yliopiston digitaalinen arkisto / E-thesis			
Muita tietoja – Övriga uppgifter – Additional information			

## I. THEORETICAL PART

### Meyer-Schuster rearrangement

## Contents of the first part

### Abbreviations

1. Introduction	1
2. Brønsted acids and early methods	2
3. Soft Lewis acids	5
3.1 Common features of gold catalysts	5
3.2 Meyer-Schuster rearrangement with gold catalysts	6
3.3 Mercury and silver catalysts	17
4. Nonmetallic and metallic hard Lewis acids	19
5. Organometal complexes of transition metals	24
6. Oxo complexes	31
7. Conclusions	37
8. References	40

## Abbreviations

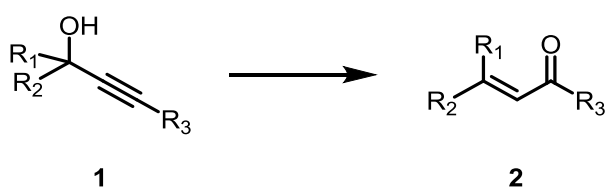
Ac	acetate
acac	acetylacetonate
BMIM	1-butyl-3-methylimidazolium
Bn	benzyl
Bu	butyl
Bz	benzoyl
cat.	catalytical
Cp	cyclopentadienyl
Cp*	pentamethylcyclopentadienyl
CSA	camphorsulfonic acid
Cy	cyclohexane
DBN	1,5-diazabicyclo[4.3.0]non-5-ene
DBU	1,8-diazabicyclo[5.4.0]undec-7-ene
DCM	dichloromethane
DFT	density functional theory
DIPEA	<i>N,N</i> -diisopropylethylamine
DMA	dimethylacetamide
DMF	dimethylformamide
eq	equivalent
Et	ethyl
HPA	heteropoly acid
HSAB	Hard-Soft Acid-Base Principle
<i>i</i> -Pr	isopropyl
IPr	<i>N,N'</i> -bis(2,6-diisopropylphenyl)imidazol-2-ylidene
ItBu	<i>N,N'</i> -bis(tert-butyl)imidazol-2-ylidene
L	ligand
Me	methyl
M-S	Meyer-Schuster
Ms	methanesulfonic acid
MW	microwave
NHC	<i>N</i> -heterocyclic carbene

<i>n</i> -Pr	propyl
Ph	phenyl
PTSA	<i>p</i> -toluenesulfonic acid
rt	room temperature
S <sub>N</sub> 2'	nucleophilic conjugate substitution
TA	1,2,3-triazole
<i>t</i> -Bu	<i>tert</i> -butyl
<i>t</i> -BuXPhos	2-di- <i>tert</i> -butylphosphino-2',4',6'-triisopropylbiphenyl
TFA	trifluoroacetic acid
THF	tetrahydrofuran
Tf	trifluoromethanesulfonate
Ts	<i>p</i> -toluenesulfonate

## 1. Introduction

$\alpha,\beta$ -unsaturated ketones and aldehydes are valuable synthetic precursors. Aldol condensation is a textbook example of preparing  $\alpha,\beta$ -unsaturated carbonyl compounds by atom-economical way, but harsh conditions and several side products limit its general applicability. Wittig reaction and its modifications offer another method for construction of olefins. In Horner-Wadsworth-Emmons reaction phosphonate carbanions react with aldehydes or ketones, and in Peterson olefination  $\alpha$ -silyl carbanions are used instead. Despite milder reaction conditions, one has to cope with waste side products, which is not in accordance with the green chemistry guidelines. In addition, these olefination methods are not necessarily suitable with bulky and demanding substrates.

Meyer-Schuster rearrangement (later M-S) gives  $\alpha,\beta$ -unsaturated carbonyl compounds from propargylic alcohols conveniently by acid treatment.<sup>1</sup> A formal 1,3-hydroxyl shift followed by tautomerization is carried out by Brønsted acid or more recently, Lewis acid often used in catalytic amounts (Scheme 1). The M-S rearrangement is atom-economical and thus, very recommendable reaction, which has gained more interest now that the catalytic methods have advanced.



**Scheme 1.** Meyer-Schuster rearrangement.

There are several mechanisms for the M-S rearrangement, depending on the catalyst and conditions. Thus, sometimes using the term “Meyer-Schuster rearrangement” for all the reactions of this group is misleading, although the result is the same.

Propargylic alcohols are widely available and affordable. They can be prepared easily by alkynylation of an aldehyde or a ketone. While Brønsted acids act by protonation followed by a dehydration-hydration mechanism, Lewis acids coordinate either with the hydroxyl group or the alkyne, depending on their tendencies (Figure 1).<sup>2</sup>

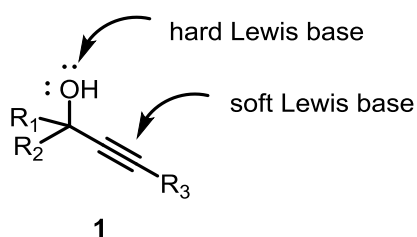
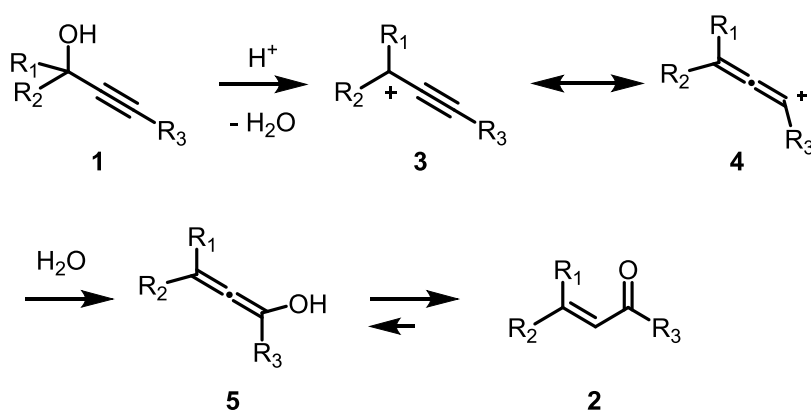


**Figure 1.** Functionalities of propargylic alcohol.

This thesis tries to shed light on the methods and mechanisms underlying the M-S rearrangement. The structure of the review is based on different groups of catalysts. The M-S reactions, which lead to the formation of  $\alpha,\beta$ -substituted ketones, aldehydes or acetates, are studied almost exclusively. Some examples of alternative pathways, for example halogen-trapped intermediates, have been added, if they exhibit special insight into the mechanism, stereoselectivity or the catalyst used. The M-S intermediates can undergo dozens of reactions, depending on substrates, solvents and catalysts, and exploiting the M-S rearrangement in cascade reactions has been under intense study recently.<sup>3,4</sup>

## 2. Brønsted acids and early methods

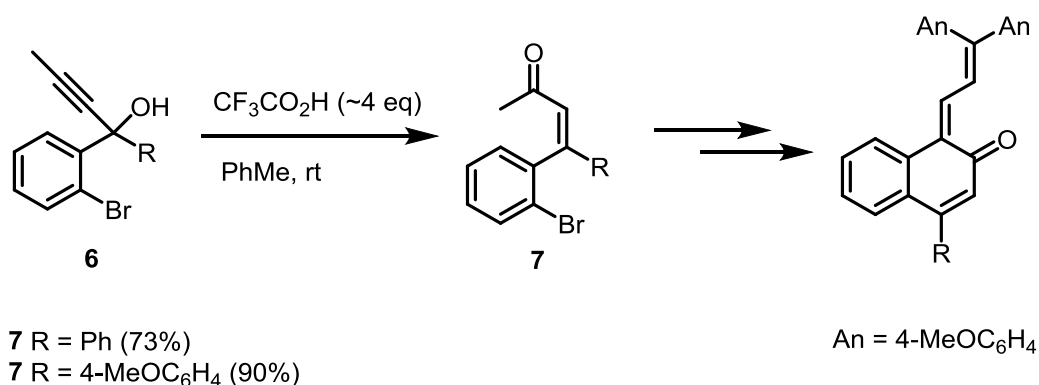
The first examples of the Meyer-Schuster rearrangement involved strong Brønsted acids in stoichiometric amounts and often heating.<sup>1, 5</sup> Acid-induced protonation and subsequent dehydration of the propargylic alcohol gives an allenic cation (**4**) (Scheme 2). The allenol formed by hydration is tautomerized into the  $\alpha,\beta$ -unsaturated carbonyl compound (**2**).



**Scheme 2.** Mechanism for the Brønsted acid-catalyzed Meyer-Schuster rearrangement.<sup>5</sup>

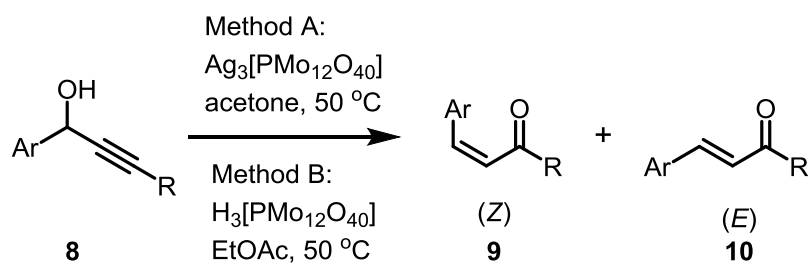


Some examples of the acids used are sulfuric<sup>6</sup> and hydrochloric acid, *p*-toluenesulfonic and benzenesulfonic acid, acetic, formic and oxalic acid. These conditions often result too harsh for many compounds, but a strong acid can be a convenient and easy choice in some cases. For example, Aiken et al. used trifluoroacetic acid at room temperature for a tertiary propargylic alcohol, when constructing naphthols (Scheme 3).<sup>7</sup> The reaction in toluene gave good to excellent yields.



**Scheme 3.** M-S reaction with trifluoroacetic acid.<sup>7</sup>

In strong acid-catalyzed reactions, *E* and *Z* isomers are formed in varying proportions, the *E* isomer being thermodynamically more stable. A special example of formation of a *Z* isomer was offered by Egi et al.<sup>8</sup> The group studied heteropoly acids (HPA) as M-S catalysts. HPAs are stronger than the usual inorganic acids, such as HCl, H<sub>2</sub>SO<sub>4</sub>, CF<sub>3</sub>SO<sub>2</sub>H.<sup>9</sup> They are non-toxic, stable and easy to handle. Keggin-type HPAs have a general formula H<sub>*n*</sub>[XM<sub>12</sub>O<sub>40</sub>], in which X is the central heteroatom and M is the addenda atom (W, Mo or V). Properties of the HPAs can easily be tuned by varying the components. The group noticed that the commercially available H<sub>3</sub>[PMo<sub>12</sub>O<sub>40</sub>] $\cdot$ *n* H<sub>2</sub>O afforded 89% of an enone with basically complete *E* selectivity (Scheme 4). Surprisingly, changing the cation to silver, mostly *Z* isomer was obtained. It was also noticed that the *Z* isomer is the initial product in either case, due to the bulkiness of the catalyst, and subsequent isomerization occurs by treatment with H<sub>3</sub>[PMo<sub>12</sub>O<sub>40</sub>] $\cdot$ *n* H<sub>2</sub>O.



Two examples, yield (Z/E, %):

Ar = 4-MeC<sub>6</sub>H<sub>4</sub>, R = *n*-C<sub>6</sub>H<sub>13</sub>

Method A: 90/8

Method B: 1/85

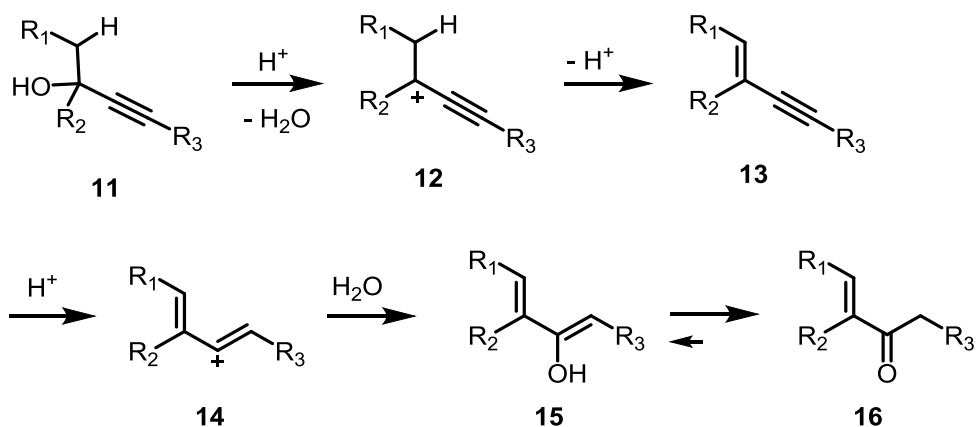
Ar = Ph, R = Me

Method A: 74/9

Method B: 1/80

**Scheme 4.** Heteropoly acid-catalyzed M-S rearrangement.<sup>8</sup>

In general, the Brønsted acid method is not usually selective, and it suffers from degradation and side reactions. The most famous side reaction, Rupe rearrangement, can occur, when the substrate bears a hydrogen in a  $\beta$ -position from the hydroxyl functionality.<sup>10</sup> Of the two rearrangements, Rupe is preferred over M-S due to lower energy.<sup>5</sup> Mechanistically, the dehydrated intermediate (**12**) undergoes  $\beta$ -elimination to afford the enyne intermediate **13** (Scheme 5). Hydration provides an  $\alpha,\beta$ -unsaturated carbonyl compound (**16**), which is a structural isomer for the M-S product.



**Scheme 5.** Mechanism for the Rupe rearrangement.<sup>5</sup>

### 3. Soft Lewis acids

According to the Hard-Soft Acid-Base Principle (HSAB), ions and elements are classified according to their tendencies to interact with certain chemical species.<sup>11</sup> “Hard” species are small, highly charged and weakly polarizable. “Soft” species have naturally opposite characteristics. Hard bases have stronger tendency to react with hard acids and soft bases with soft acids. Thus, behavior, and in this context, coordination preferences of a species can be predicted. In propargylic alcohols, the hydroxyl group represents a hard species and the triple bond a soft species (see Figure 1).

Late transition metals and their ions tend to be soft acids, which means that they prefer coordinating to acetylene over hydroxide. For this reason, gold(I), gold(III), silver(I) and mercury(I) compounds have been attractive candidates for selective activation of propargylic alcohols towards the M-S rearrangement. Nevertheless, gold(III) has been shown to be more oxophilic, while gold(I) is  $\pi$ -philic.<sup>12,13</sup> Gold(III) has smaller diameter and less electrons than gold(I) and is, thus, somewhat harder.<sup>14</sup> This selectivity might explain product formation in some cases.

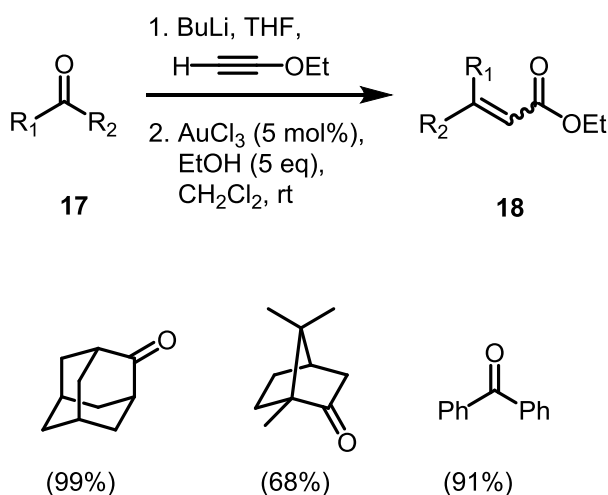
#### 3.1 Common features of gold catalysts

In general, reactions with gold catalysts require only mild conditions, and a broad selection of ligands is available, of which the most common ones are phosphines and carbenes.<sup>15</sup> Gold complexes are tolerant of oxygen and water, an exception being gold(III) halogen salts, which are hygroscopic. Gold can be employed as inorganic salts, the most commonly  $\text{AuCl}_3$  and  $\text{AuCl}$ , or organic complexes, with the oxidation state +I being the most popular. Gold(I) complexes are often used as precatalysts of the form  $\text{L}_n\text{AuX}$ . The ligand X can be exchanged into a loosely coordinating counterion, which is usually offered by a silver(I) salt, for example  $\text{AgOTf}$  and  $\text{AgBF}_4$ . The formation of the cationic gold species  $\text{L}_n\text{Au}^+\text{X}^-$  enables higher electrophilicity of gold, and the  $\text{X}^-$  ligand can be substituted by a substrate. The more loosely coordinating the counteranion, the more acidic the active gold complex. Importantly, silver salts can play an unpredicted role in the gold(I)-catalyzed reaction and lead to unwanted side reactions. Yet, there are gold(I) complexes, which do not require use of silver salts or other activating co-catalysts. For example,  $\text{LAuNTf}_2$ -type catalysts have been used for the M-S rearrangement.<sup>16</sup>

Gold catalysts do not normally act through a redox cycle, like other transition metal catalysts, but they activate the substrate by coordination. They are strong Lewis acids, and the exceptional ability to activate carbon-carbon triple bonds can be exploited in conducting the M-S rearrangement selectively.<sup>17</sup>

### 3.2 Meyer-Schuster rearrangement with gold catalysts

Gold(III) chloride gave only moderate results in the M-S rearrangement of  $\gamma$ -phenyl-substituted propargylic alcohols, as dehydrated enynes were major side products.<sup>2</sup> Instead, the acetylene group can be activated by incorporating an electron-donating ethoxy group to enhance coordination of gold. Electron-rich alkoxyacetylenes underwent the M-S rearrangement efficiently, and sterically demanding side groups were well tolerated. As a drawback, high catalyst loading of 5 mol% was needed, and low stereochemical control was achieved. A two-stage strategy for the synthesis of  $\alpha,\beta$ -unsaturated esters includes the M-S reaction as the second step, a straightforward acetylide addition to ketones being the first step (Scheme 6).

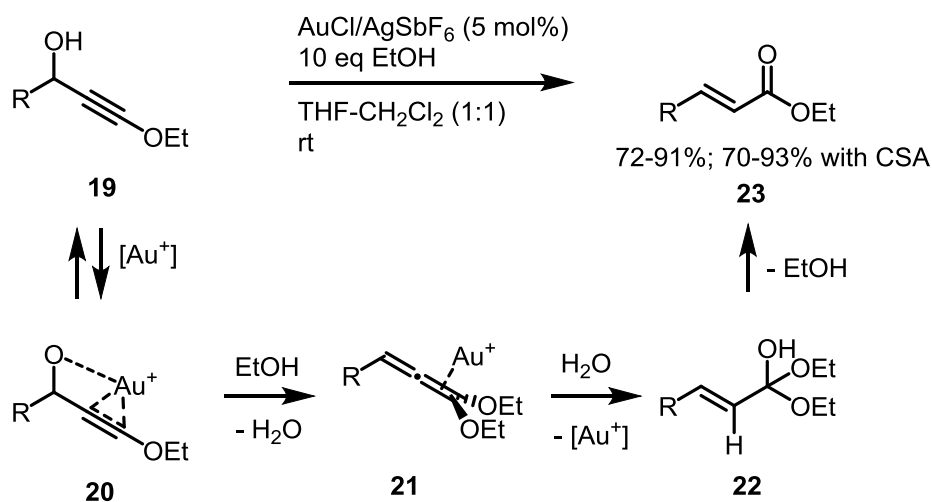


**Scheme 6.** Two-step olefination of ketones with gold(III) chloride.<sup>2</sup>

Also Rieder et al. tested AuCl<sub>3</sub> for ethoxy-activated substrates, but as it resulted capricious, other method was used instead.<sup>18</sup> NaAuCl<sub>4</sub>·2 H<sub>2</sub>O (5 mol%) has also given M-S products.<sup>13</sup>

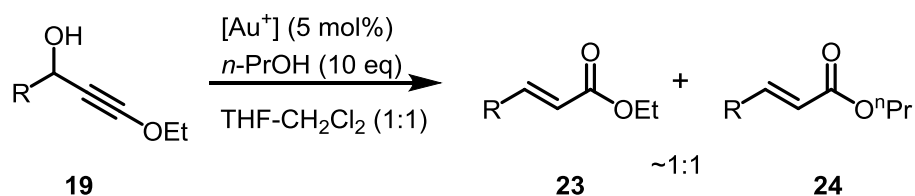
Owing to the success with the alkynylation-rearrangement by AuCl<sub>3</sub>, the Dudley group studied a set of secondary propargylic alcohols with ethoxy activation.<sup>19</sup> AuCl/AgSbF<sub>6</sub> was the best combination, and together with ethanol,  $\alpha,\beta$ -unsaturated esters were achieved with high yields (Scheme 7). *E*-selectivity was varying, but it could be further enhanced by addition of camphorsulfonic acid. Also one example of tertiary substrate was offered with 92% yield, thus the method could be expected to work with a wider range of tertiary alcohols as well. The reaction proceeds in THF-CH<sub>2</sub>Cl<sub>2</sub> mixture at room temperature. The mechanism is proposed to involve substitution by ethanol to form the 1,1-diethoxyallene (**21**) followed by the formation of the 1,1-diethoxyalken-1-ol (**22**). When ethanol

was substituted by *n*-propanol, a 1:1 mixture of ethyl and *n*-propyl esters was achieved (Scheme 8). This observation supports the necessity of ethanol in the reaction.



R = alkyl, aryl

**Scheme 7.** M-S rearrangement with AuCl/AgSbF<sub>6</sub>.<sup>19</sup>

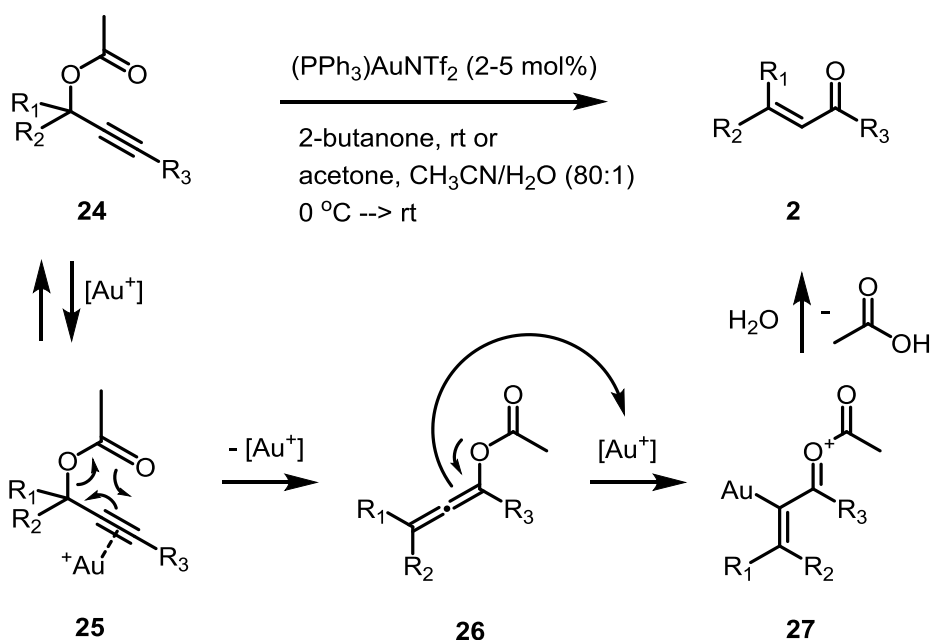


**Scheme 8.** Incorporation of *n*-propanol.<sup>19</sup>

For less activated propargylic alcohols, other gold catalysts are needed. In the first reports for the propargylic alcohols, which do not bear an ethoxy group, conversion to corresponding acetates was required.<sup>16, 20</sup> The Zhang group used the commercially available cationic [PPh<sub>3</sub>AuNTf<sub>2</sub>] (NTf<sub>2</sub> = triflimide) for the M-S rearrangement of propargylic acetates. Also other phosphine ligands were suitable. The reaction proceeded neatly and with high *E*-selectivity for internal substrates with a wide range of alkyl and aryl functionalities (Scheme 9). In the case of terminal propargylic acetates, hydration of the triple bond occurred. For secondary propargylic acetates, 2 mol% of catalyst in 2-butanone was sufficient. Tertiary substrates were prone to dehydration and other side reactions.

Still, 5 mol% of  $[\text{PPh}_3\text{AuNTf}_2]$  in acetonitrile/ $\text{H}_2\text{O}$  (80:1) gave very good yields. Acetonitrile is assumed to slow down the reaction through coordination and thus prevent side reactions, like elimination.

Gold has a dual role in activating both the triple bond during the 1,3-shift of the propargylic ester (**25**), and the subsequent alkenylacyloxocarbenium intermediate (**27**) (Scheme 9).<sup>16, 20</sup> In addition to hydrolysis, the carbenium (**27**) can attack to various electrophiles resulting in intramolecular cyclizations<sup>21</sup> and rearrangements<sup>22</sup>, or formation of  $\alpha$ -iodoenones,<sup>23</sup> to mention a few. The catalyst in wet butanone with *t*-butanol was used in the synthesis of the lower side chains of prostaglandins.<sup>24</sup> Addition of *t*-butanol was observed to suppress desilylation of the hydroxyl protection.



$\text{R}_1 = \text{H}$ ;  $\text{R}_2 = \text{alkyl, aryl}$ ;  $\text{R}_3 = \text{alkyl, aryl}$ ;

2 mol% catalyst, 2-butanone, rt; (78-92%)

$\text{R}_1 = \text{alkyl, aryl}$ ;  $\text{R}_2 = \text{alkyl, aryl}$ ;  $\text{R}_3 = \text{alkyl}$ ;

5 mol% catalyst in acetone,  $\text{CH}_3\text{CN}/\text{H}_2\text{O}$  (80:1),  $0\text{ }^\circ\text{C} \rightarrow \text{rt}$ ; (82-98%)

**Scheme 9.**  $\text{PPh}_3\text{AuNTf}_2$ -catalyzed M-S reaction of propargylic acetates.<sup>16</sup>

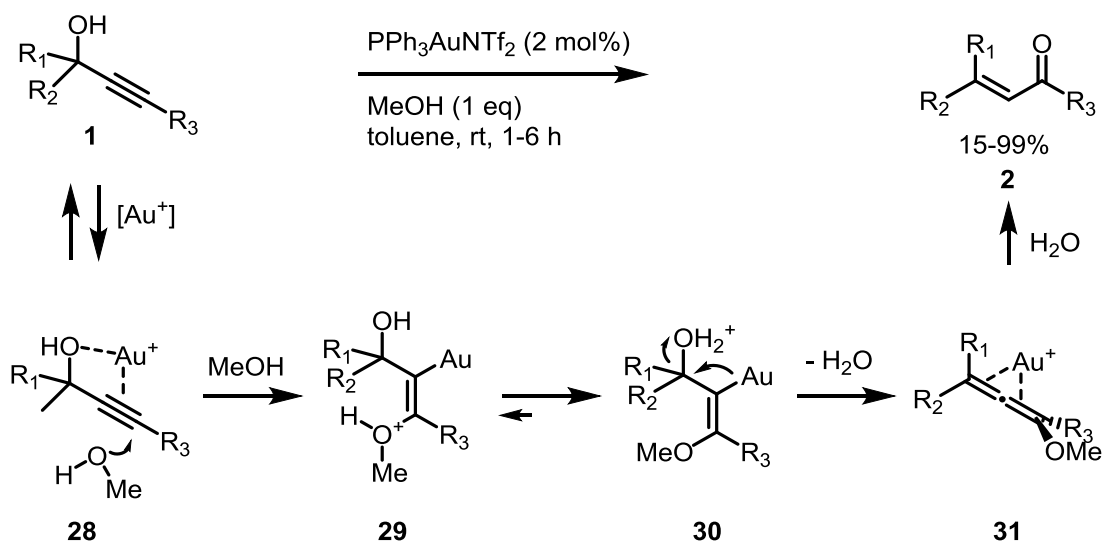
Pennell et al. investigated generation of boron enolates from alkynes catalyzed by  $\text{PPh}_3\text{AuNTf}_2$  using 4-methoxyphenylboronic acid as an additive.<sup>25, 26</sup> Instead of trapping the cyclic enolate, they obtained a  $\beta$ -hydroxyketone and an enone. Using methanol as the protic additive instead of boronic acid, the enone was acquired exclusively. A general procedure for the reaction of secondary and

tertiary propargylic alcohols with 1-2 mol% cationic gold(I) catalyst, in the presence of 1 equivalent of methanol, gives moderate to high yields (Scheme 10). The method worked notably well also for alkyl-substituted secondary and tertiary substrates. Secondary substrates gave better results than tertiary, and the dimethylamino phenyl-substituted alcohol with 15% yield was the only incompatible over the 29 tested substrates. Nitrogen-containing substrates tend to be unreactive due to coordination of gold with nitrogen and following inactivation. Primary substrates gave some methanol addition products in addition to the enone. This could be circumvented by using boronic acid instead.

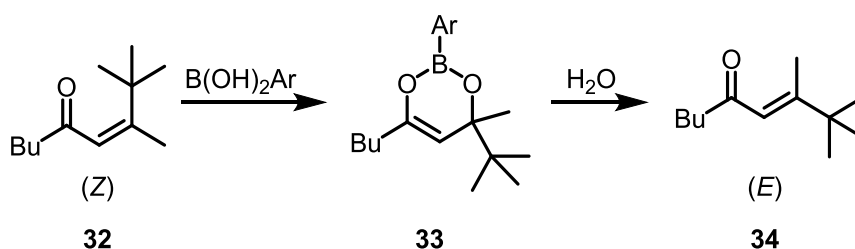
The mechanism for the MeOH-aided rearrangement is shown in Scheme 10. The carbonyl group is formed by addition of methanol.

Addition of *p*-methoxyphenylboronic acid to the enone obtained from Au/MeOH reaction increased the *E/Z* ratio significantly. This can be reasoned by the formation of a cyclic boronate intermediate (**33**), which determines the conformation (Scheme 11). The mechanism with the aid of boronic acid resembles the 3,3-rearrangement mechanism of the propargylic acetate (see Scheme 9).

Terminal propargylic alcohols yielded  $\alpha$ -hydroxyketones but, interestingly,  $\alpha,\beta$ -unsaturated aldehydes together with  $\alpha$ -methoxyketones were obtained with a catalyst batch possibly contaminated with silver salt, which indicates a two-step reaction catalyzed by two different metals.



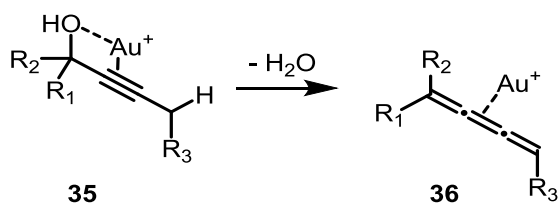
**Scheme 10.** PPh<sub>3</sub>AuNTf<sub>2</sub>-catalyzed M-S reaction of propargylic alcohols.<sup>26</sup>



**Scheme 11.** Isomerization of Z-product by boronic acid treatment.<sup>26</sup>

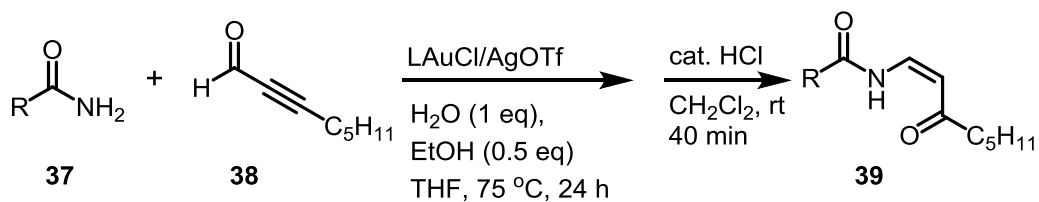
During the catalyst screening by the Zhang group, [PPh<sub>3</sub>AuCl]/AgSbF<sub>6</sub> resulted unstable.<sup>16</sup> Still, [PPh<sub>3</sub>AuCl] precatalyst is often a suitable option, and it can be activated by various salts. Silver(I) triflate was used by Mou et al. in a rearrangement/cyclization cascade reaction.<sup>27</sup> Lee et al. screened several catalysts for their alkyl-chained substrate, and 5 mol% [PPh<sub>3</sub>AuCl]/AgOTf resulted the most efficient, but no stereocontrol was noticed.<sup>28</sup> Due to more rapid conversion of substrates with a hydrogen in the  $\alpha$ -position to the alkyne, the group proposed a cumulene intermediate caused by dehydration of the Au-coordinated propargylic substrate (Scheme 12). This was also supported by the unreactivity of double-substituted propargylic alcohols. Nevertheless, Nolan and co-workers showed that M-S products are obtained even in the absence of the  $\alpha$ -hydrogen, and they discarded the cumulene-involving mechanism.<sup>29</sup>



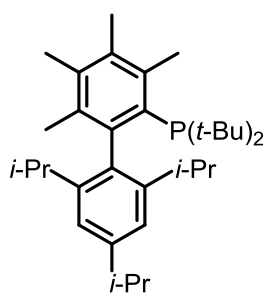


**Scheme 12.** Formation of the cumulene intermediate.<sup>28</sup>

Kim et al. developed a tandem synthesis of enamides starting from propargylic aldehydes (Scheme 13).<sup>30</sup> A phosphine-based gold complex [Me<sub>4</sub>-*t*-BuXPhosAuCl] (L = 2-di-*tert*-butylphosphino-3,4,5,6-tetramethyl-2',4',6'-triisopropyl-1,1'-biphenyl, **40**) with AgOTf was used to catalyze both the nucleophilic addition of the amide to the aldehyde and the M-S rearrangement of the resulting propargylic hemiaminal. Decrease in solvent polarity increased the *Z/E* ratio due to intramolecular hydrogen bonding between the amide proton and the carbonyl oxygen of the ketone. Enamides are important intermediates in synthesis, but traditionally their syntheses have been accompanied by several difficulties.



R = alkyl, aryl, heterocycle



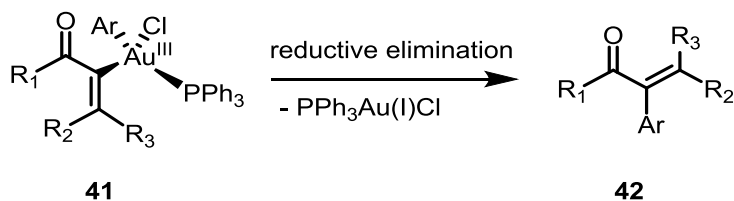
L = Me<sub>4</sub>-*t*-BuXPhos

**40**

**Scheme 13.** Tandem enamide synthesis with LAuCl/AgOTf.<sup>30</sup>

The groups of Shin and Glorius introduced independently a fascinating method to activate the [PPh<sub>3</sub>AuCl] precatalyst during tandem M-S rearrangement/aryl coupling.<sup>31, 32</sup> Au(I) is oxidized to

active Au(III) by light-induced Ru-catalyzed redox cycle, which introduces an aryl ligand into the  $[L_nAu(I)X]$  complex (Scheme 14). After the M-S rearrangement, reductive elimination gives the arylated enone **42**.



**Scheme 14.** Reductive elimination step of Au-redox cycle.<sup>32</sup>

*N*-heterocyclic carbene-ligated gold complex  $[(\text{NHC})\text{AuCl}]$  together with a silver(I) salt in THF/H<sub>2</sub>O was used as a catalyst by the Nolan group for the M-S reaction of propargylic acetates.<sup>33</sup> Later, they achieved to apply the catalyst for propargylic alcohols by changing the solvent system into MeOH/H<sub>2</sub>O.<sup>29</sup> The most suitable ligands were IPr and ItBu (**43-45** in Figure 2). The catalyst was activated with AgSbF<sub>4</sub>, though AgBF<sub>4</sub> and AgPF<sub>6</sub> showed similar potential. A broad variety of conjugated enones were obtained from electron-rich and electron-withdrawing aryl-substituted compounds, as well as from unactivated secondary propargylic alcohols and acetates (Scheme 15). The common thing for all the substrates was the aryl substituent in either end of the molecule. Two examples of alkyl-substituted secondary substrates gave only 58% and 28% yields. The special feature in the acetate method was the reactivity of terminal alkynes, which gave poor results as free alcohols.

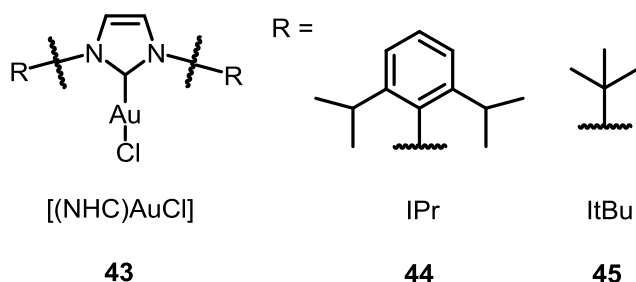
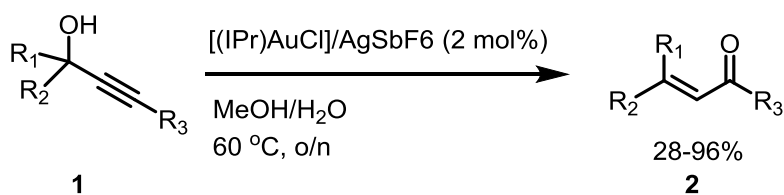


**Figure 2.** Successful NHC-ligands.



$\text{R}_1$  = H, alkyl, aryl  
 $\text{R}_2$  = alkyl, aryl  
 $\text{R}_3$  = alkyl, aryl, alkoxy, ester

**Scheme 15.** Gold-NHC complex-catalyzed M-S rearrangement.<sup>29</sup>

Water was found to be essential for the reactions. Anhydrous conditions have been noticed to lead to formation of indenenes.<sup>34</sup> The group suggested that instead of activating the carbon-carbon triple bond, the catalyst activates a water molecule to facilitate its attack (Figure 3). In their suggested  $\text{S}_{\text{N}}2'$  mechanism based on DFT calculations, the active  $[(\text{NHC})\text{AuOH}]$  species **46** coordinates *via* the oxygen atom to the electron-deficient end of the triple bond offering the carbonyl group (Scheme 16). They postulated that an allene could not be an intermediate, like in 3,3-rearrangement, because an isolated allene did not react under the earlier reaction conditions (Scheme 17).<sup>20</sup> Also, in THF/ $\text{H}_2\text{O}$  propargylic methyl ether reacted, while propargylic alcohol remained unreactive. As a methoxy group is not able to undergo 3,3-rearrangement, it was tempting to exclude that mechanism.

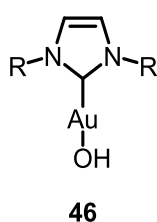
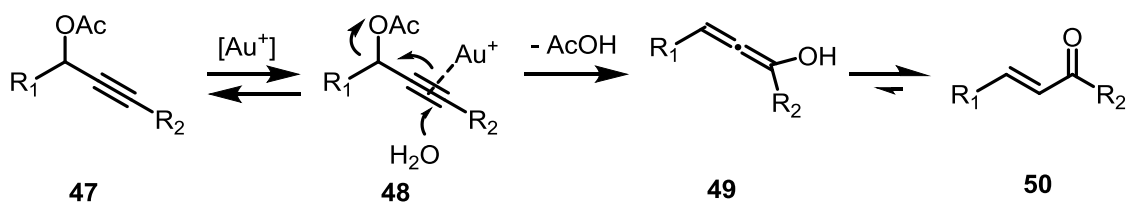
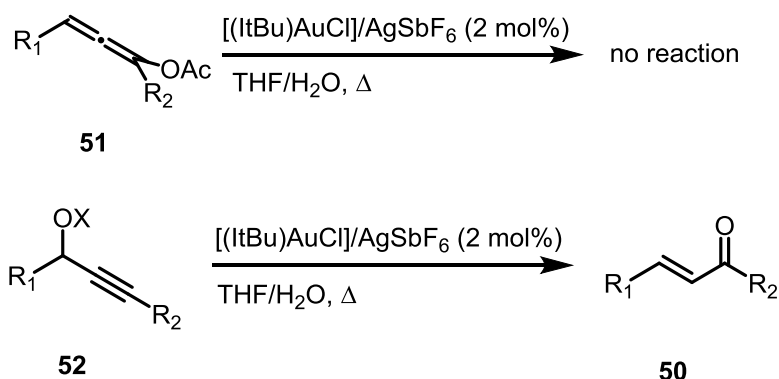


**Figure 3.** Proposed active NHC-catalyst.<sup>33</sup>



**Scheme 16.** Suggested  $S_N2$  mechanism with NHC-gold.<sup>33</sup>



X = H: no reaction

X = Me: 62%

**Scheme 17.** Suggested evidence for the incorporation of the [NHC-Au-OH] active species and the absence of 3,3-rearrangement..<sup>33</sup>

Nevertheless, the group succeeded with the reaction of propargylic alcohols using mixture of methanol and water at 60 °C.<sup>29</sup> This suggests that methanol plays a role in this case, or THF as a solvent was a bad choice. On the other hand, with alkoxy-substituted substrates, quantitative transesterification with methanol was observed. Thus, the mechanism suggested by the Dudley group<sup>19</sup> (see Scheme 8) can be discarded in the case of NHC-ligated gold.

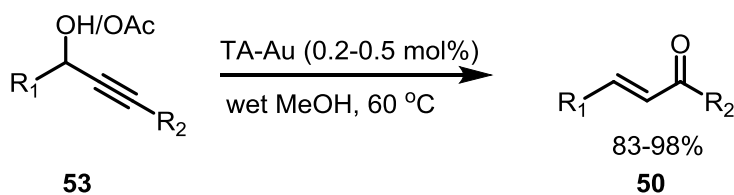
Later, the Nolan group defined that the active species cannot be the gold hydroxyl complex due to low activity of the isolated complex in the absence of protic acid activator  $\text{HBF}_4$ .<sup>34</sup> Instead, the catalyst is  $[(\text{NHC})\text{Au}]^+$ , which is formed from  $[(\text{NHC})\text{AuOH}]$  via the dinuclear species  $[\{\text{Au}(\text{NHC})\}_2(\mu\text{-OH})]^+$  activated by a Brønsted acid.<sup>35</sup> The precatalyst  $[(\text{NHC})\text{AuOH}]$  is prepared easily, and expensive silver additives are not needed. Still, NHC ligands are expensive. Additionally, other DFT calculations by the Nolan group<sup>36</sup> for NHC ligands and acetate substrates suggest coordination of gold with a triple bond, enabling the 1,3-shift via a cyclic intermediate, like in the previously depicted case of

propargylic acetate (see Scheme 9). The  $S_N2'$  mechanism cannot be excluded at this point, though. The exact mechanism for propargylic alcohols remained unclear.

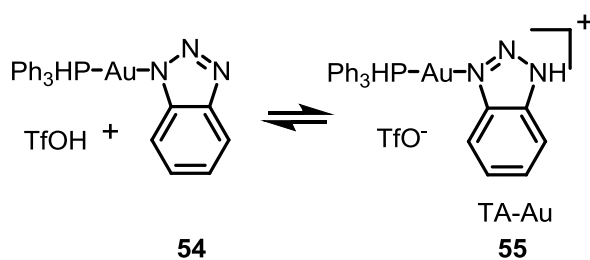
In addition to Nolan's preliminary work with IPr ligand, it has been used in the synthesis of prostanoids, irones and  $\alpha$ -ionones, as well as in M-S rearrangement of propargylic acetates followed by  $\alpha$ -fluorination.<sup>37, 38, 39, 40</sup> IPr was used also in a tandem one-pot synthesis of  $\beta$ -disubstituted ketones.<sup>41</sup> The M-S rearrangement of a secondary alcohol was followed by asymmetric boronic acid 1,4-addition. Choosing an orthogonal ligand system of gold and rhodium was the key to success for the first known Au(I)/Rh(I) tandem reaction.

Shi and co-workers introduced a 1,2,3-triazole coordinated gold(I) complex (TA-Au) (Scheme 18).<sup>42, 43, 44</sup> In addition to being air, moisture and thermally stable, the complex was promoted as a cheaper option compared with the NHC ligands. However, it bears a counterion, which is introduced by a silver(I) salt. The precatalyst  $[\text{Ph}_3\text{P-Au-triazole}]^+\cdot\text{X}^-$  reveals the active species  $[(\text{Ph}_3\text{P})\text{Au}]^+$ , and the role of the triazole counter ligand is to dynamically stabilize the gold catalyst from degradation. Since simple  $[(\text{Ph}_3\text{P})\text{Au}]^+$  catalysts suffer from low stability and oxidation,<sup>42, 45</sup> development of bulkier phosphorus ligands was one approach to circumvent the problem. Triazole ligands, instead, allow the use of inexpensive  $\text{Ph}_3\text{P}$ .

M-S rearrangement for propargylic acetates and alcohols has been made with TA-Au (Scheme 18).<sup>44</sup> It was suggested that an equilibrium between the neutral (**54**) and ionized (**55**) forms of TA-Au and liberation of HOTf causes hydration of the allene after the 1,3-shift. A large group of secondary substrates were reactive, including terminal alkyne, as well as *t*-butyl-substituted propargylic acetate, which did not react with NHC-ligated gold.<sup>33</sup> Also, entirely alkyl-substituted alcohols and acetates were reactive, so aryl group was not necessary. Instead, no rearrangements of primary or tertiary substrates were reported. Despite the limited substrate scope, the TA-Au method is highly interesting because of the low catalyst loading and affordable price of the ligand.



$R_1$  = alkyl, aryl  
 $R_2$  = H, alkyl, aryl



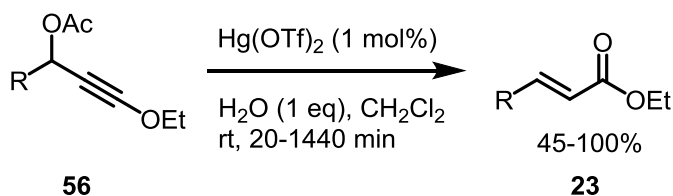
**Scheme 18.** TA-Au-catalyzed M-S rearrangement and equilibrium between ionic and neutral forms of TA-Au.<sup>44</sup>

Another special feature of TA-Au catalysts is the chemoselectivity, which allows coordination between gold and an alkyne, but not with an allene. As a consequence, stereoselectivity is dictated by the kinetic pathway, opposite to the thermodynamic pathway used by other gold catalysts. When  $\alpha$ -haloenones were synthesized *via* propargylic acetate rearrangement followed by halogenation of allene, kinetically favored *E* isomers were formed with good to excellent selectivity.<sup>43</sup> While other gold catalysts coordinate to the allene, the lack of coordination of TA-Au leaves this site open for the halogenating reagent.

In conclusion, there are several gold catalyst systems, which give great results under mild conditions. Gold(I) complexes seem to be more reliable than gold(III). As the field of gold catalysis is still fresh and growing, better and more affordable methods are expected in near future.

### 3.3 Mercury and silver catalysts

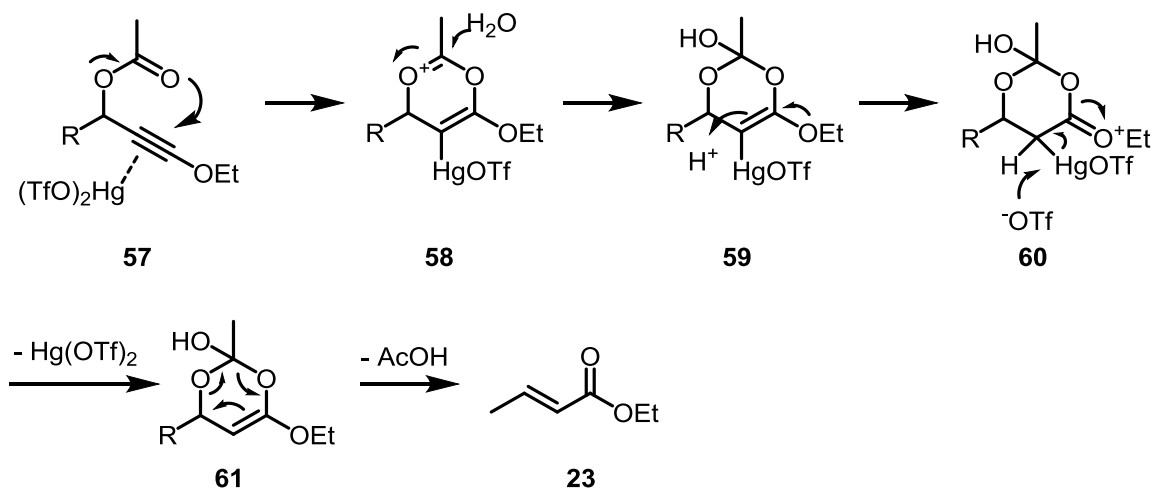
In addition to gold, late transition metals silver and mercury can act as soft Lewis acids and activate the triple bond. Although mercury sounds suspicious, one can recall that many organomercuric compounds are not toxic. Mercury(II) triflate catalyzes the M-S rearrangement of secondary ethoxyalkynyl acetates with good to excellent yields and practically perfect *E*-selectivity (Scheme 19).<sup>46</sup> Bulky *t*-butyl-substituted substrate gave only 45%. Primary, internal alkynyl acetates also react fairly well (51-84%, 5 examples),<sup>47</sup> but the activating effect of electron-donating alkoxy group can be observed as better yields. Optimized conditions for the reaction of ethoxyalkynyl acetates at room temperature include 1 mol% of Hg(OTf)<sub>2</sub>, dichloromethane and 1 eq of water.



R = *n*-alkyl, Ar, BuOBn, BuOBz,  
*t*-Bu, *p*-NO<sub>2</sub>Ph

**Scheme 19.** M-S rearrangement with Hg(OTf)<sub>2</sub>.<sup>46</sup>

The mechanism for the rearrangement of the ethoxyalkynyl acetate is proposed to undergo through cyclization, which resembles the 1,3-shift already seen for various systems (Scheme 20; see Scheme 9). After coordination of the alkyne with Hg(OTf)<sub>2</sub>, acetate attacks the triple bond to form a cyclic oxonium cation (**58**). Water attacks the carbonyl carbon, and subsequently, the ethoxy group helps with protonation to form another oxonium cation (**60**). Demercuration regenerates the catalyst, and fragmentation yields the unsaturated ester. The perfect *E/Z* stereoselectivity can be reasoned by noticing, that the side group prefers an equatorial orientation on the chair structure.

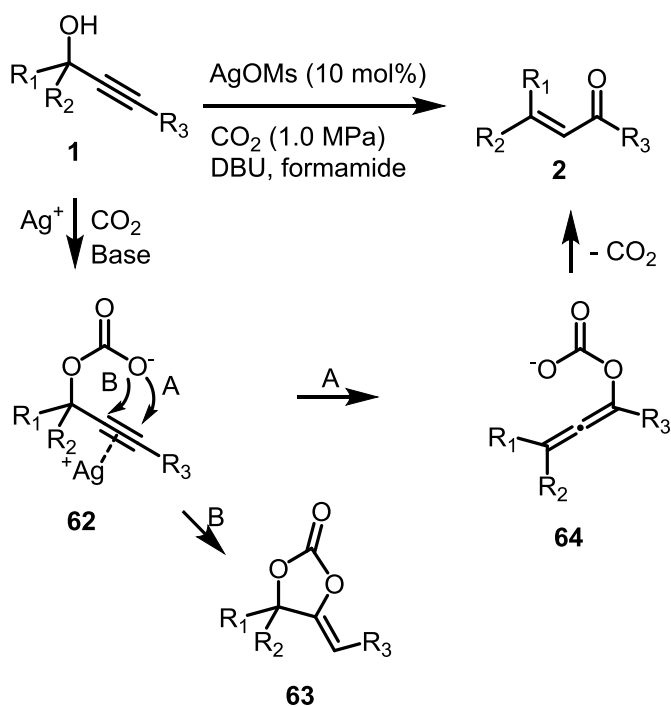


**Scheme 20.** Mechanism for the  $\text{Hg}(\text{OTf})_2$ -catalyzed M-S rearrangement.<sup>46</sup>

A sophisticated method to activate a secondary or tertiary propargylic alcohol towards M-S rearrangement was introduced by Sugawara et al.<sup>48</sup> Using 10 mol% of AgOMs and 1 eq of DBU in formamide under 1 MPa of  $\text{CO}_2$ , high yields (70-98%) were obtained for several tertiary and secondary, internal propargylic alcohols with alkyl or ethoxy substituents (Scheme 21). The substrate with terminal alkyne was less reactive. Also DBN and DIPEA worked, and catalytic amount of base was sufficient at elevated temperature. No stereoselective control was observed.

The hydroxyl group is converted into carbonate by carbon dioxide (Scheme 21). Silver salt activates the triple bond, and 3,3-sigmatropic rearrangement occurs in the presence of base to form an allene-enolate (**64**). Release of  $\text{CO}_2$  yields the enone. The incorporation of  $\text{CO}_2$  was proved by isotopic studies. A polar solvent is crucial to prevent the attack to the  $\alpha$  carbon of the triple bond and the formation of a cyclic carbonate (**63**) (route B in Scheme 21). Polar solvents, like DMF and DMA, stabilize the polarized carbonate structure with an elongated C-O bond, which is directed to attack the  $\beta$  carbon. The drawback of the system is the high loading (10 mol%) of AgOMs.





$\text{R}_1, \text{R}_2 = \text{alkyl, aryl}$   
 $\text{R}_3 = \text{alkyl, aryl, alkoxy}$

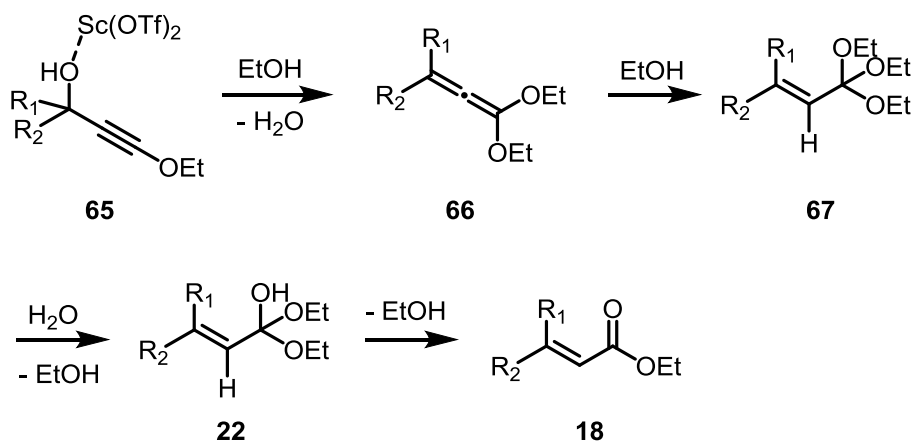
**Scheme 21.** M-S rearrangement with silver salt and carbon dioxide, and an alternative fate.<sup>48</sup>

#### 4. Nonmetallic and metallic hard Lewis acids

Lewis acid metal salts are very convenient choices for the M-S reaction, as they are easy to handle and sometimes recyclable from water. Among the tested salts,  $\text{InCl}_3$ ,  $\text{Sc}(\text{OTf})_3$ ,  $\text{FeCl}_3$ ,  $\text{Y}(\text{OTf})_3$  and  $\text{Cu}(\text{OTf})_2$  are soluble in water, while  $\text{Bi}(\text{OTf})_3$  and  $\text{Ca}(\text{NTf}_2)_2$  are insoluble. During studies conducted by the group of Dudley,<sup>49</sup> they implied that the tested salts act like soft Lewis acids and coordinate with the triple bond. It is more probable, though, that they coordinate with the hard hydroxyl oxygen, because  $\text{In}(\text{III})$ ,  $\text{Sc}(\text{III})$ ,  $\text{Fe}(\text{III})$ ,  $\text{Ca}(\text{II})$  and  $\text{Y}(\text{III})$  are hard, while  $\text{Cu}(\text{II})$  and  $\text{Bi}(\text{III})$  are borderline Lewis acids.

Scandium(III) triflate is a fast and efficient catalyst for ethoxylated propargylic alcohols.<sup>49</sup> Exploiting one-pot olefination including alkynylation followed by M-S reaction, hindered  $\alpha,\beta$ -unsaturated carbonyls can be synthesized, of which many cannot be prepared by traditional methods. It can be noticed that more hindered substrates exhibit even better chemoselectivity, as other mechanistic routes are inhibited. Copper(II) triflate give nearly similar results as scandium triflate.

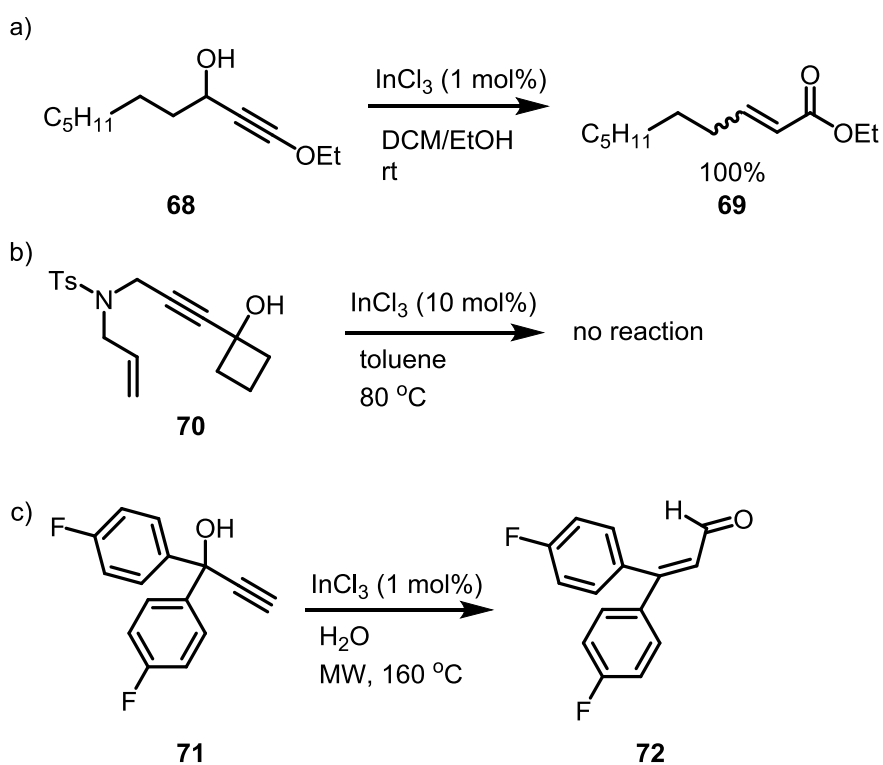
During mechanistic studies for the  $\text{Sc}(\text{OTf})_3$  catalyzed reaction, the group of Dudley conducted the same experiment as for the  $\text{AuSBF}_6$  (Scheme 8),<sup>19</sup> in which substitution of ethanol by *n*-propanol resulted in 50% of *n*-propyl ester in the product. This time, 75% incorporation of *n*-propanol was observed and hence, a modified mechanism was proposed (Scheme 22). After the formation of a diethoxy allene (**66**), another equivalent of ethanol is added, which yields an ortho-ester (**67**), which in turn hydrolyzes to the unsaturated ester.



**Scheme 22.** Mechanism for  $\text{Sc}(\text{OTf})_3$ -catalyzed M-S rearrangement.<sup>19</sup>

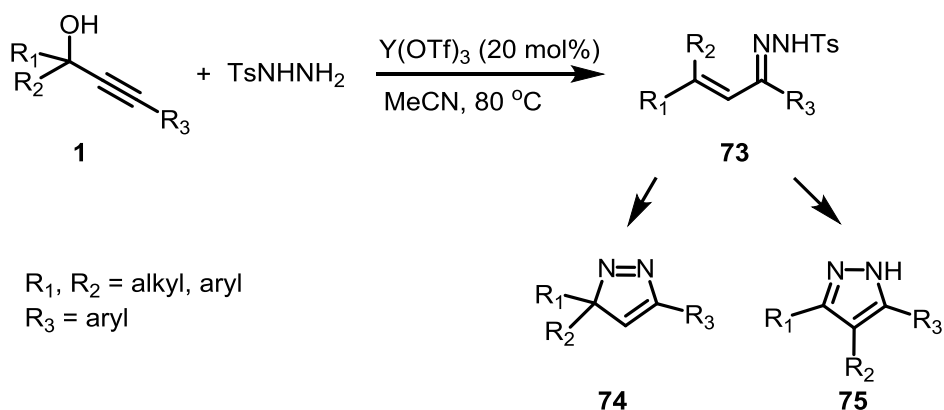
Although not as active as scandium or copper, indium(III) chloride works well for ethoxy-activated propargylic alcohols.<sup>49</sup> 1 mol% of the catalyst in DCM/EtOH at room temperature catalyzed the M-S reaction of the secondary ethoxydecynol **68** with 100% yield (Scheme 23a). Camphorsulfonic acid accelerated the reaction significantly. The mechanism could be assumed to be same type as with  $\text{Sc}(\text{OTf})_3$ .

For nonactivated tertiary propargylic alcohol **70**,  $\text{InCl}_3$  did not show any activity at 80 °C after 24 hours (Scheme 23b).<sup>28</sup> Nevertheless, terminal and internal alkynols with different aryl rings were transformed into enals and enones with excellent yields under microwave irradiation in water, in a timescale of 5 to 360 minutes (one example in Scheme 23c).<sup>50</sup> The conditions tolerate aryl rings even with electron-withdrawing groups, therefore it would be tempting to consider MW irradiation for nonactivated substrates like **70**, as well. Better solubility of substrates is based on superheating of water, which modifies its properties towards polar organic solvents.<sup>51</sup> This green method would be highly recommended, although results might be unpredictable, as there are several influencing factors compared to traditional chemistry.



**Scheme 23.** Reactions of different substrates with  $\text{InCl}_3$ : **a)** Ethoxy-activated<sup>49</sup>, **b)** alkyl-substituted<sup>28</sup> and **c)** terminal, aryl-substituted<sup>50</sup>.

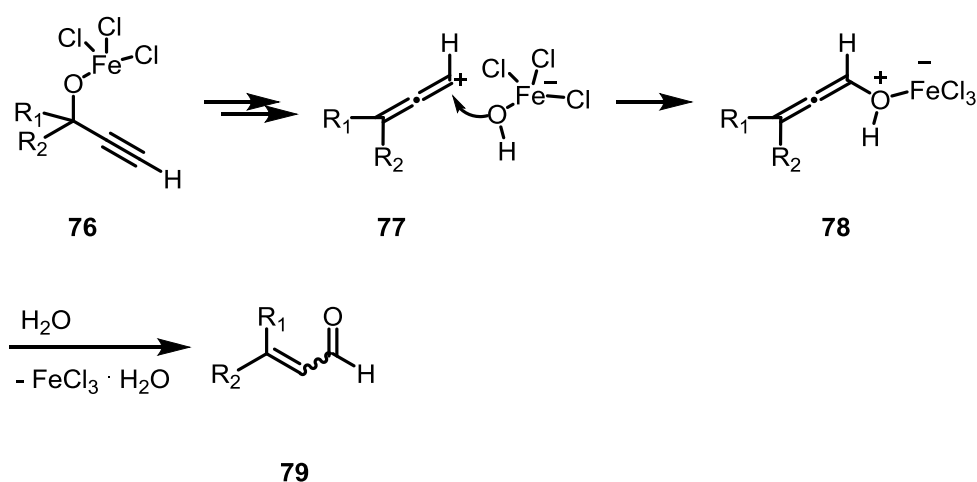
Yttrium(III) triflate was used by Liu et al. to produce pyrazoles *via* hydrazones.<sup>52</sup> The unsaturated hydrazones were produced either by aza-Meyer-Schuster reaction or M-S reaction of a propargylic alcohol followed by nucleophilic attack of tosyl hydrazide (Scheme 24). Also other salts of lanthanides Ce(III), Yb(III) and La(III) gave moderate yields. Lanthanide triflate salts have been called promising green catalysts, because of their selectivity and stability in water. Still, there are few examples of their use as catalyst. The major disadvantage is the high price.



**Scheme 24.** Y(OTf)<sub>3</sub> catalyzed synthesis of hydrazones and their conversion into pyrazoles.<sup>52</sup>

The same propargylic substitution/aza-Meyer-Schuster rearrangement<sup>53</sup>, as well as M-S rearrangement of terminal and internal propargylic alcohols as part of formation of pyrroles<sup>54</sup>, have been catalyzed by 10 mol% iron(III) chloride. Additionally, El Douhaibi et al. studied reactions with stoichiometric amount of FeCl<sub>3</sub>.<sup>55</sup> Therefore, success in catalytic utilization of FeCl<sub>3</sub> in traditional M-S rearrangement might be expected. The reactions require heating in tetrahydrofuran, dichloroethane or nitromethane. By using anhydrous conditions, El Douhaibi et al. proved that the catalyst is in fact FeCl<sub>3</sub> and not HCl formed by hydrolysis. Alcaide et al. also demonstrated that 10 mol% HCl in absence of FeCl<sub>3</sub> did not induce desired transformation.

Anhydrous conditions also rule out the hydration-dehydration mechanism. El Douhaibi et al. propose occurrence of an allylic cation intermediate (**77**) formed by the departure of the activated hydroxyl group (Scheme 25).<sup>55</sup>

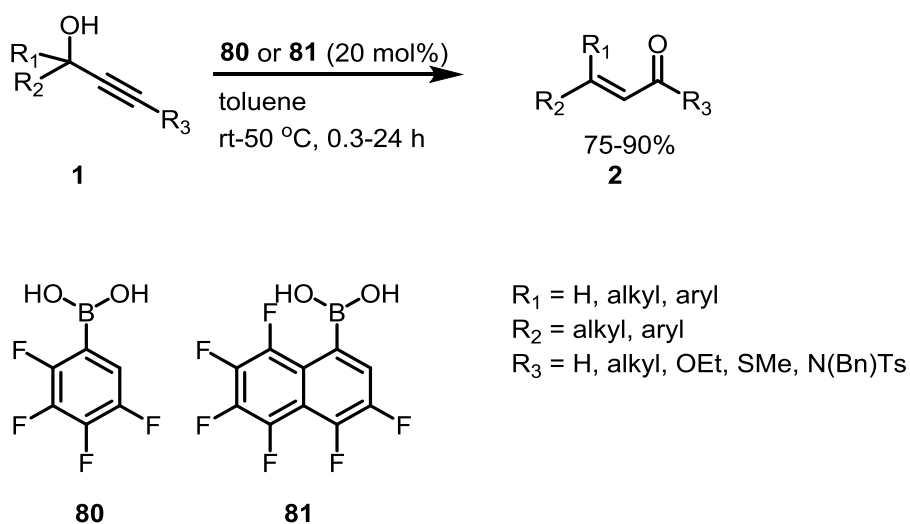


**Scheme 25.** Proposed mechanism for FeCl<sub>3</sub>-catalyzed M-S rearrangement.<sup>55</sup>

On the other hand, presence of traces of water has been shown indispensable in many occasions, anhydrous conditions leading to inhibition or other routes. This is true as well for a catalyst comprising  $\text{Ca}(\text{NTf}_2)_2/\text{KPF}_6$ .<sup>56</sup> Like Begouin and Niggemann explain, water hydrates the Lewis acid metal ion, which causes acidification of the water molecule.<sup>57</sup> The resulting Lewis/Brønsted acid system has superior activity than either of the acids separately. Accordingly, the combination of  $\text{FeCl}_3/\text{HCl}$  formed by partial hydrolysis could facilitate the M-S reaction.

An exceptional feature in the study of Okamoto et al. is that primary propargylic alcohols with aromatic substitution on the acetylenic end were reactive upon treatment with several metal salts.<sup>58</sup> There are only few examples of the M-S reactivity of primary substrates.<sup>25, 26</sup> Bismuth(III) triflate was selected as the most promising catalyst in a tandem reaction including the M-S rearrangement and 1,4-addition of an alcohol. Also  $\text{Cu}(\text{OTf})_2$ ,  $\text{Al}(\text{OTf})_3$ ,  $\text{Sc}(\text{OTf})_3$  and  $\text{AgOTf}$  showed activity.

Electron-deficient fluorinated aryl boronic acids are a mild alternative for the M-S reaction of secondary and tertiary propargylic alcohols (Scheme 26).<sup>59</sup> Boronic acid was seen to function together with a gold catalyst and especially enhance the *E*-selectivity,<sup>25, 26</sup> but it works individually even at room temperature.



**Scheme 26.** M-S rearrangement with boronic acid catalysts.<sup>59</sup>

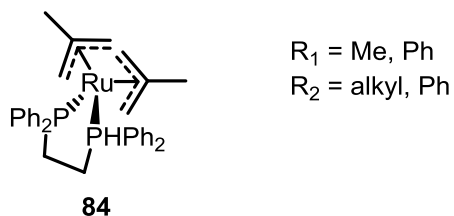
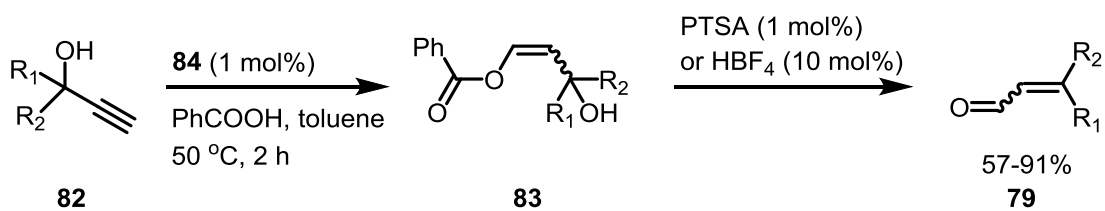
Another boron compound,  $\text{BF}_3$ , has activity as a catalyst.<sup>60</sup> During the synthesis of Taxol AB-ring system, ethoxylated substrate gave an  $\alpha,\beta$ -unsaturated ester and a  $\beta$ -hydroxy ester. Although the

reaction proceeded at room temperature,  $\text{BF}_3$  is not a recommendable option because of its toxicity.

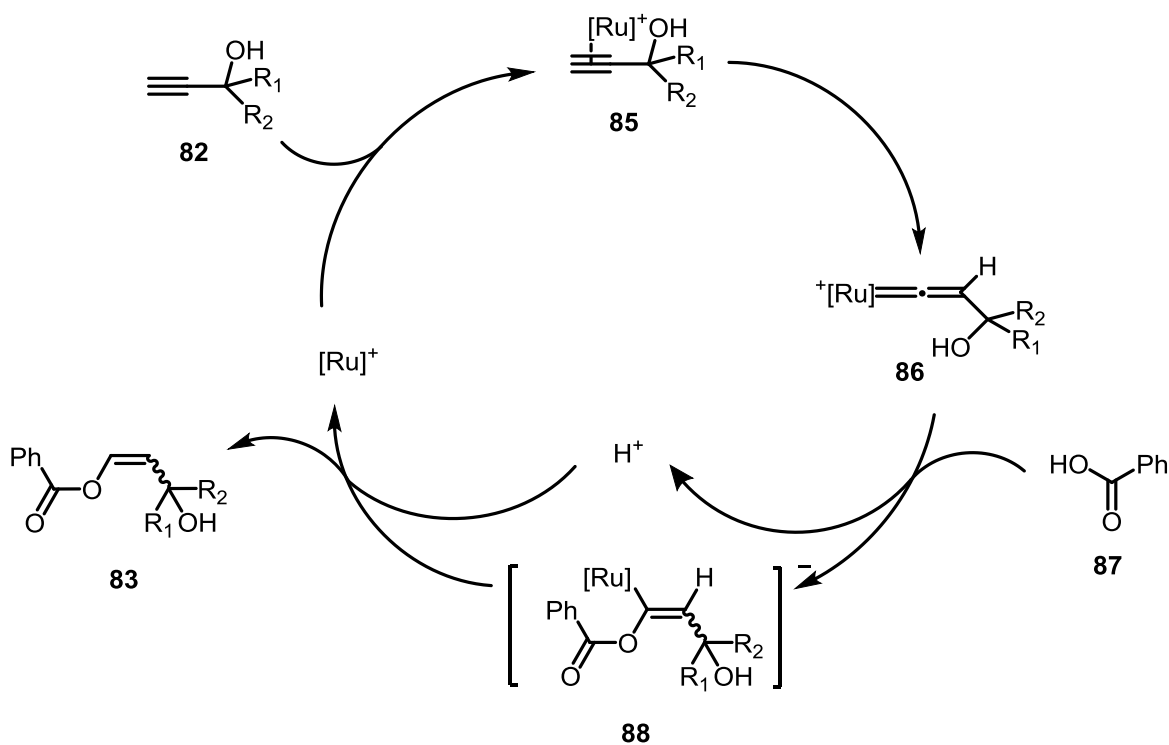
## 5. Organometal complexes of transition metals

In addition to gold, several transition metal-containing organometal complexes catalyze the Meyer-Schuster rearrangement. By definition, organometallic compounds have at least one bond between a carbon atom and a metal. Ligands are coordinated with the metal ion with bonds that have both ionic and covalent character. The metals discussed in this chapter are ruthenium, rhenium and iridium, which are located next to each other on the second and third row of transition metal block, meaning that they have similar properties and various oxidation states. It has to be remembered that the following complexes used for the M-S rearrangement are not commercially available, and the use of these catalysts serves primarily for the investigation of the catalysts themselves. In addition, iridium and rhenium are very expensive. Therefore, they might not be reasonably deployed for common use. Nevertheless, they follow a special mechanism, which is suitable for terminal propargylic alcohols, and is worth mentioning.

The pioneering work on ruthenium-catalyzed M-S rearrangement was done by the group of Dixneuf.<sup>61</sup> Anti-Markovnikov addition to alkynes was achieved by tuning the Ru catalyst with hydrocarbon ligands, followed by the discovery of the M-S rearrangement.<sup>62,63</sup> The method includes addition of the benzoic carboxylate to the terminal propargylic alcohol catalyzed by  $\text{Ru}[\eta^3\text{-CH}_3\text{C}(\text{Me})\text{CH}_2]_2(\text{dppe})$  (**84**) (Scheme 27). Allylic ligands in the Ru complex **84** are labile in acidic conditions and afford a vacant coordination site for the substrate. The ruthenium-alkyne **85** is transformed into the more stable ruthenium-vinylidene species **86** by 1,2-hydride shift, and this Fischer carbene-like structure is able to react by anti-Markovnikov addition of benzoic acid (Scheme 28). Protonolysis affords a hydroxyalkenyl benzoate **83**, which is then transformed into an enone *in situ*.

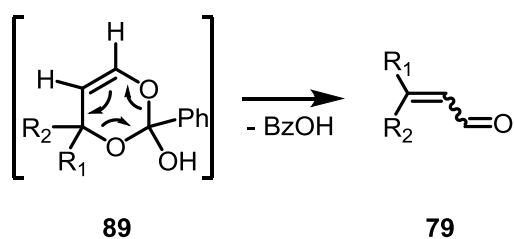


**Scheme 27.** M-S rearrangement of tertiary substrates with  $\text{Ru}[\eta^3\text{-CH}_3\text{C}(\text{Me})\text{CH}_2]_2(\text{dppe})$  complex.<sup>63</sup>



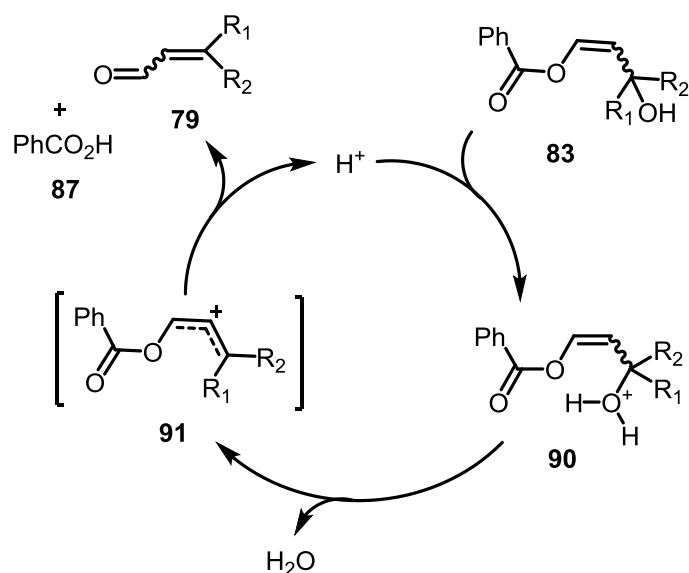
**Scheme 28.** Catalytic cycle for the  $\text{Ru}[\eta^3\text{-CH}_3\text{C}(\text{Me})\text{CH}_2]_2(\text{dppe})$  complex.<sup>63</sup>

There are two ways to form the  $\alpha,\beta$ -unsaturated aldehyde: In the first method, the benzoate intermediate undergoes a concerted rearrangement upon heating at 110 °C. This method requires the Z isomer, as the rearrangement occurs through a cyclic structure (**89**) (Scheme 29).



**Scheme 29.** Concerted mechanism for the benzoate intermediate rearrangement into an enal.<sup>62</sup>

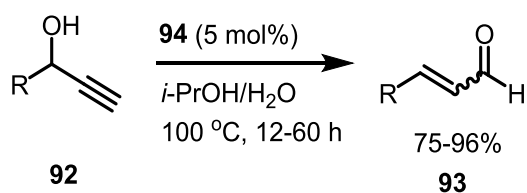
More convenient method is to use a catalytic amount of acid ( $\text{HBF}_4$  or PTSA) (Scheme 30). The protonated hydroxyalkenyl benzoate (**90**) releases benzoic acid to form the  $\alpha,\beta$ -enal (**79**). By this method, both *Z* and *E* benzoates are reactive. The method is suitable only for tertiary alcohols.



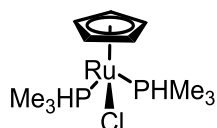
**Scheme 30.** Acid-catalyzed route for enals.<sup>63</sup>

Secondary alcohols react with a half-sandwich Ru(II) catalyst  $[\text{RuClCp}(\text{PMe}_3)_2]$  (**94**) in *i*-PrOH/ $\text{H}_2\text{O}$  at  $100\text{ }^\circ\text{C}$ , giving predominantly *E* isomers (Scheme 31), as shown by the Wakatsuki group.<sup>64</sup> The drawback of this reaction is the high temperature needed and unreactivity of tertiary alkynols.





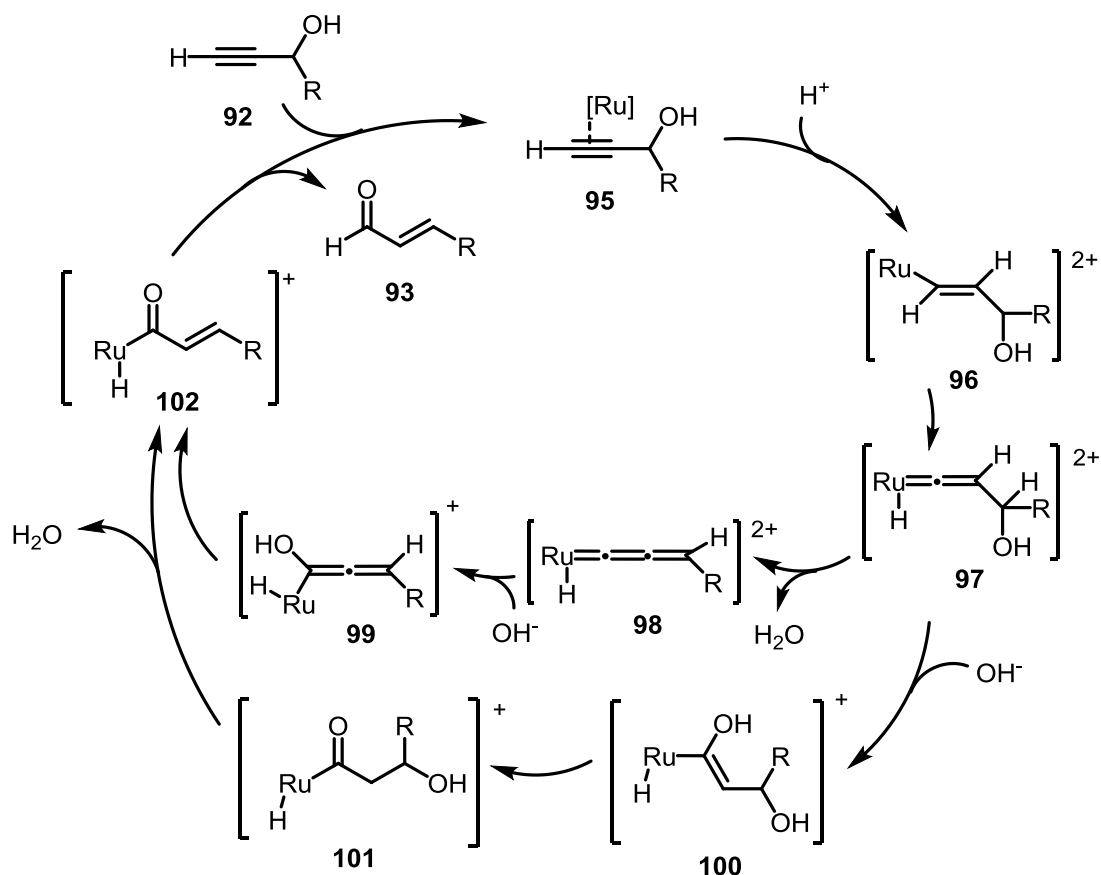
R = alkyl, Ph



**94**

**Scheme 31.** M-S rearrangement of secondary substrates with  $[\text{RuClCp}(\text{PMe}_3)_2]$  complex.<sup>64</sup>

One possible reaction mechanism is shown on Scheme 32. It includes anti-Markovnikov hydration of the terminal alkyne, and it is based on allenylidene and vinylidene intermediates and the group's formerly proposed aldehyde synthesis mechanism.<sup>65, 66</sup> Their mechanism involved protonation of the Ru(II)-(hydroxy)alkyne complex **95**, followed by formation of the Ru(IV)-hydride-(hydroxy)vinylidene intermediate **97** (Scheme 32). It is unclear, whether the dehydration of the initial hydroxyl group takes place before or after the hydration (upper or lower route, respectively). The first option would yield the Ru(IV)-allenylidene intermediate **98**, which would be attacked by  $\text{OH}^-$  to obtain **102** after tautomerization of **99**. The attack on  $\alpha$ -carbon is facilitated by weaker back-donation ability of Ru(IV). Late dehydration would occur from the  $\gamma$ -hydroxyacyl complex **101** to form Ru(IV)-acyl **102**. In both cases, reductive elimination liberates the enal (**93**) and recovers the Ru(II) active species.

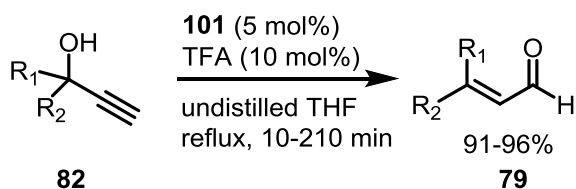


**Scheme 32.** Catalytic cycle for the [RuClCp(PMe<sub>3</sub>)<sub>2</sub>] complex.<sup>64, 65, 66</sup>

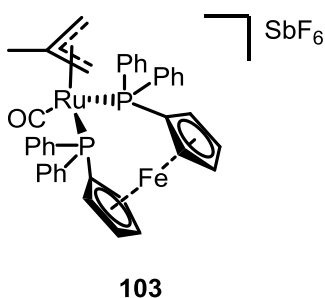
The outcome of the reaction of a propargylic alcohol with Ru depends on solvent, electronic properties of the ligands and substitution on the  $\gamma$ -carbon. The cationic 16 e<sup>-</sup> compound [Ru( $\eta^3$ -2-C<sub>3</sub>H<sub>4</sub>Me)(CO)(dppf)][SbF<sub>6</sub>] (**103**) catalyzed formation of propargylic ethers, when alcohol was acting as a solvent and a nucleophile (Scheme 33).<sup>67, 68, 69</sup> In undistilled THF under reflux, nearly quantitative rearrangement into enals occurred instead. Trifluoroacetic acid improved the catalytic activity. Secondary and tertiary propargylic alcohols were suitable, and thermodynamic *E* products were observed exclusively. Rupe rearrangement occurs if the propargylic alcohol bears a C-H bond in the  $\beta$ -position of the alcohol. Thus, a variety of substrates is excluded. This is a severe drawback of the method, while many other catalysts can suppress the Rupe route. Another fate in absence of water is dehydration and formation of enynes.

The dictating *E* isomer is formed due to the addition of water to the allenylidene complex in a stereoselective manner. The mechanism was suggested the same as the dehydration-hydration mechanism of the Wakatsuki group (see Scheme 32). As the aforementioned half-sandwich Ru-complex yields mostly *E* isomers too, it might be considered to proceed partly through dehydration-

hydration process, and not *vice versa*. A substantial proof for the formation of the Ru-vinylidene complex is the unreactivity of substrates bearing an internal alkyne.



$\text{R}_1 = \text{H, aryl, } t\text{-Bu}$   
 $\text{R}_2 = \text{aryl, } t\text{-Bu}$

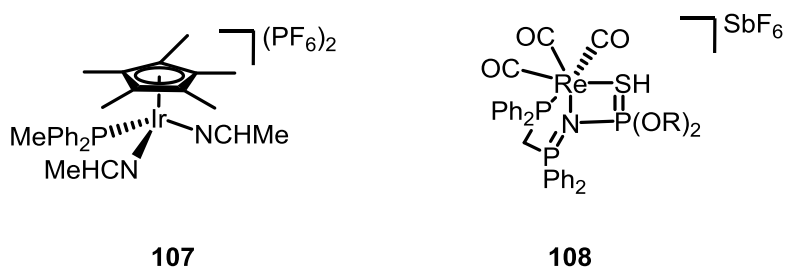
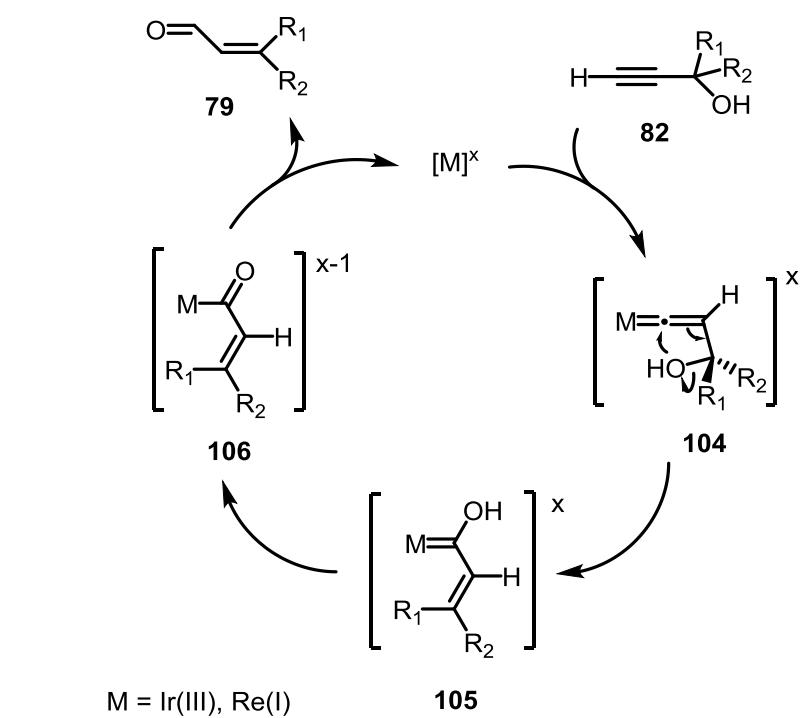


**Scheme 33.** M-S rearrangement with  $\text{Ru}(\eta^3\text{-2-C}_3\text{H}_4\text{Me})(\text{CO})(\text{dppf})[\text{SbF}_6]$  complex.<sup>68</sup>

The  $[\text{Ru}(\eta^3\text{-2-C}_3\text{H}_4\text{Me})(\text{CO})(\text{dppf})][\text{SbF}_6]$  (**103**) complex has been used in tandem isomerization-aldol condensations to construct conjugated dienones and diene-diones,<sup>70, 71</sup> which in turn, were used in the synthesis of dyes.<sup>72</sup>

Finally, a special case of reactivity of internal propargylic alcohols was shown by the Dixneuf group.<sup>73</sup> Instead of a carbene-like structure, possibly a cationic intermediate was formed in the reaction with  $[(p\text{-cymene})\text{Ru}(\text{OTf})(\text{CO})(\text{PCy}_3)][\text{OTf}]$ .

The cationic iridium complex  $[\text{IrCp}^*(\text{NCMe})_2(\text{PPh}_2\text{Me})][\text{PF}_6]_2$  (**107**) catalyzed the M-S reaction of terminal, tertiary propargylic alcohols with excellent yields at room temperature (Scheme 34).<sup>74</sup> At least one phenylic R group was required. No stereoselectivity was noticed. As the reactions were made in anhydrous conditions, previously suggested formation of allenylidene and hydroxyacyl complexes by hydration/dehydration can be ruled out. Instead, intramolecular attack of the OH group at the  $\alpha$  carbon gives a (hydroxy)alkenylcarbene complex (**105**), which tautomerizes into an acyl complex.



**Scheme 34.** Mechanism for Ir and Re-catalyzed M-S rearrangement and structures of the complexes.<sup>74, 75</sup>

Cationic rhenium(I) complexes of type  $[\text{Re}(\kappa^3\text{-}P,N,S\text{-Ph}_2\text{PCH}_2\text{PPh}_2)(\text{CO})_3][\text{SbF}_6]$  (R = Et, Ph) (**108**) catalyze the M-S reaction of terminal secondary and tertiary propargylic alcohols with high yields and *E* selectivity under microwave irradiation (Scheme 34).<sup>75</sup> Also selective Rupe reaction was obtained for compounds bearing a C-H bond in the  $\beta$ -position. The reactions were successful also in the ionic liquid [BMIM][PF<sub>6</sub>] (BMIM = 1-butyl-3-methylimidazolium), enabling recycling of the catalyst up to 10 times.

The reaction mechanism is similar to the mechanism of the Ir catalyst above (see Scheme 34), including formation of the (hydroxy)vinylidene complex, and probable subsequent intramolecular

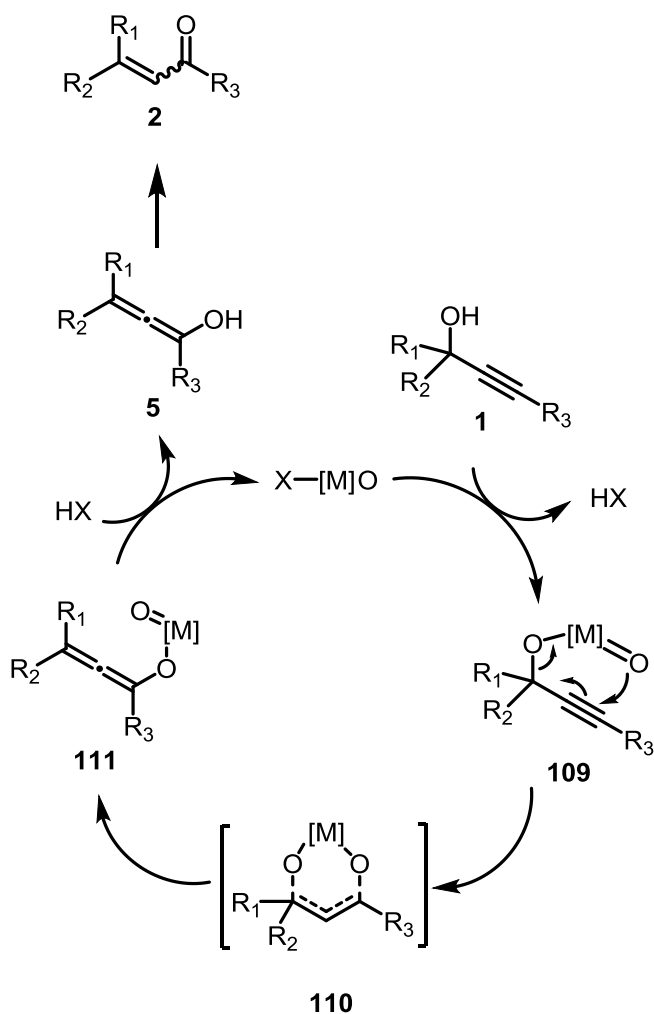
attack of hydroxide. The difference in *E* selectivity between the Ir and Re catalysts remains a mystery.

Ru, Re and Ir complexes catalyze the Meyer-Schuster rearrangement of primary substrates, including one example of secondary substrates. The special mechanistic feature is the formation of metal-allenyldiene or metal-vinylidene intermediate. These catalysts may give good results for aromatic compounds, but the catalytic compounds have to be prepared beforehand.

## 6. Oxo complexes

The first real catalysts for the M-S rearrangement were metal oxides and oxo ligands, which activated the hydroxyl group of propargylic alcohols. Vanadium, rhenium, titanium and molybdenum oxides have shown good selectivity towards M-S rearrangement, but they have traditionally required high temperatures (>100 °C), which causes degradation of substrates and catalysts and, naturally, is not reasonable in terms of green chemistry.<sup>6, 76, 77, 78</sup>

The widely accepted 3,3-rearrangement mechanism is similar to the propargylic acetate rearrangement with gold (Scheme 35; see Scheme 9). A metal-oxo-propargyloxo complex (**109**) is formed by transesterification between a propargylic alcohol and an oxo-metal precatalyst. 3,3-sigmatropic rearrangement yields the allenyl-oxo intermediate (**111**), which donates the metal-oxo group to the next substrate. The resulting allenol (**5**) tautomerizes into an  $\alpha,\beta$ -unsaturated product. It can be noticed that the competing Rupe rearrangement is not possible, when this mechanism is applied, leading to high M-S selectivity.



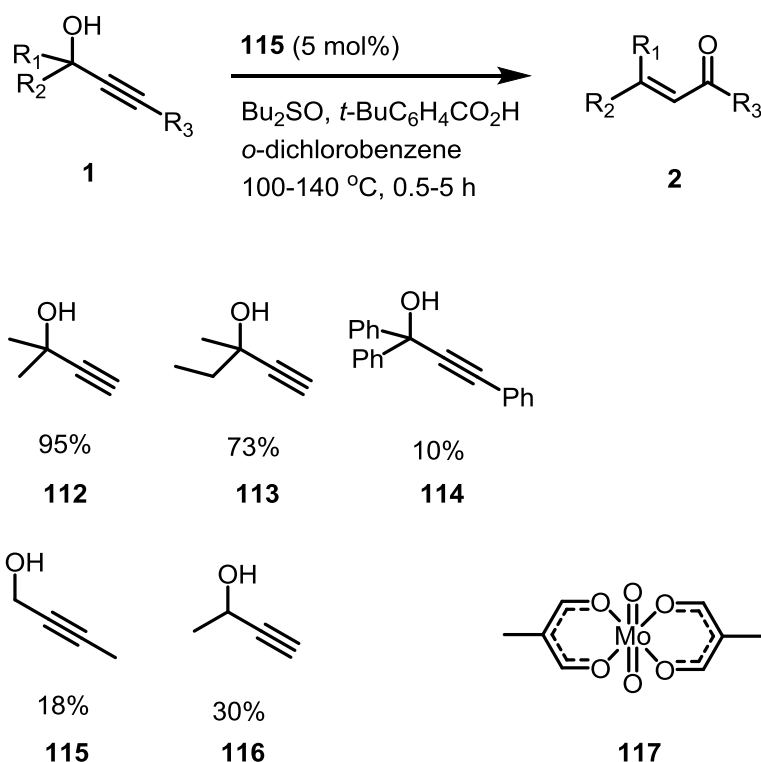
M = V, Mo, Re  
X = halide, alkoxide

**Scheme 35.** General mechanism for oxo-metal complex catalysis.<sup>78</sup>

Vanadium has been used in the form  $\text{VO}(\text{OR})_3$ , but it has suffered from thermal instability.<sup>79, 80</sup> Whether substrate or catalyst-specific, in some cases, it has been possible to run the reaction at 80 °C.<sup>18, 81</sup> Carrillo-Hermosilla and García-Álvarez also made an important improvement to the reactivity of the catalyst by substituting one of the alkoxide groups with chloride.<sup>81</sup> The resulting  $\text{VO}(\text{Cl})(\text{OEt})_2$  has an exhaustive substrate scope of internal and terminal propargylic alcohols, giving yields of 95-99% (20 examples), but no stereoselectivity. The reactions were conducted in toluene under microwave irradiation at 80 °C. The catalyst was used by Alibés in the synthesis of sesquiterpenes.<sup>82</sup>

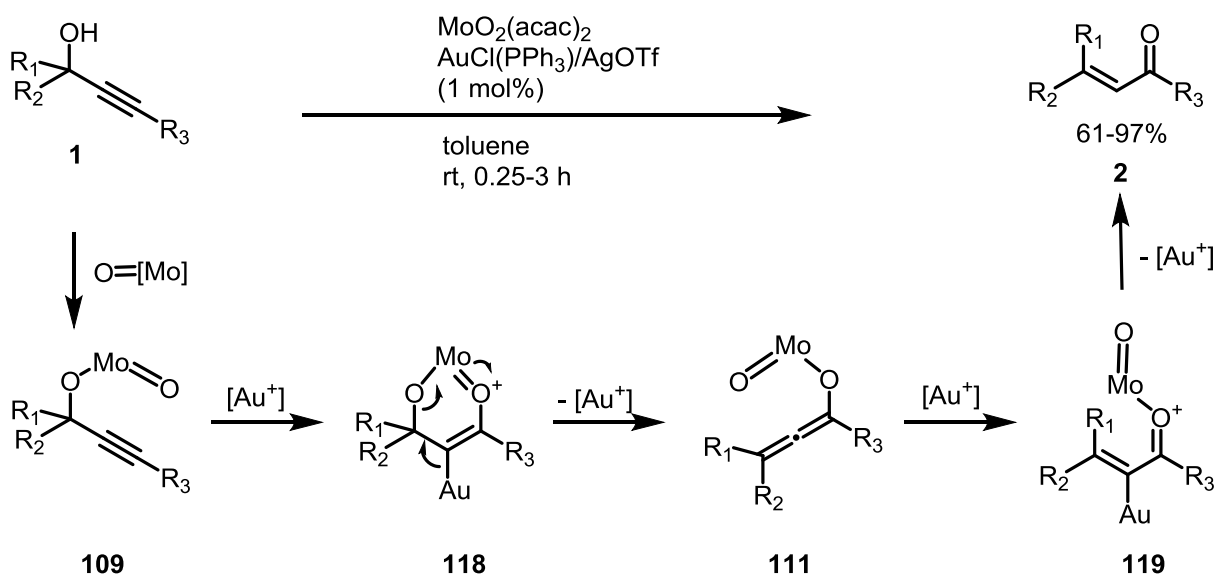
*cis*-dioxomolybdenum(VI) compound needed an additive, preferably a sulfoxide, to catalyze the reaction of tertiary, terminal propargylic alcohols (Scheme 36).<sup>78</sup> Additionally, carboxylic acid

improved the yields notably. The role of the additives remained unclear, but the other oxo ligand was suggested to stabilize the cyclic intermediate **110** (Scheme 35).  $\text{MoO}_2(\text{acac})_2$  gave the best results, although several other ligands worked as well. Despite the stabilizing effect of the cationic intermediate, phenyl-substituted substrate was incompatible, as well as a primary alcohol. The best results gave exceptionally alkyl-substituted, terminal propargylic alcohols. The nucleophilic attack of the oxygen of the metal ester to the triple bond can be less preferred, if the alkyne is connected to electron-donating R groups, such as ethoxide.



**Scheme 36.** Scope of  $\text{MoO}_2(\text{acac})_2$ -catalyzed M-S rearrangement.<sup>78</sup>

A gold catalyst in combination with molybdenum affords great results at room temperature (Scheme 37).<sup>83, 84</sup> The oxomolybdenum complex offers the carbonyl functionality by 1,3-shift, and gold activates the triple bond. The advantages of this method are mild reaction conditions, shortened reaction times and wide scope of substrates: Primary substrates react easily, and even a rare example of an *N*-alkynyl amide rearrangement is offered. The mild reaction conditions have been exploited in the synthesis of (+)-antheicotulide derivatives and platencin.<sup>85, 86, 87</sup>

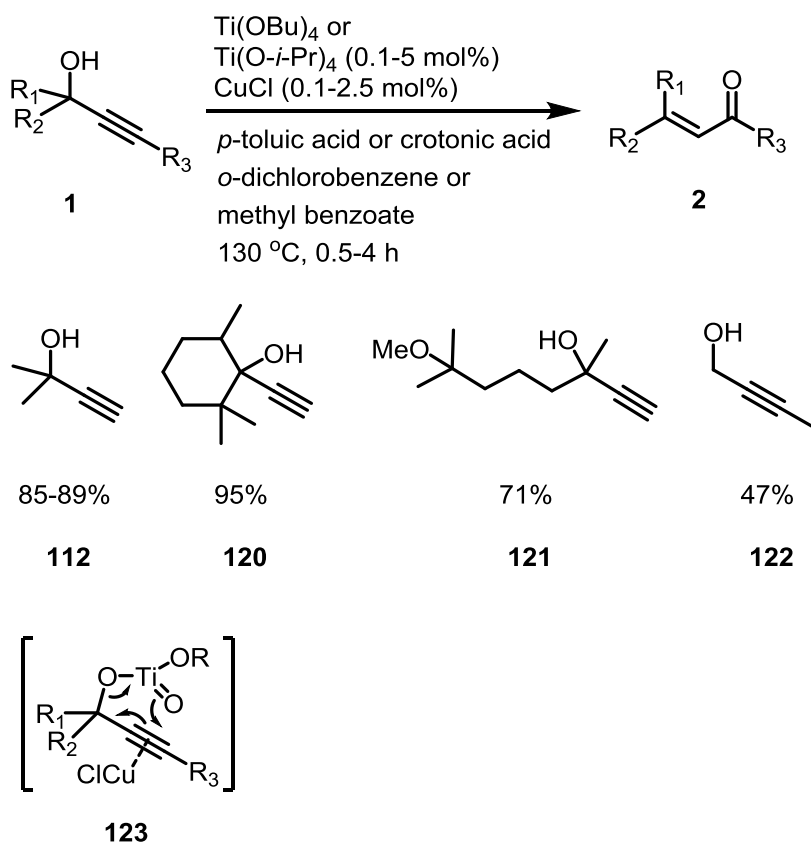


$R_1, R_2 = \text{H, alkyl, aryl}$   
 $R_3 = \text{H, alkyl, aryl, OPh, N(Bn)Ts}$

**Scheme 37.** Reaction scope and mechanism of Mo/Au-catalyzed M-S rearrangement.<sup>83, 84</sup>

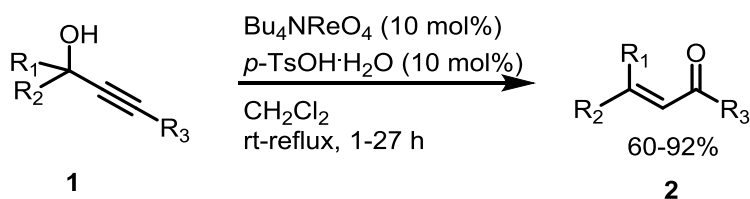
Same kind of coordination is shown by a combination of titanium alkoxide and copper(I) chloride (Scheme 38).<sup>6, 88</sup>  $\text{Ti}(\text{OR})_4$  is activated by carboxylic acid, and it gives a titanium propargyloxo complex with a propargylic alcohol substrate.  $\text{CuCl}$  coordinates with the triple bond and thus activates the complex (**123**) towards 3,3-sigmatropic rearrangement, which yields the  $\alpha,\beta$ -unsaturated carbonyl compound. Again, high temperatures (130 °C) are needed, but the recyclable catalyst system brings benefit. The method seems promising in terms of substrates, as primary and tertiary, internal and terminal propargylic alcohols with alkyl R groups were reactive (4 examples).





**Scheme 38.** M-S rearrangement with Ti/Cu catalyst.<sup>6, 88</sup>

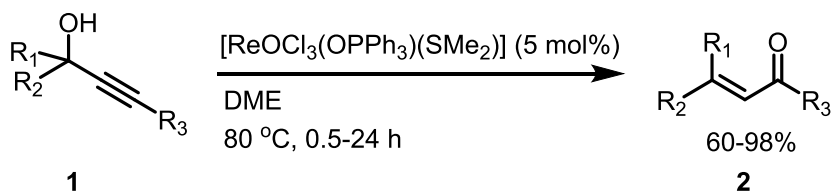
Rhenium(VII) oxide can catalyze the M-S rearrangement in acidic conditions at room temperature (Scheme 39).<sup>89, 90</sup> Tetrabutylammonium perrhenate ( $\text{Bu}_4\text{NReO}_4$ ) with catalytic amount of  $p$ -toluenesulfonic acid hydrate in dichloromethane gave good to excellent yields for tertiary and secondary phenyl-substituted propargylic alcohols, including (trialkylsilyl)alkyne alcohols. Secondary alkyl-substituted alcohols required heating up to accelerate the reaction, and primary substrates only gave a trace of product. Due to its chemoselectivity, perrhenate salt has been used in several total syntheses.<sup>79, 80</sup>



$\text{R}_1 = \text{Ph, Ph(CH}_2\text{)}_2, \text{Bu}$   
 $\text{R}_2 = \text{H, Me}$   
 $\text{R}_3 = \text{H, Bu, Ph, Ph(CH}_2\text{)}_2, \text{SiMe}_3$

**Scheme 39.** Perrhenate-catalyzed M-S rearrangement.<sup>89, 90</sup>

The readily available rhenium(V) complex  $[\text{ReOCl}_3(\text{OPPh}_3)(\text{SMe}_2)]$  has proven to be efficient catalyst for several secondary and tertiary substrates (Scheme 40).<sup>91</sup> Although the reaction proceeds at room temperature, heating up to 80 °C accelerates the rate and improves the yield significantly. Being moderately coordinating, dimethoxyethane turned out to be the most suitable solvent. Reactions have high *E*-selectivity, and complete enantioselectivity can be achieved by prolonged treatment with the catalyst.

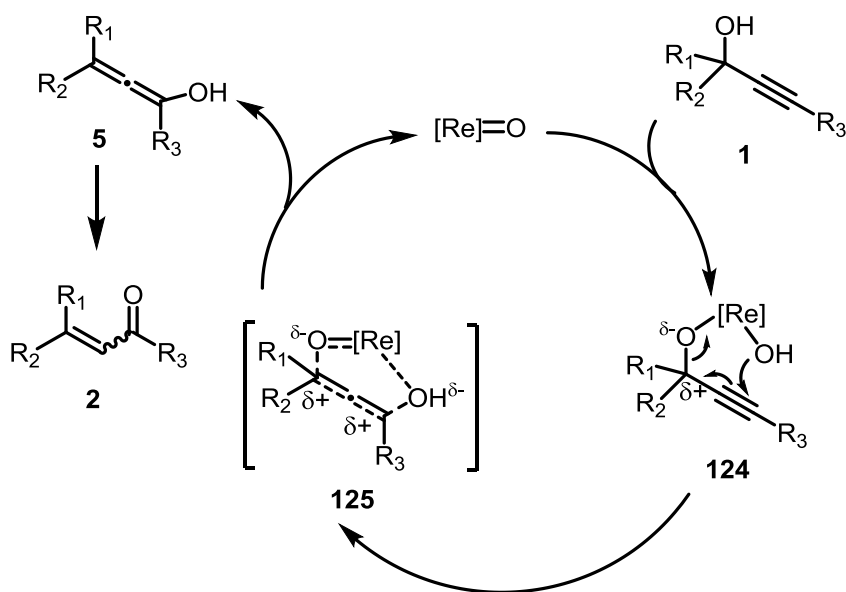


$\text{R}_1 = \text{alkyl, aryl}$   
 $\text{R}_2 = \text{H, Me, Ph}$   
 $\text{R}_3 = \text{H, alkyl, aryl, ester, carboxylic acid}$

**Scheme 40.** M-S rearrangement with  $[\text{ReOCl}_3(\text{OPPh}_3)(\text{SMe}_2)]$ .<sup>91</sup>

The catalyst has shown applicability in tandem reactions, as well.<sup>92, 93, 94</sup> Nolin et al.<sup>92</sup> prepared enantioenriched allylic alcohols by one-pot rearrangement-reduction reaction by addition of chiral ligands into the mixture. They conducted also conjugate addition of thiols into enones to form  $\beta$ -sulfanyl ketones.<sup>93</sup> Vidari and co-workers<sup>94</sup> used the alkynylation-rearrangement route already introduced by Dudley and co-workers<sup>49</sup> to produce enones.

The generally accepted mechanism was supported by labeling tests, but as no free acid was detected in the reaction mixture arising from the chlorine-alkoxy ligand exchange, Stefanoni et al. proposed a modified mechanism (Scheme 41).<sup>91</sup> First, the hydroxyl group of the substrate adds across the Re-oxo bond and, as a consequence, the resulting polarized complex **124** undergoes easily the 1,3-shift. Finally, the resulting allenol structure **5** leads to the enone.



**Scheme 41.** Modified mechanism for  $[ReOCl_3(OPPh_3)(SMe_2)]$ -catalyzed M-S rearrangement.<sup>91</sup>

## 7. Conclusions

As it can be seen, there are no general conditions for the Meyer-Schuster rearrangement. There are some guidelines for the substrate scope and temperature applied, but unfortunately, often one has to apply the “trial and error” approach. Generally, aryl and alkoxy-substituted propargylic alcohols react efficiently. Unactivated *n*-alkyl-substituted substrates tend to be very unreactive or suffer from the Rupe rearrangement. It may be advisable to transform them into acetates, which changes the mechanism applied. This, in turn, weakens the effort to apply only few synthetic steps.

Activation of the hydroxyl group by protonation or with a Lewis acid is a traditional approach for the M-S rearrangement. A wide selection of different metal salts is available, and they are easy to use. The benefit of oxo metals is their high selectivity, but the harsh conditions are not suitable for all the substrates. Also strong Brønsted acids can find their applications in some simple cases.

Recently, the attention has turned to the activation of the triple bond instead of the hydroxyl. As gold catalysis is still a relatively fresh field, new methods and lower catalyst loading may be expected also for the M-S rearrangement. Gold is not as expensive as platinum or palladium, which are used routinely in modern synthesis. Organometal complexes of ruthenium and similar metals would be a great choice for terminal alkynes, but practically these catalysts are not applicable without proficient organometallic chemistry skills.

At the moment, there are few examples of *Z* selectivity,<sup>8, 43</sup> and that is the most challenging theme for the future work. Most probably the selectivity could be developed based on sterically demanding ligands, which allow the electrophile attack on one side only. Additionally, microwave-assisted reactions preferably in water are expected to be seen, following the lead of Cadierno et al.<sup>50</sup> Some characters of the different catalyst groups are collected in Table 1.

**Table 1.** Groups of M-S rearrangement catalysts and their utility.

	Price	Temperature	Special positive feature	Special drawback	Availability	Substrate requirements
Brønsted acids	Cheap	Room temperature to high (>100 °C)	Heteropoly acids are Z selective	Harsh conditions; Rupe rearrangement	Generally very good	Varying; β-hydrogen exposes to the Rupe rearrangement
Gold salts and complexes	Expensive	Room temperature to moderate	Methods for higher <i>E</i> selectivity; Tandem reactions; Gold catalysis under development	Several possible side reactions, but the catalysts are selective	Several available catalysts; Easy preparing methods	Often acetylated or alkoxyated; Also hindered and primary
Other soft Lewis acids (Ag, Hg)	Expensive	Room temperature	Greener CO <sub>2</sub> method by Sugawara et al. <sup>48</sup>	-	Very good	Acetylated, not primary
Metallic hard Lewis Acids	From cheap to expensive	Room temperature to moderate	Convenient to handle	Some salts are rare	Good to very low	Large scope, also primary
Other hard Lewis acids	Affordable	Room temperature to moderate	Mild	Special boronic acid for every substrate	Good	Large scope
Other transition metal complexes	Very expensive	Moderate heating	Tuning of ligands for different substrates	Have to be prepared	Not available	Only terminal (1 exception)
Metal-oxo complexes and oxides	From affordable to expensive	High	Good chemoselectivity; Tandem reactions	High temperature	Good	Large scope

## 8. References

1. Meyer, K. H. and Schuster, K. *Ber. Dtsch. Chem. Ges. (A and B Series)* **1922**, 55 (4), 819-823.
2. Engel, D. A. and Dudley, G. B. *Org. Lett.* **2006**, 8 (18), 4027-4029.
3. Zhu, Y., Sun, L., Lu, P. and Wang, Y. *ACS Catal.* **2014**, 4, 1911-1925.
4. Zhang, L., Fang, G., Kumar, R. K. and Bi, X. *Synthesis* **2015**, 47, 2317-2346.
5. Swaminathan, S. and Narayan, K. V. *Chem. Rev.* **1971**, 71, 429-438.
6. Mercier, C. and Chabardes, P. *Pure Appl. Chem.* **1994**, 66 (7), 1509-1518.
7. Aiken, S., Armitage, B., Gabbutt, C. D. and Heron, B. M. *Tetrahedron Lett.* **2015**, 56, 4840-4842.
8. Egi, M., Umemura, M., Kawai, T. and Akai, S. *Angew. Chem. Int. Ed.* **2011**, 50, 12197-12200.
9. Timofeeva, M. N. *Appl. Catal., A* **2011**, 256, 19-35.
10. Rupe, H. and Kambli, E. *Helv. Chim. Acta* **1926**, 9 (1), 672.
11. Pearson, R. G. *J. Chem. Educ.* **1968**, 45 (9), 581.
12. Sromek, A. W., Rubina, M. and Gevorgyan, V. *J. Am. Chem. Soc.* **2005**, 127, 10500-10501.
13. Georgy, M., Boucard, V. and Campagne, J.-M. *J. Am. Chem. Soc.* **2005**, 127, 14180-14181.
14. Morita, N., Yasuda, A., Shibata, M., Ban, S., Hashimoto, Y., Okamoto, I. and Tamura, O. *Org. Lett.* **2015**, 17, 2668-2671.
15. Kramer, S. and Gagosz, F. in *Gold Catalysis: An Homogeneous Approach.*, Michelet, V. and Toste, F. D., Eds. Imperial College Press: London, 2014; pp 1-49.
16. Yu, M., Li, G., Wang, S. and Zhang, L. *Adv. Synth. Catal.* **2007**, 349, 871-875.
17. Hashmi, A. S. K. and Hutchings, G. J. *Angew. Chem. Int. Ed.* **2006**, 45, 7896-7936.
18. Rieder, C. J., Winberg, K. J. and West, F. G. *J. Org. Chem.* **2010**, 76, 50-56.
19. Lopez, S. S., Engel, D. A. and Dudley, G. B. *Synlett* **2007**, 6, 0949-0953.
20. Marion, N. and Nolan, S. P. *Angew. Chem. Int. Ed.* **2007**, 46, 2750-2752.

21. Zhang, L. and Wang, S. *J. Am. Chem. Soc.* **2006**, *128*, 1442-1443.
22. Wang, S. and Zhang, L. *J. Am. Chem. Soc.* **2006**, *128*, 8414-8415.
23. Yu, M., Zhang, G. and Zhang, L. *Org. Lett.* **2007**, *9* (11), 2147-2150.
24. Zanoni, G., D'Alfonso, A., Porta, A., Feliciani, L., Nolan, S. P. and Vidari, G. *Tetrahedron* **2010**, *66*, 7472-7478.
25. Pennell, M. N., Unthank, M. G., Turner, P. and Sheppard, T. D. *J. Org. Chem.* **2011**, *76*, 1479-1482.
26. Pennell, M. N., Turner, P. G. and Sheppard, T. D. *Chem. Eur. J.* **2012**, *18*, 4748-4758.
27. Mou, X.-Q., Xu, Z.-L., Wang, S.-H., Zhu, D.-Y., Wang, J., Bao, W., Zhou, S.-J., Yanga, C. and Zhang, D. *Chem. Commun.* **2015**, 51.
28. Lee, S. I., Baek, J. Y., Sim, S. H. and Chung, Y. K. *Synthesis* **2007**, *14*, 2107-2114.
29. Ramón, R. S., Marion, N. and Nolan, S. P. *Tetrahedron* **2009**, *65*, 1767-1773.
30. Kim, S. M., Lee, D. and Hong, S. H. *Org. Lett.* **2014**, *16*, 6168-6171.
31. Um, J., Yun, H. and Shin, S. *Org. Lett.* **2016**, *18*, 484-487.
32. Tlahuext-Aca, A., Hopkinson, M. N., Garza-Sanchez, R. A. and Glorius, F. *Chem. Eur. J.* **2016**, *22*, 5909-5913.
33. Marion, N., Carlqvist, P., Gealageas, R., Frémont, P. d., Maseras, F. and Nolan, S. P. *Chem. Eur. J.* **2007**, *13*, 6437-6451.
34. Ramón, R. S., Gaillard, S., Slawin, A. M. Z., Porta, A., D'Alfonso, A., Zanoni, G. and Nolan, S. P. *Organometallics* **2010**, *29*, 3665-3668.
35. Gaillard, S., Bosson, J., Ramón, R. S., Nun, P., Slawin, A. M. Z. and Nolan, S. P. *Chem. Eur. J.* **2010**, *16*, 13729-13740.
36. Correa, A., Marion, N., Fensterbank, L., Malacria, M., Nolan, S. P. and Cavallo, L. *Angew. Chem. Int. Ed.* **2008**, *47*, 718-721.
37. Beretta, R., Giambelli-Gallotti, M., Pennè, U., Porta, A., Gil-Romero, J. F., Zanoni, G. and Vidari, G. *J. Org. Chem.* **2015**, *80* (3), 1601-1609.
38. Bugoni, S., Boccato, D., Porta, A., Zanoni, G. and Vidari, G. *Chem. Eur. J.* **2015**, *21*, 791-799.

39. Merlini, V., Gaillard, S., Porta, A., Zanoni, G., Vidari, G. and Nolan, S. P. *Tetrahedron Lett.* **2011**, *52*, 1124-1127.
40. de Haro, T. and Nevado, C. *Chem. Commun.* **2011**, *47*, 248-249.
41. Hansmann, M. M., Hashmi, A. S. K. and Lautens, M. *Org. Lett.* **2013**, *15* (13), 3226-3229.
42. Duan, H., Sengupta, S., Petersen, J. L., Akhmedov, N. G. and Shi, X. *J. Am. Chem. Soc.* **2009**, *131*, 12100-12102.
43. Wang, D., Ye, X. and Shi, X. *Org. Lett.* **2010**, *12* (9), 2088-2091.
44. Wang, D., Zhang, Y., Harris, A., Gautam, L. N. S., Chen, Y. and Shi, X. *Adv. Synth. Catal.* **2011**, *353*, 2584-2588.
45. Chen, Y., Yan, W., Akhmedov, N. G. and Shi, X. *Org. Lett.* **2010**, *12* (2), 344-347.
46. Nishizawa, M., Hirakawa, H., Nakagawa, Y., Yamamoto, H., Namba, K. and Imagawa, H. *Org. Lett.* **2007**, *9* (26), 5577-5580.
47. Imagawa, H., Asai, Y., Takano, H., Hamagaki, H. and Nishizawa, M. *Org. Lett.* **2006**, *8* (3), 447-450.
48. Sugawara, Y., Yamada, W., Yoshida, S., Ikeno, T. and Yamada, T. *J. Am. Chem. Soc.* **2007**, *129*, 12902-12903.
49. Engel, D. A., Lopez, S. S. and Dudley, G. B. *Tetrahedron* **2008**, *64*, 6988-6996.
50. Cadierno, V., Francos, J. and Gimeno, J. *Tetrahedron Lett.* **2009**, *50*, 4773-4776.
51. Kappe, C. O., Stadler, A. and Dallinger, D., *Microwave Theory*. 2 ed.; Wiley-VCH Verlag GmbH & Co. KGaA: Weinheim, 2012; p 9-39.
52. Liu, W., Wang, H., Zhao, H., Li, B. and Chen, S. *Synlett* **2015**, *26*, 2170-2174.
53. Hao, L., Wu, F., Ding, Z.-C., Xu, S.-X., Ma, Y.-L., Chen, L. and Zhan, Z.-P. *Chem. Eur. J.* **2012**, *18*, 6453-6456.
54. Alcaide, B., Almendros, P. and Quirós, M. T. *Adv. Synth. Catal.* **2011**, *353*, 585-594.
55. el Douhaibi, A. S., Judeh, Z. M. A., Basri, H., Moussa, Z., Messali, M. and Qi, G. *Synth. Commun.* **2011**, *41* (4), 533-540.
56. Passet, M., Michelet, B., Guillot, R., Bour, C., Bezenine-Lafollée, S. and Gandon, V. *Chem. Commun.* **2015**, *51*.



57. Begouin, J.-M. and Niggemann, M. *Chem. Eur. J.* **2013**, *19*, 8030-8041.
58. Okamoto, N., Sueda, T. and Yanada, R. *J. Org. Chem.* **2014**, *79*, 9854-9859.
59. Zheng, H., Lejkowski, M. and Hall, D. G. *Chem. Sci.* **2011**, *2*, 1305-1310.
60. Crich, D., Natarajan, S. and Crich, J. Z. *Tetrahedron* **1997**, *53* (21), 7139-7158.
61. Bruneau, C. and Dixneuf, P. H. *Chem. Commun.* **1997**, 507-512.
62. Picquet, M., Bruneau, C. and Dixneuf, P. H. *Chem. Commun.* **1997**, 1201-1202.
63. Picquet, M., Fernández, A., Bruneau, C. and Dixneuf, P. H. *Eur. J. Org. Chem.* **2000**, 2361-2366.
64. Suzuki, T., Tokunaga, M. and Wakatsuki, Y. *Tetrahedron Lett.* **2002**, *43*, 7531-7533.
65. Tokunaga, M. and Wakatsuki, Y. *Angew. Chem. Int. Ed.* **1998**, *37* (20), 2867-2869.
66. Tokunaga, M., Suzuki, T., Koga, N., Fukushima, T., Horiuchi, A. and Wakatsuki, Y. *J. Am. Chem. Soc.* **2001**, *123*, 11917-11924.
67. Cadierno, V., Díez, J., García-Garrido, S. E. and Gimeno, J. *Chem. Commun.* **2004**, 2716-2717.
68. Cadierno, V., García-Garrido, S. E. and Gimeno, J. *Adv. Synth. Catal.* **2006**, *348*, 101-110.
69. Cadierno, V., Crochet, P. and Gimeno, J. *Synlett* **2008**, *8*, 1105-1124.
70. Onodera, G., Matsumoto, H., Nishibayashi, Y. and Uemura, S. *Organometallics* **2005**, *24*, 5799-5801.
71. Cadierno, V., Díez, J., García-Garrido, S. E., Gimeno, J. and Nebra, N. *Adv. Synth. Catal.* **2006**, *348*, 2125-2132.
72. Borge, J., Cadierno, V., Díez, J., García-Garrido, S. E. and Gimeno, J. *Dyes Pigments* **2010**, *87*, 209-217.
73. Bustelo, E. and Dixneuf, P. H. *Adv. Synth. Catal.* **2007**, *349*, 933-942.
74. Talavera, M., Bravo, J., Gonsalvi, L., Peruzzini, M., Zuccaccia, C. and Bolaño, S. *Eur. J. Inorg. Chem.* **2014**, 6268-6274.
75. García-Álvarez, J., Díez, J., Gimeno, J. and Seifried, C. M. *Chem. Commun.* **2011**, *47*, 6470-6472.

76. Pauling, H., Andrews, D. A. and Hindley, N. C. *Helv. Chim. Acta* **1976**, *59*, 1233-1243.
77. Chabardes, P., Kuntz, E. and Varagnat, J. *Tetrahedron* **1977**, *33*, 1775-1783.
78. Lorber, C. Y. and Osborn, J. A. *Tetrahedron Lett.* **1996**, *37* (6), 853-856.
79. Engel, D. A. and Dudley, G. B. *Org. Biomol. Chem.* **2009**, *7*, 4149-4158.
80. Cadierno, V., Crochet, P., García-Garrido, S. E. and Gimeno, J. *Dalton Trans.* **2010**, *39*, 4015-4031.
81. Antiñolo, A., Carrillo-Hermosilla, F., Cadierno, V., García-Álvarez, J. and Otero, A. *ChemCatChem* **2012**, *4*, 123-128.
82. Parés, S., Alibés, R., Figueredo, M., Font, J. and Parella, T. *Eur. J. Org. Chem.* **2012**, 1404-1417.
83. Egi, M., Yamaguchi, Y., Fujiwara, N. and Akai, S. *Org. Lett.* **2008**, *10* (9), 1867-1870.
84. Ye, L. and Zhang, L. *Org. Lett.* **2009**, *11* (16), 3646-3649.
85. Hodgson, D. M., Talbot, E. P. A. and Clark, B. P. *Org. Lett.* **2011**, *13* (21), 5751-5753.
86. Hodgson, D. M., Talbota, E. P. A. and Clark, B. P. *Chem. Commun.* **2012**, *48*, 6349-6350.
87. Wang, J., Sun, W.-B., Li, Y.-Z., Wang, X., Sun, B.-F., Lina, G.-Q. and Zou, J.-P. *Org. Chem. Front.* **2015**, *2*, 674-676.
88. Lorber, C. Y., Youinou, M.-T., Kress, J. and Osborn, J. A. *Polyhedron* **2000**, *19*, 1693-1698.
89. Narasaka, K., Kusama, H. and Hayashi, Y. *Chem. Lett.* **1991**, 1413-1416.
90. Narasaka, K., Kusama, H. and Hayashi, Y. *Tetrahedron* **1992**, *48* (11), 2059-2068.
91. Stefanoni, M., Luparia, M., Porta, A., Zanoni, G. and Vidari, G. *Chem. Eur. J.* **2009**, *15*, 3940-3944.
92. Nolin, K. A., Ahn, R. W., Kobayashi, Y., Kennedy-Smith, J. J. and Toste, F. D. *Chem. Eur. J.* **2010**, *16*, 9555-9562.
93. Garst, A. E., Badiceanu, A. D. and Nolin, K. A. *Tetrahedron Lett.* **2013**, *54*, 459-461.
94. Mattia, E., Porta, A., Merlini, V., Zanoni, G. and Vidari, G. *Chem. Eur. J.* **2012**, *18*, 11894-11898.

## II. EXPERIMENTAL PART

### Synthesis of potential FtsZ inhibitors

## Contents of the second part

### II. EXPERIMENTAL PART

Synthesis of potential FtsZ inhibitors

Abbreviations

1. Background and aim of the work	1
2. Results	4
2.1 Design and preparation of the inhibitors	4
2.2 Synthesis of compounds of Set I	5
2.3 Synthesis of compounds of Set II	7
2.4 Synthesis of compounds of Set III	13
2.5 Biological evaluation	16
3. Conclusions	19
4. Experimental methods	20
4.1 Set I	21
4.2 Set II	27
4.3 Set III	35
3.4 Biological evaluation	37
5. References	38
6. Appendix	

## Abbreviations

3-MBA	3-methoxybenzamide
4-DPPBA	4-diphenylphosphinobenzoic acid
AIBN	azobisisobutyronitrile
BS-FtsZ	<i>Bacillus subtilis</i> FtsZ
dansyl	(dimethylamino)naphthalene-1-sulfonyl
dba	dibenzylideneacetone
DCM	dichloromethane
DMF	dimethylformamide
ESI	electrospray ionization
Et	ethyl
FtsZ	filamenting temperature-sensitive mutant Z
GDP	guanosine 5'-diphosphate
GMPCPP	guanosine 5'-[( $\alpha,\beta$ )-methylene]triphosphate
GTP	guanosine 5'-triphosphate
HPLC	high performance liquid chromatography
IR	infrared
Me	methyl
MS	mass spectrometry
NBD	nitrobenzoxadiazole
NBS	<i>N</i> -bromosuccinimide
Ph	phenyl
PS	polystyrene
TLC	thin-layer chromatography

## 1. Background and aim of the work

FtsZ (filamenting temperature-sensitive mutant Z) is a bacterial homologue for eucaryotic tubulin.<sup>1</sup> This widely conserved GTPase has an essential role in bacterial cell division and has recently been proposed as an attractive target for antibacterial drug discovery.

The function of FtsZ and the bacterial cell division have been reviewed by Errington and Lutkenhaus.<sup>2, 3</sup> FtsZ exists in the bacterial cells as both monomers and highly ordered polymers, depending on whether it is bound to guanosine 5'-triphosphate (GTP) or guanosine 5'-diphosphate (GDP). At the earliest step of cell division, it undergoes self-assembly of individual subunits at the mid-cell, and GTP-binding promotes the FtsZ polymerization by head-to-tail association. On the contrary, when GTP is hydrolyzed to GDP, the protofilament adapts a curved conformation and disintegrates. The protofilaments polymerize in different shaped filaments leading to the formation of Z-ring, which is a highly dynamic structure with a half-time of a few seconds. Several other division proteins are then recruited to regulate and form the divisome, a complex that finally constricts to generate two new daughter cells.

FtsZ is a tempting target for antibiotics, as it is the principal protein in Z-ring formation and cytokinesis. Over the last decade, several compounds have been identified as FtsZ inhibitors perturbing the protein polymerization and the GTPase activity. Schaffner-Barbero et al. and Li et al. have reviewed groups of molecules with antimicrobial activity based on FtsZ.<sup>4, 5</sup>

The biggest contribution to the synthetic FtsZ inhibitors came from the development of 3-methoxybenzamide (3-MBA) derivatives. Ohashi et al. found out that 3-MBA (Figure 1) inhibits weakly cell division in *Bacillus subtilis in vitro*.<sup>6</sup> Based on this finding, Haydon et al. screened through more than 500 benzamide analogs.<sup>7</sup> They found out that a compound PC190723 and its derivative 8J (Figure 1) are potent inhibitors of staphylococci and *Bacillus subtilis in vitro*.<sup>7, 8</sup>

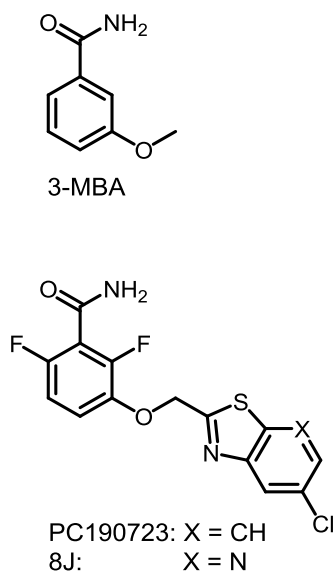


**Figure 1.** Structures of 3-MBA, PC190723 and 8J.

The crystal structure of *S. aureus* FtsZ-GDP in complex with PC190723 has been reported (Figure 2).<sup>9</sup> PC190723 binds to a narrow pocket in FtsZ formed by the C-terminal half of the H7 helix, the T7 loop and the C-terminal four-stranded  $\beta$ -sheet. The difluorobenzamide substituent fits into the top portion of the cleft by directly interacting with the T7 loop. The chlorine at the lipophilic end enters into a hydrophobic tunnel formed by two residues from the H7 helix (Gln<sup>192</sup> and Gly<sup>193</sup>) and two from the C-terminal  $\beta$ -sheet (Met<sup>226</sup> and Ile<sup>228</sup>). The tunnel leads to a wide pocket, which could be structurally mapped to the equivalent of tubulin's taxol-binding site.

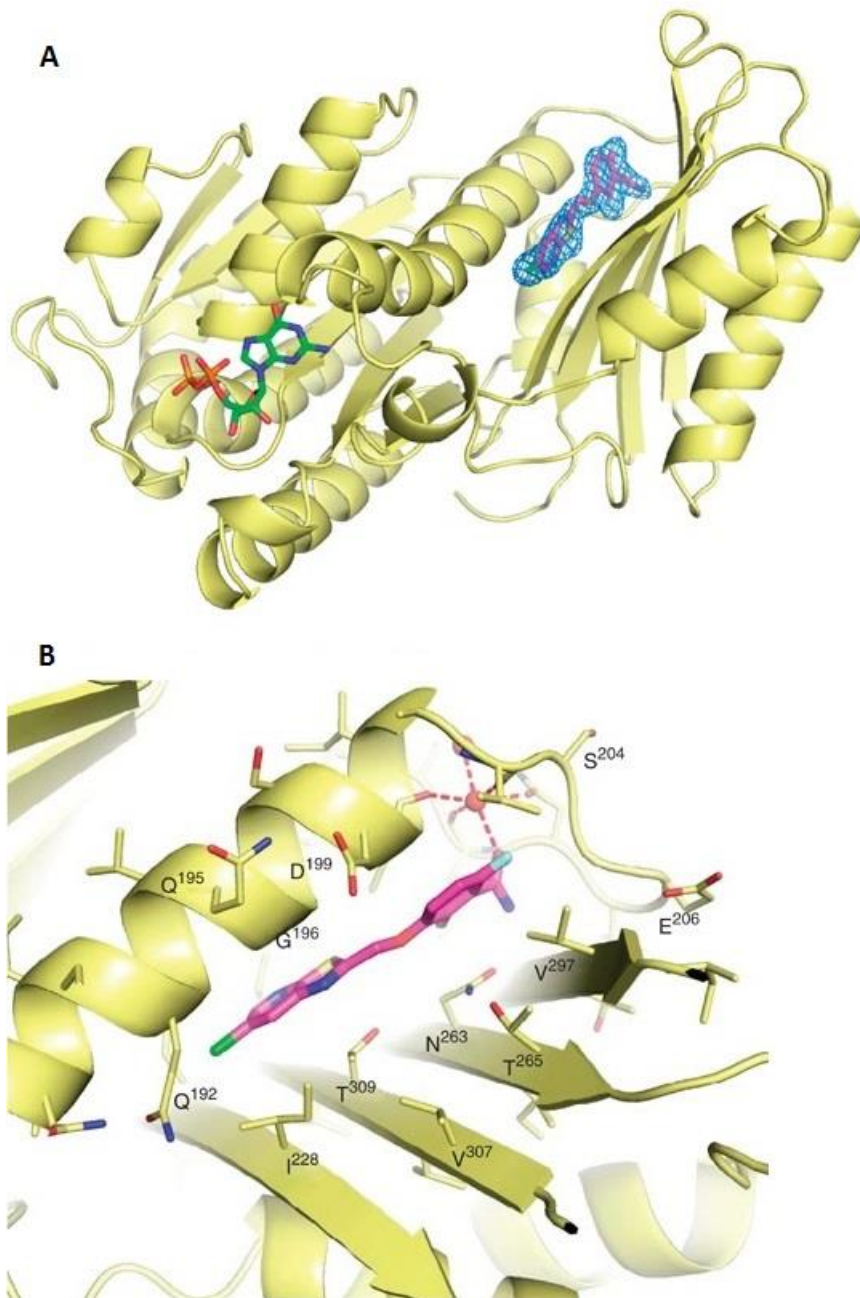


**Figure 2. A:** Structure of FtsZ protein of *S. Aureus* with PC190723 (in magenta) and GDP (green). **B:** Detailed view of the PC190723-binding pocket.<sup>9</sup> (Reprinted with permission of The American Association for the Advancement of Science.)

PC190723 acts as an FtsZ polymer-stabilizing agent that modulates the flexibility and the assembly of the protein.<sup>10</sup> It triggers a conformational change in which the H7 helix and the C-terminal domain move away from the N-terminal domain in the presence of GDP. The forming linear protofilament encloses GDP, which prevents dissociation of the filament.



The antibacterial activity of PC190723 seems to be caused by its 2,6-difluoro-3-hydroxybenzamide (DFMBA) moiety.<sup>11</sup> The compound inhibits the GTPase activity at 10  $\mu$ M and has been characterized as a potent selective bactericide. Notably, it is the first inhibitor shown to be efficacious in an *in vivo* model of bacterial infection.<sup>7</sup> In this context, the Medical Chemistry Laboratory led by Prof. M. Luz López-Rodríguez started a project aimed at the discovery of FtsZ inhibitors targeting the GTP-binding pocket and the PC190723 binding site. The present research project was focused on the last one, and the main objective was the design and synthesis of a set of fluorescent derivatives of inhibitors PC190723 and 8J, which could be used to obtain information about the interactions between the inhibitors and the protein.

## 2. Results

### 2.1 Design and preparation of the inhibitors

The design of the compounds was started based on the structure of PC190723/8J and the previous work done by the research group. Thus, three sets of fluorescent derivatives that contain the DFMBA subunit were designed following three approaches (Figure 3): i) the replacement of the heterocyclic subunit of PC190723/8J by a fluorescent tag (Set I); ii) the attachment of a fluorophore through a spacer at position 5 of the benzothiazole of 8J, replacing the chlorine atom (Set II); iii) the attachment of the fluorescent tag to the position 6 of the benzothiazole using an amino group as bonding group (Set III). The selected fluorophores were a coumarin, dansyl (5-(dimethylamino)naphthalene-1-sulfonyl) and nitrobenzoxadiazole (NBD).

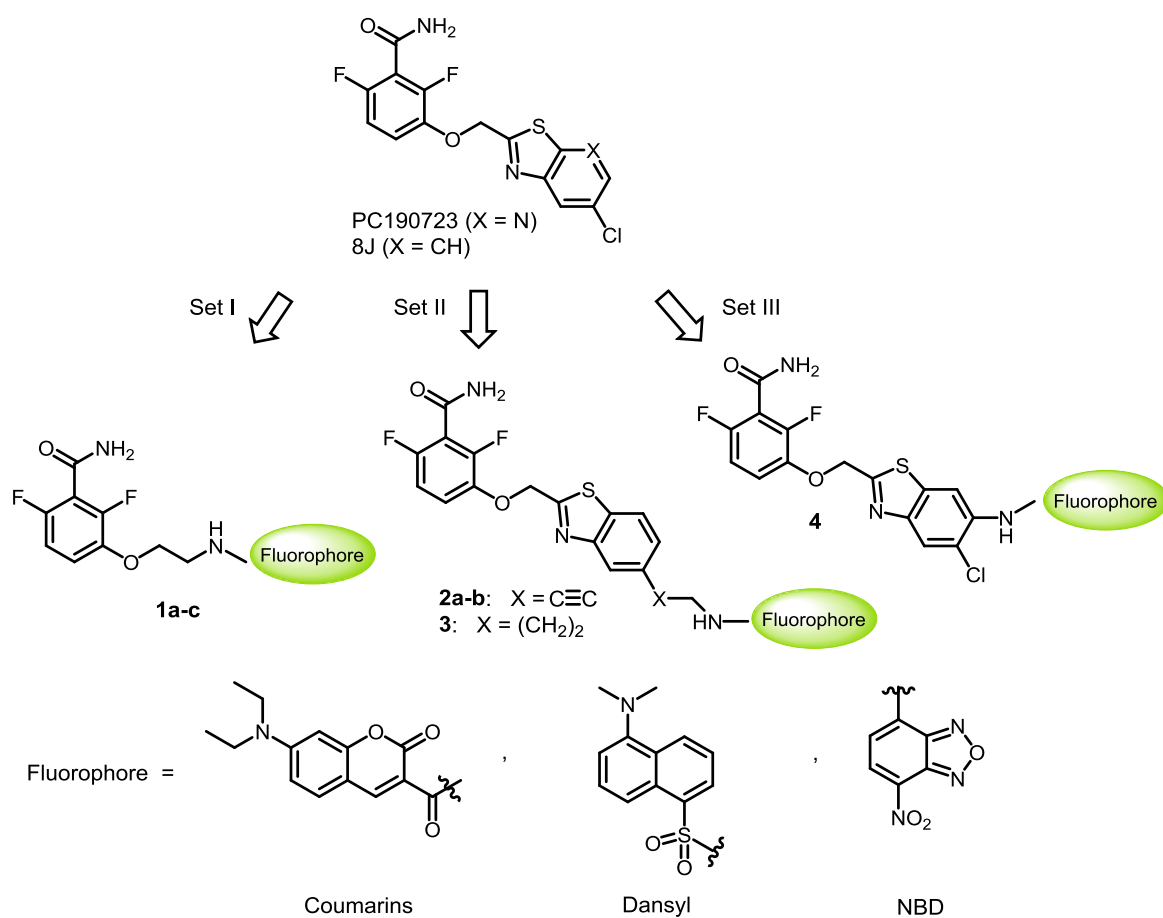


**Figure 3.** Designed Sets I-III of fluorescent derivatives based on PC190723 and 8J.

## 2.2 Synthesis of compounds of Set I

Regarding the first set of fluorescent compounds, the heterocyclic subunit of PC190723/8J was replaced by a fluorophore and an ethyl chain bearing an amino group as attachment point was used as a spacer. The retrosynthetic analysis is presented in the Figure 4.

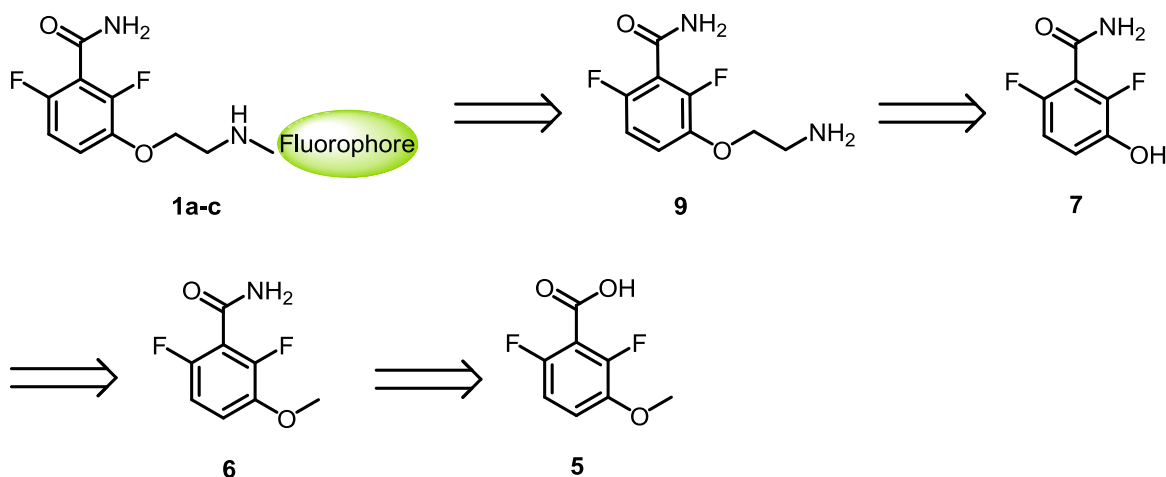
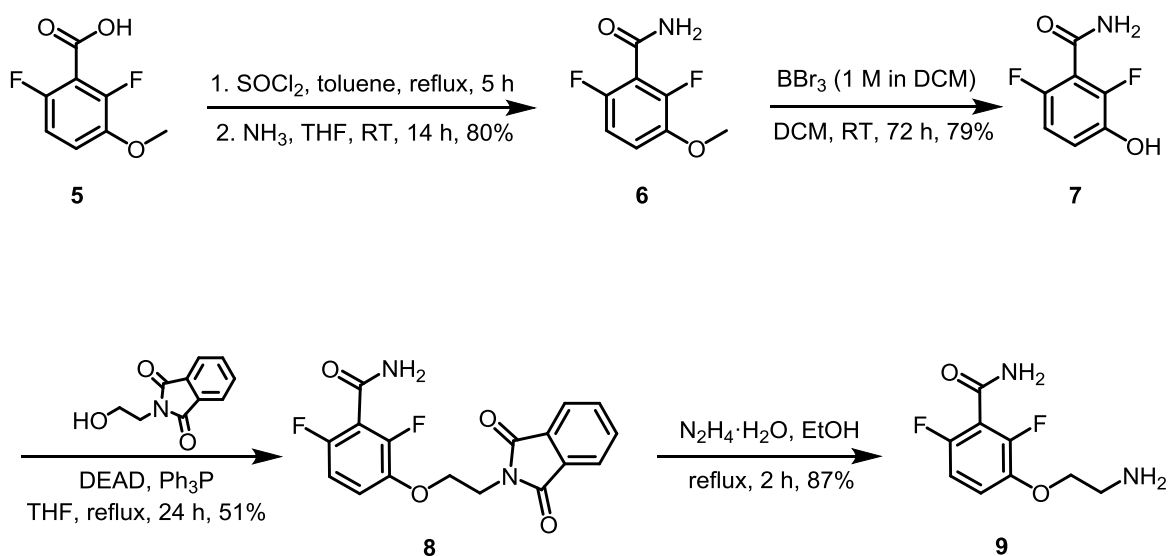
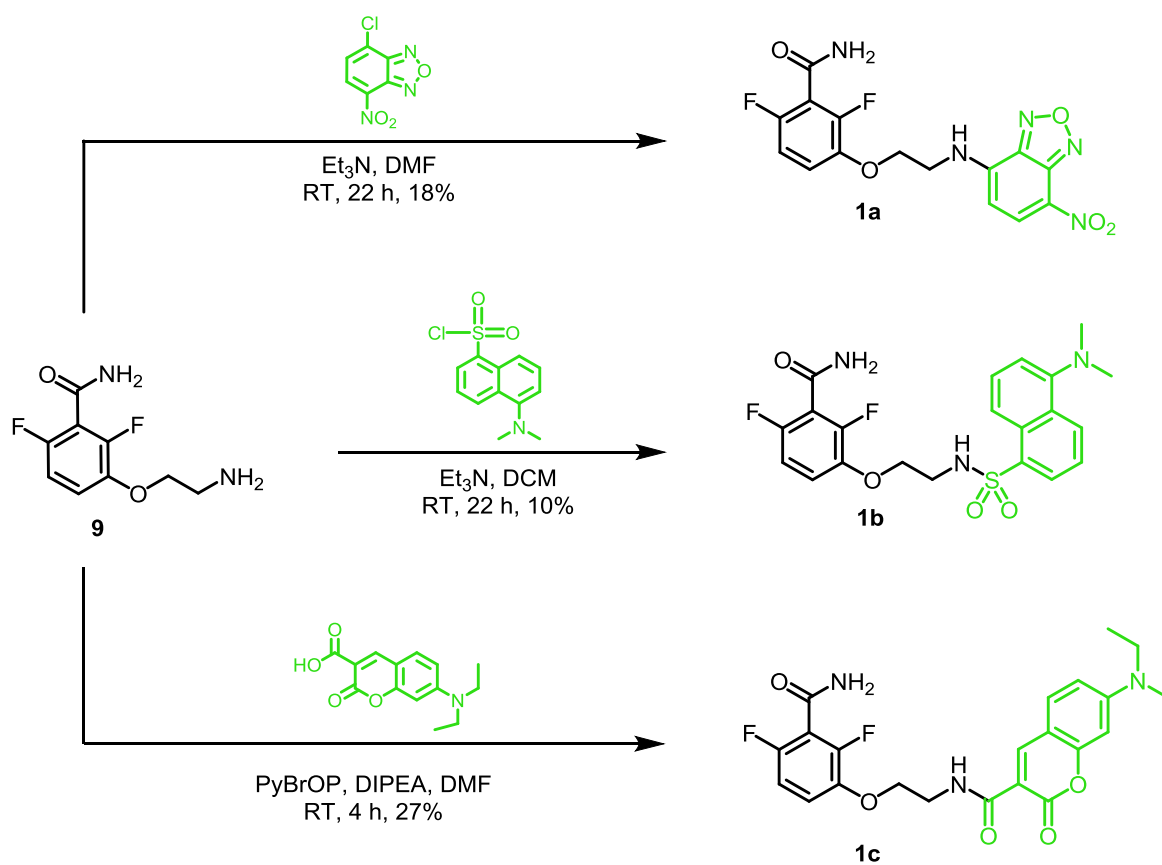


**Figure 4.** Retrosynthetic analysis for Set I compounds.

The commercially available 2,6-difluoro-3-methoxybenzoic acid (**5**) was first converted into its corresponding amide (**6**) via acid chloride (Scheme 1). Then, the methoxy group was deprotected with boron tribromide, and Mitsunobu reaction of the resulting phenol (**7**) with hydroxyethylphthalimide followed by removal of the protecting group afforded the corresponding amine (**9**). This 3-(2-aminoethoxy)-2,6-difluorobenzamide was further treated with Cl-NBD, dansyl chloride or 7-diethylaminocoumarin-3-carboxylic acid using the appropriate coupling-reaction conditions to afford the NBD (**1a**), dansyl (**1b**) and coumarin (**1c**) derivatives, respectively (Scheme 2).



**Scheme 1.** Synthesis of intermediate **9**.



**Scheme 2.** Syntheses of fluorescent compounds **1a-c**.

### 2.3 Synthesis of compounds of Set II

The compounds of Set II were constructed by attachment of the fluorophore to the position 5 of the benzothiazole ring of **8J** by replacement of the chlorine atom and using an aliphatic spacer. The route for Set II compounds was adapted from Haydon et al.<sup>8</sup> and Sorto et al.<sup>12</sup>, and the retrosynthetic analysis is shown on Figure 5.

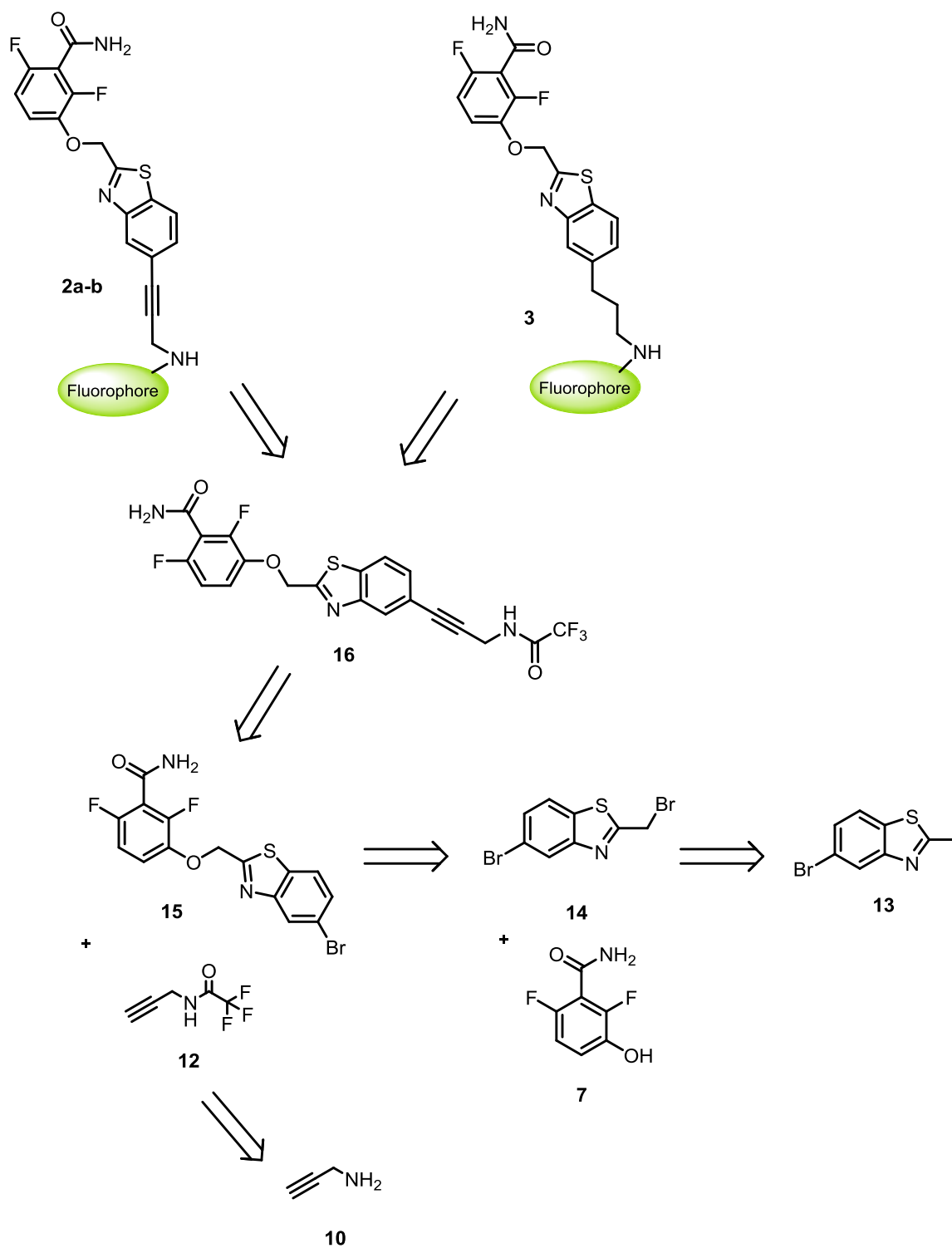
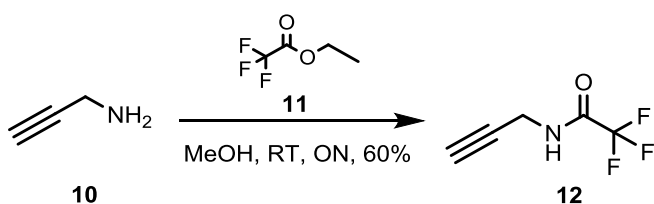


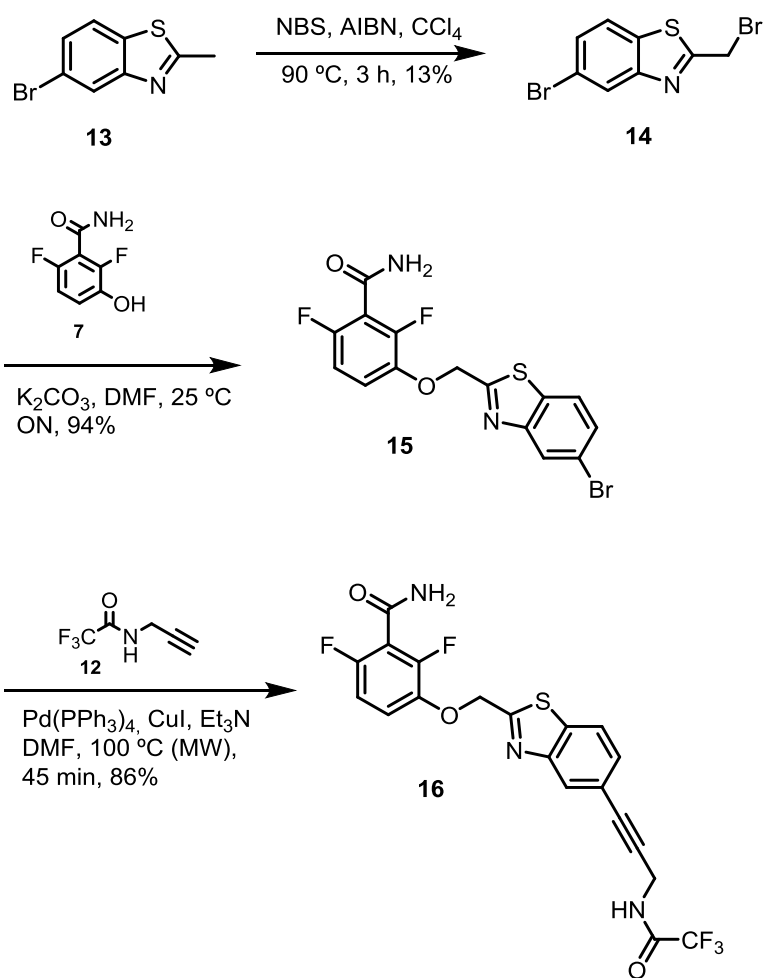
**Figure 5.** Retrosynthetic analysis for Set II.

The first task was to synthesize the *N*-protected intermediate amine **12** by reaction of propargylamine (**10**) with ethyl trifluoroacetate (**11**) (Scheme 3).



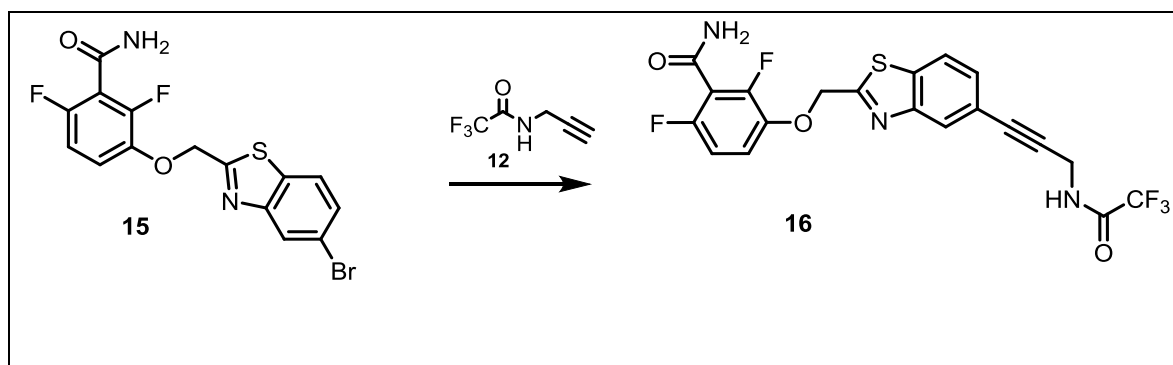
**Scheme 342.** Synthesis of *N*-protected amine **12**.

Commercial 5-bromo-2-methylbenzothiazole (**13**) was brominated with *N*-bromosuccinimide (NBS) in the presence of azobisisobutyronitrile (AIBN), followed by Williamson alkylation of intermediate **14** with 2,6-difluoro-3-hydroxybenzamide (**7**) to afford derivative **15** (Scheme 4).<sup>8</sup> Next, Sonogashira coupling reaction of **15** with 2,2,2-trifluoro-*N*-(prop-2-ynyl)acetamide (**12**) was explored under microwave conditions (Table 1 and Scheme 4). Carbon-supported palladium (Pd/C) and 4-diphenylphosphinobenzoic acid (4-DPPBA) were firstly tested as catalytic system and unfortunately yielded no product. The coupling reaction was then tried with dipalladium-tris(dibenzylideneacetone)chloroform complex [Pd<sub>2</sub>(dba)<sub>3</sub>·CHCl<sub>3</sub>] and polystyrene-supported triphenylphosphine (PS-PPh<sub>3</sub>) affording the desired compound **16** with 54% yield. Finally, the use of tetrakis(triphenylphosphine)palladium [(PPh<sub>3</sub>)<sub>4</sub>Pd] as catalyst yielded derivative **16** with high yield (86%).



**Scheme 4.** Synthesis of intermediate **16**.

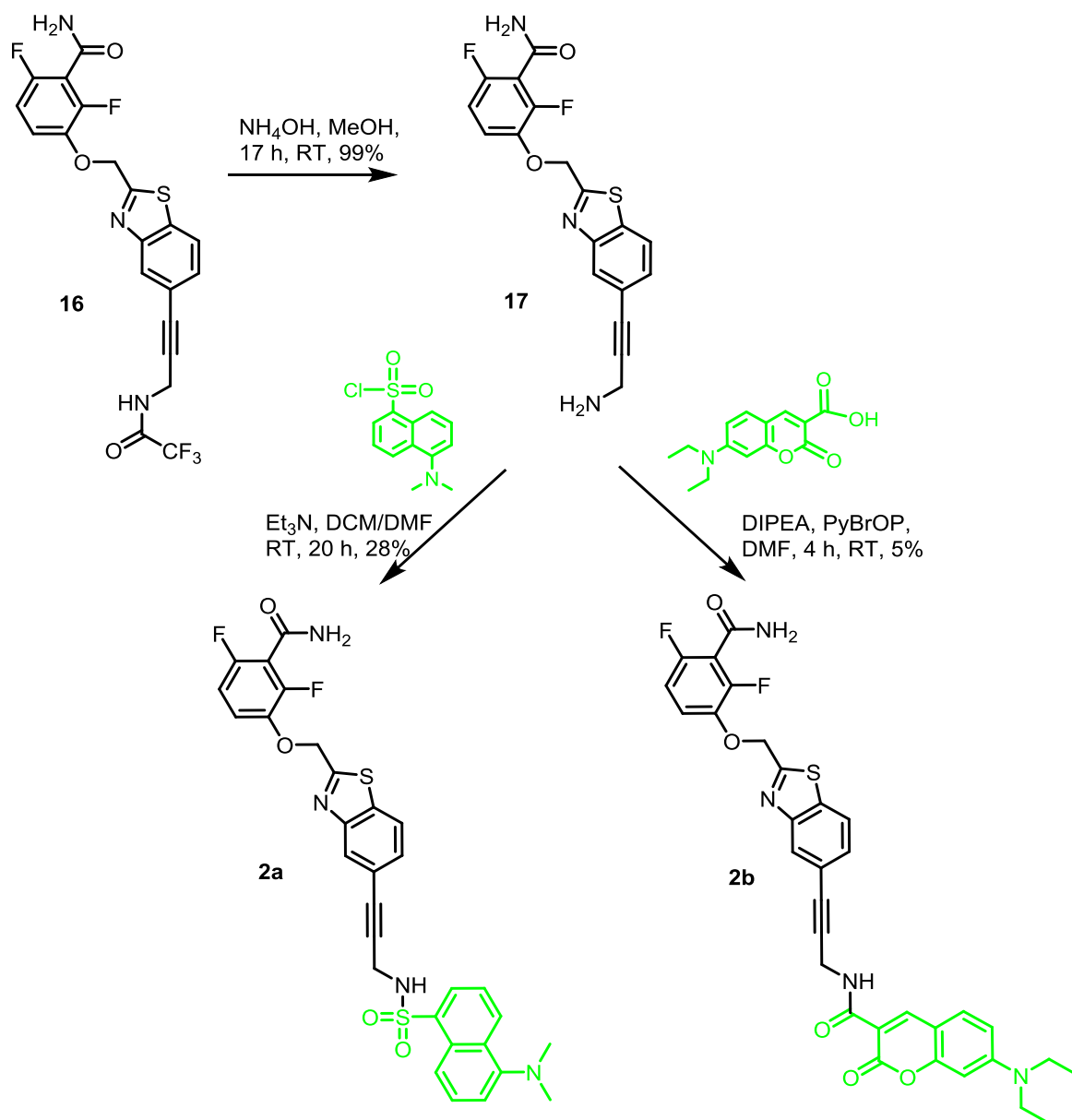
**Table 1.** Catalysts used for Sonogashira coupling of **15** and **12**.



Catalytic system	Reaction conditions	Yield (%)
Pd/C, 4-DPPBA	CuI, Cs <sub>2</sub> CO <sub>3</sub> , DMF, H <sub>2</sub> O, 120 °C (MW), 15 min	0
Pd <sub>2</sub> (dba) <sub>3</sub> · CHCl <sub>3</sub> , PS-PPh <sub>3</sub>	CuI, Et <sub>3</sub> N, DMF, 120 °C (MW), 1 h	54
Pd(PPh <sub>3</sub> ) <sub>4</sub>	CuI, Et <sub>3</sub> N, DMF, 100 °C (MW), 45 min	86

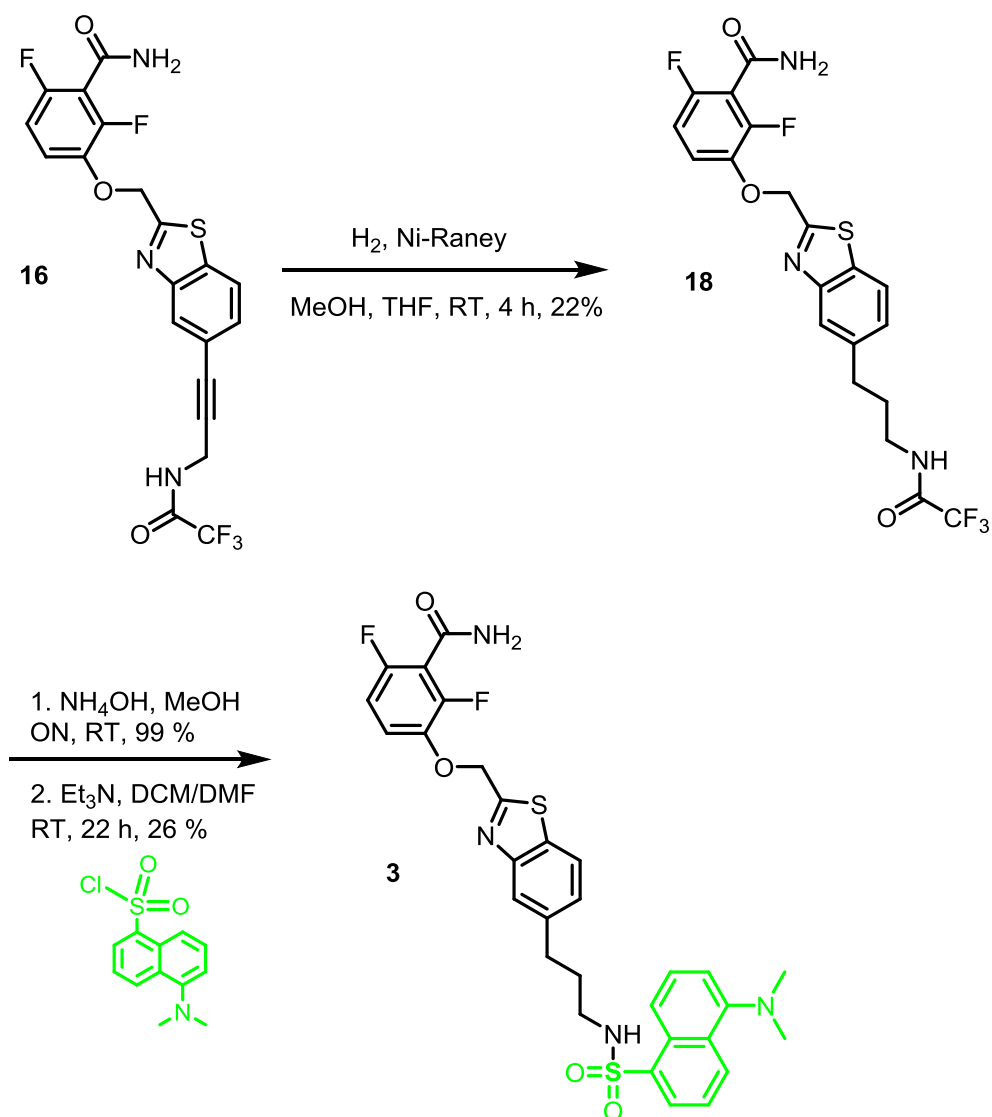
Next, compound **16** was deprotected by reaction with ammonia solution and the intermediate amine **17** treated with dansyl chloride or 7-diethylaminocoumarin-3-carboxylic acid to obtain fluorescent derivatives **2a** and **2b**, respectively (Scheme 5).





**Scheme 543.** Syntheses of fluorescent compounds **2a** and **2b**.

In order to study the influence of a more flexible spacer, the triple bond present in **16** was hydrogenated in the presence of Raney-Ni to afford aliphatic amide **18** (Scheme 6). Amino group was then deprotected, followed by condensation of the resulting amine with dansyl chloride to obtain the fluorescent derivative **3**.



**Scheme 6.** Synthesis of fluorescent derivative **3**.

## 2.4 Synthesis of compounds of Set III

In Set III, the fluorophore was attached to the position 6 of the benzothiazole ring of **8J** using an amino group as attachment point. This route was also based on the synthesis described by Haydon et al.<sup>8</sup> In this case, benzothiazole intermediate **24** bearing a nitro group was constructed by thionation of the corresponding amide **21** and subsequent cyclization (Figure 6).

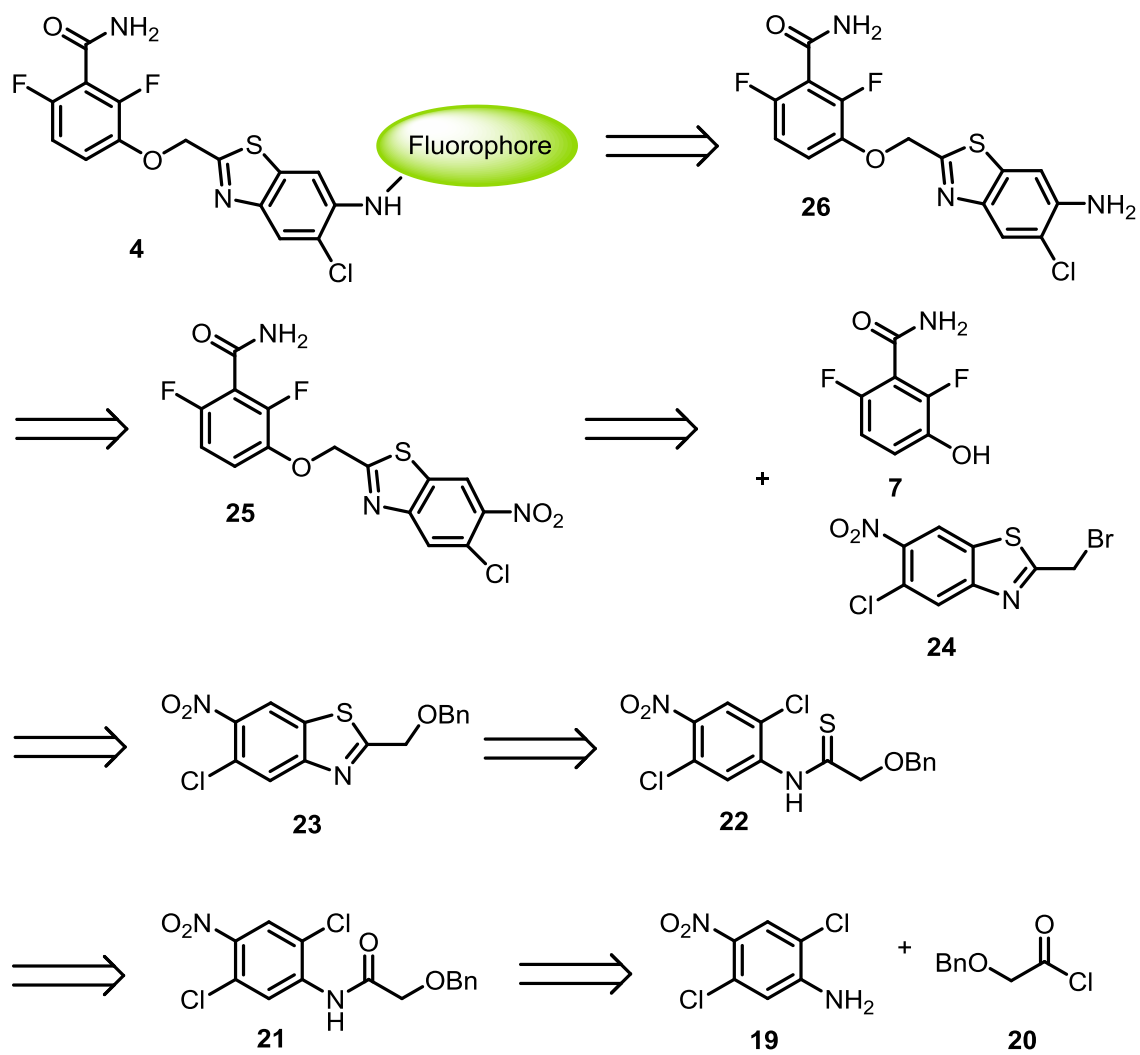
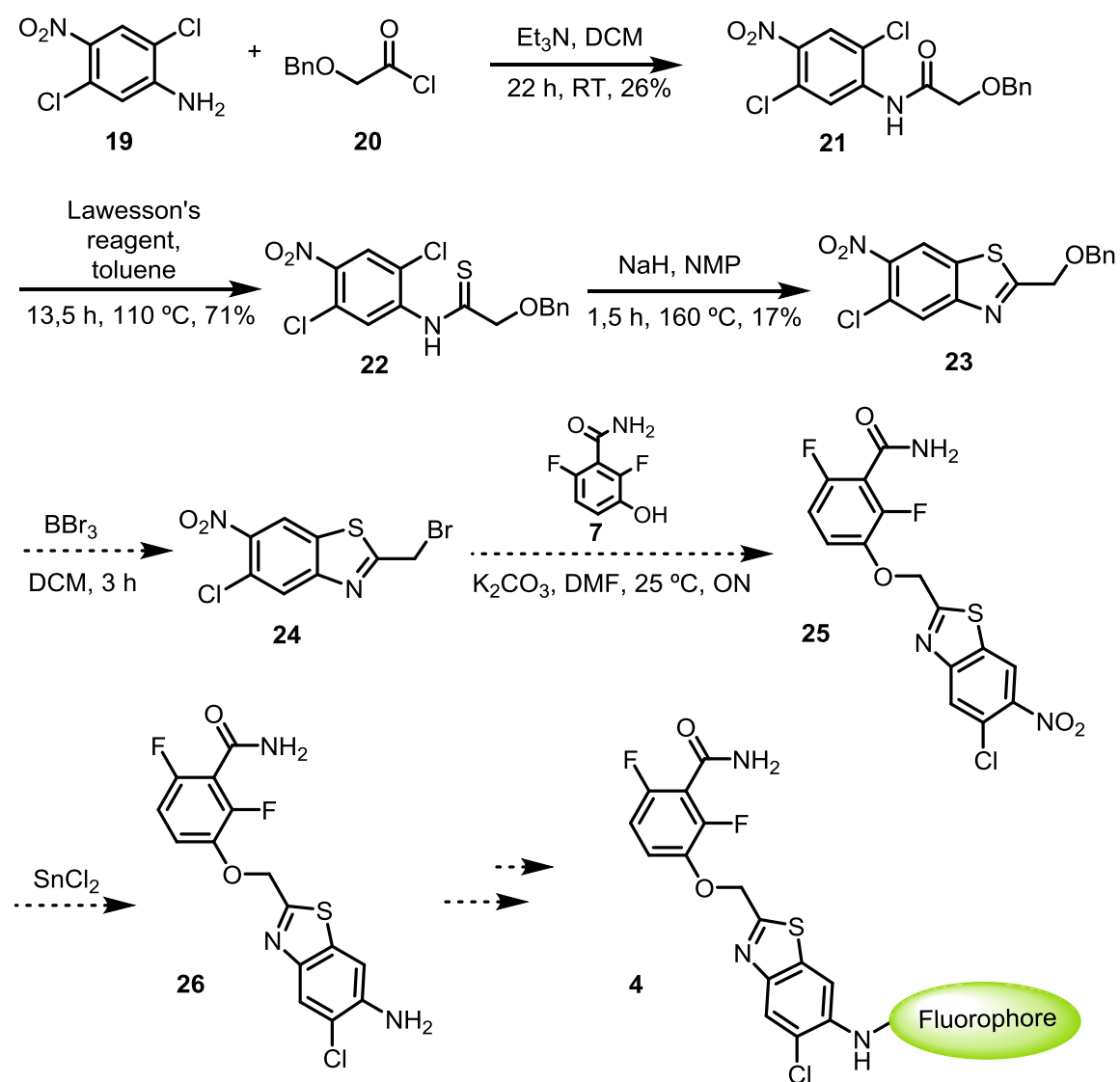


**Figure 6.** Retrosynthetic analysis for Set III.

During my stay, I managed to proceed to the compound **23** (Scheme 7). The synthesis started with reaction of 2,5-dichloro-4-nitroaniline (**19**) with benzyloxyacetyl chloride (**20**) to yield the corresponding amide (**21**). Then, thionation of the carbonyl group with Lawesson's reagent was followed by cyclization of intermediate **22** with NaH to get 2-((benzyloxy)methyl)-5-chloro-6-nitrobenzo[*d*]thiazole (**23**).

To terminate the synthesis of compounds of Set III, the proposed route includes bromination of **23**, Williamson alkylation with 2,5-difluoro-3-hydroxybenzamide (**7**), reduction of the nitro group of **26** and condensation with the fluorophore to yield the corresponding fluorescent derivatives **4** (Scheme 7, dotted reaction arrows).

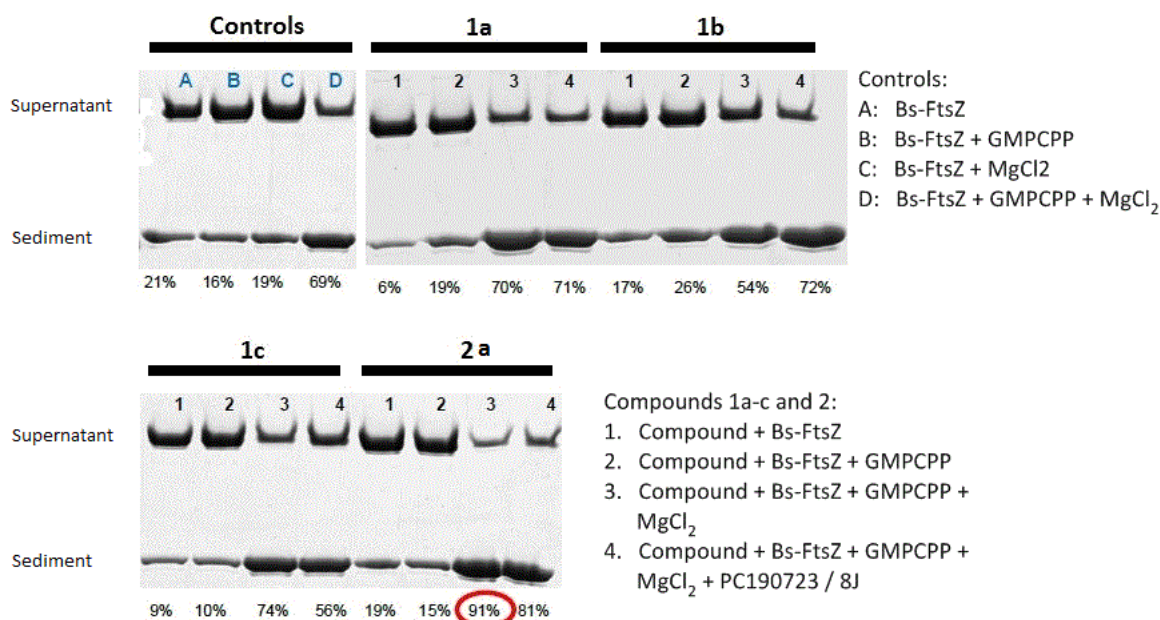


**Scheme 7.** Synthesis of intermediate **23** and proposed synthesis of fluorescent compounds **4**.

## 2.5 Biological evaluation

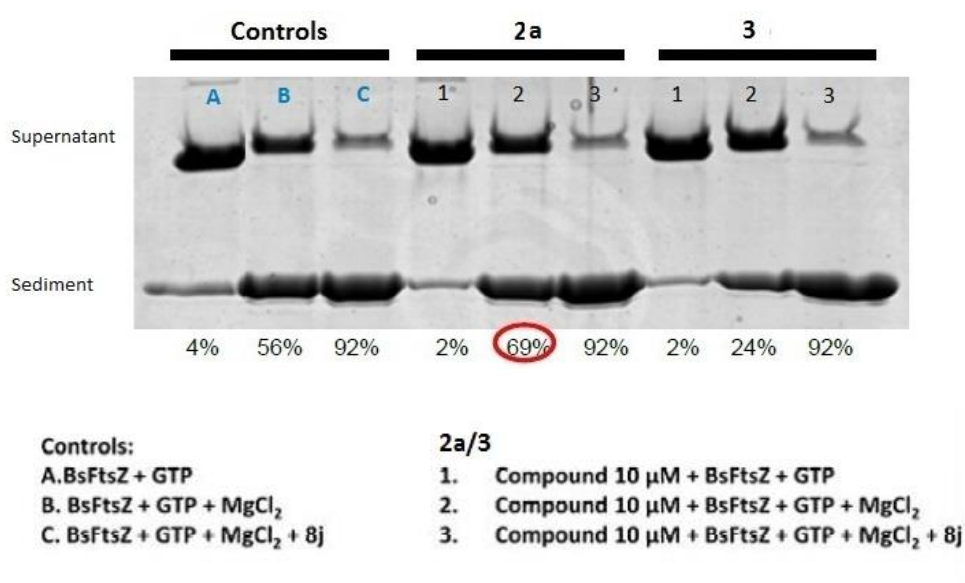
Biological evaluation of the synthesized compounds was carried out in collaboration with the research group led by Dr. José Manuel Andreu at the “Centro de Investigaciones Biológicas” (CIB, Biological Research Center). First, the effect of compounds **1a-c**, **2a-b** and **3** on FtsZ assembly was investigated. This was done using *Bacillus subtilis* FtsZ (Bs-FtsZ) polymer sedimentation assays. Fluorescence spectra of the compounds were also measured in order to find potential probe molecules for future investigation.

Polymer pelleting experiments were made by sedimenting the FtsZ polymers formed under well-controlled assembly conditions in the presence of the compound under study and quantifying them after loading the pellets and supernatants with a time lag into polyacrylamide gel electrophoresis. Proportions of polymerized pellets in presence of the compounds were compared. Bs-FtsZ with GTP or GMPCPP (non-hydrolyzable form of GTP) and  $MgCl_2$  were used as basal controls. Also, PC190723 or **8J** were used as additional controls. Figure 7 shows the effect of compounds **1a-c** and **2a** on FtsZ assembly in the presence of GMPCPP. Compound **2a** was the only compound able to inhibit FtsZ filament assembly by stabilizing filament polymerization, as the percentage of the pellet in sediment is larger than that of the control (91% of pellet in conditions 3 vs 69% in basal conditions D).



**Figure 7.** Sedimentation assays for **1a-c** and **2a**.

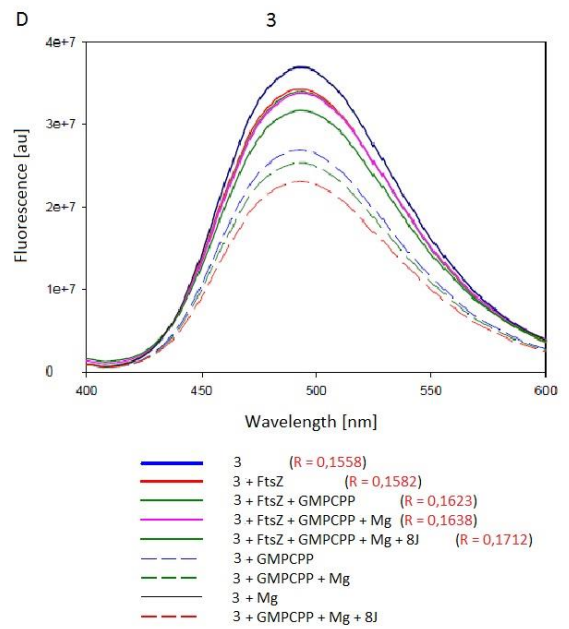
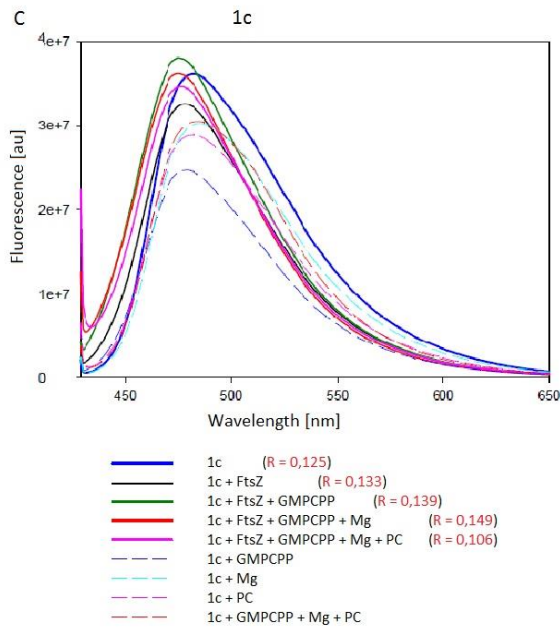
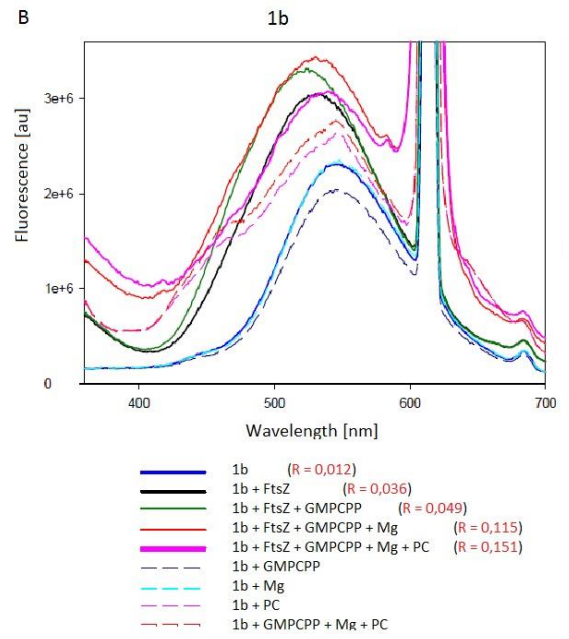
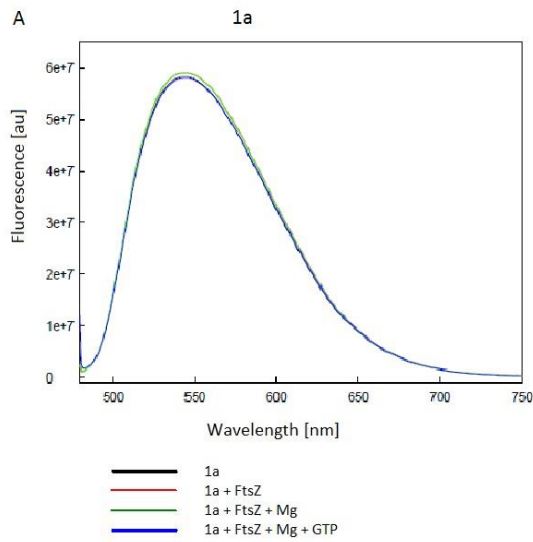
The polymerization effects of dansyl derivatives **2a** and **3** using GTP were also compared (Figure 8). It can be seen that compound **2a** had some activity (69% of pellet in conditions 2 vs 56% in basal conditions B), whereas compound **3** showed no activity (24% of pellet in conditions 2). This result could be explained because of the flexibility of the hydrogenated chain of **3**, which prevents the molecule from entering the cavity of action. It is noteworthy that compound **2a** is active only in presence of GMPCPP or GTP and MgCl<sub>2</sub> (data not shown), while PC190723 does not require MgCl<sub>2</sub> to induce formation of coil structures of FtsZ.<sup>11</sup> These results demonstrate that fluorescent derivative **2a** is an FtsZ polymer stabilizing agent and therefore an inhibitor of FtsZ activity.



**Figure 8.** Sedimentation assays for **2a** and **3**.

Fluorescence emission spectra for compounds **1a-c**, **2a** and **3** were measured to investigate wavelength and intensity displacements when binding to the protein (Figure 9A-E). Major changes of intensity and maximum wavelength were observed only for dansyl derivative **1b** (Figure 9B, displacement between blue and red lines), while the other compounds show minor or no changes.

At last, fluorescence anisotropy values (R) were measured for **1b-c**, **2a** and **3**. The anisotropy values change significantly only for **1b**, from 0.012 to 0.115 (Figure 9B), which indicates that this fluorescent compound binds to the protein. However, the presence of PC190723 does not restore the initial values, meaning that it is not able to replace the fluorescent derivative **1b**.



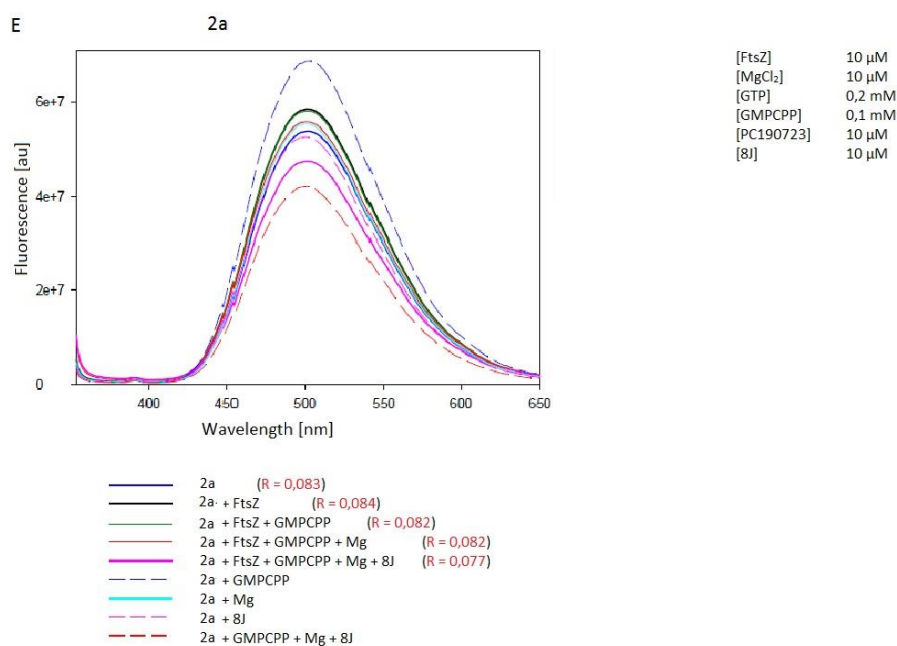


**Figure 9.** Fluorescence emission spectra for compounds **1a-c**, **2a** and **3**. **A:** Compound **1a** (20  $\mu$ M),  $\lambda_{ex}$  = 474 nm. **B:** Compound **1b** (10  $\mu$ M),  $\lambda_{ex}$  = 306 nm. **C:** Compound **1c** (10  $\mu$ M),  $\lambda_{ex}$  = 422 nm. **D:** Compound **3** (10  $\mu$ M),  $\lambda_{ex}$  = 345 nm. **E:** Compound **2a** (10  $\mu$ M),  $\lambda_{ex}$  = 345 nm.

### 3. Conclusions

In this project, compounds **1a-c**, **2a-b** and **3** were synthesized. They are fluorescent derivatives of PC190723 and 8J, known FtsZ inhibitors. Synthetic route for Set III compounds was started as well.

Compound **2a** has an FtsZ polymer-stabilizing effect, and acts as an inhibitor. On the other hand, only **1b** is capable of changing its fluorescent properties when binding to FtsZ. Hence, more accurate structural design based on the protein crystal structure is needed. There is little information about interactions between PC190723 and other bacterial FtsZ than *S. aureus*.<sup>13</sup> Calculations made by Miguel et al.<sup>13</sup> propose that the PC190723 binding pocket varies across species and polymerization states, and taking that into account, Bs-FtsZ may have different binding mechanism and place of action. More species-specific structural studies are needed to be able to design better fitting inhibitory molecules.



## 4. Experimental methods

### General methods:

All chemicals were purchased from Sigma-Aldrich, ABCR, Acros, Lancaster, Invitrogen, ATTO-TEC or Scharlab and were used without further purification. Anhydrous dichloromethane and tetrahydrofuran were freshly distilled over sodium hydride and sodium benzophenone ketyl, respectively. Triethylamine was dried over calcium hydride and distilled prior use. Hydrogenation reactions were carried out with a Parr hydrogenator. Reactions under microwave irradiation were carried out in a Biotage Initiator 2.5 reactor.

The reactions were followed with analytical thin-layer chromatography (TLC) on Merck silica gel plates (Kieselgel 60 F-254) with detection by UV light. Flash chromatography was performed on a Varian 971-FP flash purification system using SuperFlash Si50 silica gel cartridges.

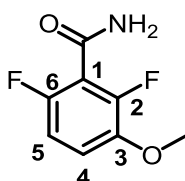
Melting points were determined on a Stuart Scientific electrothermal apparatus. IR spectra were measured on a Bruker Tensor 27 spectrometer equipped with a Specac ATR accessory of 5200-650  $\text{cm}^{-1}$  transmission range, and the frequencies are expressed in  $\text{cm}^{-1}$ . Nuclear magnetic resonance (NMR) spectra were recorded on a Bruker DPX 300 ( $^1\text{H}$ , 300 MHz;  $^{13}\text{C}$ , 75 MHz) and Bruker Avance 500 ( $^1\text{H}$ , 500 MHz;  $^{13}\text{C}$ , 125 MHz) at the Universidad Complutense de Madrid (UCM) NMR facilities. Chemical shifts ( $\delta$ ) are expressed in parts per million relative to internal tetramethylsilane. Coupling constants ( $J$ ) are in hertz (Hz).

Mass spectrometry (MS) was carried out on a Bruker LC-Esquire spectrometer in electrospray ionization (ESI) mode at the UCM's mass spectrometry core facility. High performance liquid chromatography coupled to mass spectrometry (HPLC-MS) analysis was performed using an Agilent 1200LC-MSD VL instrument. LC separation was achieved with a Zorbax Eclipse XDB-C18 column (5  $\mu\text{m}$ , 4.6 mm x 150 mm) for naphthalene derivatives and a Zorbax SB-C3 column (5  $\mu\text{m}$ , 2.1 mm x 50 mm) for biphenyl derivatives, both together with a guard column (5  $\mu\text{m}$ , 4.6 mm x 12.5 mm). The gradient mobile phases consisted of A (95:5 water/MeOH) and B (5:95 water/MeOH) with 0.1% ammonium hydroxide and 0.1% formic acid as the solvent modifiers. MS analysis was performed with an ESI source. The capillary voltage was set to 3.0 kV and the fragmentor voltage was set at 72 eV. The drying gas temperature was 350  $^{\circ}\text{C}$ , the drying gas flow was 10 L/min, and the nebulizer pressure was 20 psi. Spectra were acquired in positive or negative ionization mode from 100 to 1200  $m/z$  and in UV-mode at four different wavelengths (210, 230, 254, and 280 nm).

Elemental analyses (C, H, N, S) were obtained on a LECO CHNS-932 apparatus at the UCM's Elemental Microanalysis services. Purity of final compounds was determined by elemental analyses and HPLC-MS, confirming at least a 95% of purity.

#### 4.1 Set I

##### **2,6-Difluoro-3-methoxybenzamide (6):**



To a suspension of 2,6-difluoro-3-methoxybenzoic acid **5** (1 g, 5.32 mmol) in anhydrous toluene (8 mL) thionyl chloride (580  $\mu$ L, 7.98 mmol) was added slowly under an argon atmosphere. The reaction mixture was refluxed for 5 hours. The solvent was evaporated under reduced pressure on a rotary evaporator. Then, the residue was dissolved in tetrahydrofuran (2 mL), 28% aqueous ammonia solution (4 mL) was added and the mixture was stirred at room temperature for 14 hours. The solvent was evaporated under reduced pressure and the resulting precipitate was suspended in water and filtered. The collected solid was dried under vacuum to afford 2,6-difluoro-3-methoxybenzamide **6** as a white solid in 80% yield.

Melting point: 167-169  $^{\circ}$ C.

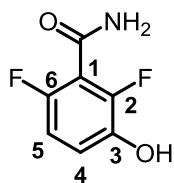
IR (ATR): 3386 (NH<sub>2</sub>), 3180 (NH<sub>2</sub>), 1651 (CO), 1590, 1491, 1452 (Ar).

<sup>1</sup>H NMR ((CD<sub>3</sub>)<sub>2</sub>CO, 300 MHz)  $\delta$ : 3.88 (s, 3 H, OCH<sub>3</sub>), 6.97 (td app,  $J$  = 9.0; 2.0, 1 H, C<sub>5</sub>H), 7.18 (td app,  $J$  = 9.3; 5.1, 2 H, C<sub>4</sub>H, NH), 7.44 (s br, 1 H, NH).

<sup>13</sup>C NMR ((CD<sub>3</sub>)<sub>2</sub>CO, 125 MHz)  $\delta$ : 57.1 (CH<sub>3</sub>), 111.4 (dd,  $J$  = 23.1; 4.2, C<sub>5</sub>H), 115.1 (d,  $J$  = 9.4; 2.8, C<sub>4</sub>H), 117.3 (t,  $J$  = 21.6, C<sub>1</sub>), 145.3 (dd,  $J$  = 11.0; 3.2, C<sub>3</sub>), 149.5 (dd,  $J$  = 250.1; 8.1, CF), 153.4 (dd,  $J$  = 241.6; 6.5, CF), 162.2 (CONH<sub>2</sub>).

MS (ESI): 188.1 [M+H]<sup>+</sup>.

### 2,6-Difluoro-3-hydroxybenzamide (7):



A solution of boron tribromide in dichloromethane (1 M, 8.6 mL, 8.60 mmol) was added dropwise to a solution of 2,6-difluoro-3-methoxybenzamide **6** (805 mg, 4.30 mmol) in anhydrous dichloromethane (25 mL) under an argon atmosphere. The mixture was stirred for 3 days at room temperature. The solvent was evaporated under reduced pressure on a rotary evaporator, the residue was dissolved in ethyl acetate (2 x 40 mL) and then washed with water (40 mL). The organic layer was dried with sodium sulfate, filtered and concentrated on a rotary evaporator. The residue was purified by silica gel column chromatography (hexane → hexane/ethyl acetate 3:7) to obtain 2,6-difluoro-3-hydroxybenzamide **7** as a white solid in 79% yield.

Melting point: 123-124 °C.

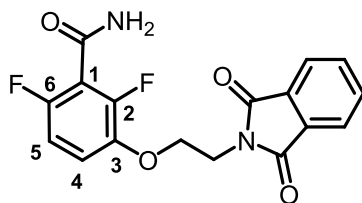
IR (ATR): 3196 (NH<sub>2</sub>), 1666 (CO), 1598, 1493, 1394 (Ar).

<sup>1</sup>H NMR ((CD<sub>3</sub>)<sub>2</sub>CO, 300 MHz) δ: 6.87 (td app, *J* = 8.8; 1.8, 1 H, C<sub>5</sub>H), 7.01 (td app, *J* = 9.2; 5.4, 1 H, C<sub>4</sub>H), 7.17 (s a, 1 H, CONH<sub>2</sub>), 7.41 (s a, 1 H, CONH<sub>2</sub>), 8.79 (s, 1 H, OH).

<sup>13</sup>C NMR ((CD<sub>3</sub>)<sub>2</sub>CO, 125 MHz) δ: 111.7 (dd, *J* = 23.3; 4.0, C<sub>5</sub>H), 117.0 (t, *J* = 21.6, C<sub>1</sub>), 118.7 (dd, *J* = 9.1; 3.7, C<sub>4</sub>H), 142.3 (dd, *J* = 13.5; 3.2, C<sub>3</sub>), 148.5 (dd, *J* = 245.4; 7.9, CF), 152.6 (dd, *J* = 240.3; 6.2, CF), 162.4 (CONH<sub>2</sub>).

MS (ESI): 172.0 [M-H]<sup>-</sup>.

### 3-[2-(1,3-Dioxisoindolin-2-yl)ethoxy]-2,6-difluorobenzamide (8):



To a solution of 2,6-difluoro-3-hydroxybenzamide **7** (292 mg, 1.69 mmol), *N*-(2-hydroxyethyl)phthalimide (478 mg, 2.50 mmol) and triphenylphosphine (873 mg, 3.33 mmol) in

anhydrous tetrahydrofuran (10 mL), diethyl azodicarboxylate (DEAD) (610  $\mu$ L, 3.33 mmol) was added under an argon atmosphere. The mixture was refluxed for 24 hours. The solvent was evaporated under reduced pressure on a rotary evaporator and the residue was purified by silica gel column chromatography (hexane  $\rightarrow$  hexane/ethyl acetate 1:1) to afford 3-[2-(1,3-dioxoisindolin-2-yl)ethoxy]-2,6-difluorobenzamide **8** as a white solid in 51% yield.

Melting point: 169-171  $^{\circ}$ C.

IR (ATR): 3397 (NH<sub>2</sub>), 1710 (CO), 1655 (CO), 1492 (Ar).

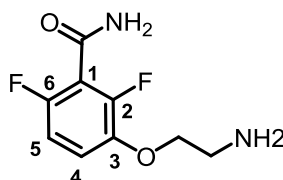
<sup>1</sup>H NMR ((CD<sub>3</sub>)<sub>2</sub>CO, 300 MHz)  $\delta$ : 4.01 (t,  $J$  = 5.7, 2 H, CH<sub>2</sub>N), 4.29 (t,  $J$  = 5.7, 2 H, CH<sub>2</sub>O), 5.82 (s br, 1 H, NH<sub>2</sub>), 5.97 (s br, 1 H, NH<sub>2</sub>), 6.85 (td app,  $J$  = 9.1; 1.8, 1 H, C<sub>5</sub>H), 7.05 (td app,  $J$  = 9.0; 5.1, 1 H, C<sub>4</sub>H), 7.74 (dd,  $J$  = 5.4; 3.0, 2 H, 2H<sub>Pht</sub>), 7.87 (dd,  $J$  = 5.5; 2.9, 2 H, 2H<sub>Pht</sub>).

<sup>13</sup>C NMR ((CD<sub>3</sub>)<sub>2</sub>CO, 75 MHz)  $\delta$ : 37.9 (CH<sub>2</sub>N), 67.7 (OCH<sub>2</sub>), 111.6 (dd,  $J$  = 23.5; 3.9, C<sub>5</sub>H), 116.9 (t,  $J$  = 23.5, C<sub>1</sub>), 117.1 (d,  $J$  = 7.1, C<sub>4</sub>H), 123.9 (2 CH<sub>Pht</sub>), 133.0 (2 C<sub>Pht</sub>), 135.2 (2 CH<sub>Pht</sub>), 144.0 (dd,  $J$  = 10.8; 3.2, C<sub>3</sub>), 150.6 (dd,  $J$  = 251.0; 8.9, CF), 153.0 (dd,  $J$  = 242.0; 6.5, CF), 162.0 (d,  $J$  = 6.7, CONH<sub>2</sub>), 168.6 (2 CO<sub>Pht</sub>).

Elemental Analysis of C<sub>17</sub>H<sub>12</sub>F<sub>2</sub>N<sub>2</sub>O<sub>4</sub>: Calculated (%): C: 58.96; H: 3.49; N: 8.09. Observed (%): C: 58.41; H: 3.93; N: 7.78.

MS (ESI): 347.1 [M+H]<sup>+</sup>.

### 3-(2-Aminoethoxy)-2,6-difluorobenzamide (**9**)



To a mixture of 3-[2-(1,3-dioxoisindolin-2-yl)ethoxy]-2,6-difluorobenzamide **8** (180 mg, 0.52 mmol) in ethanol (15 mL), monohydrated hydrazine (50.6  $\mu$ L, 1.04 mmol) was added. The reaction mixture was refluxed for 2 hours and then, the solvent was evaporated under reduced pressure. The crude was purified by silica gel column chromatography (ethyl acetate  $\rightarrow$  ethanol) to obtain 3-(2-aminoethoxy)-2,6-difluorobenzamide **9** as a white solid in 87% yield.

Melting point: 98-100  $^{\circ}$ C.

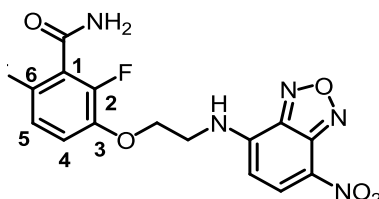
IR (ATR): 3310 (NH<sub>2</sub>), 1675 (CO), 1489 (Ar).

<sup>1</sup>H NMR (CD<sub>3</sub>OD, 500 MHz)  $\delta$ : 3.22 (t,  $J$  = 5.1, 2 H, CH<sub>2</sub>NH<sub>2</sub>), 4.20 (t,  $J$  = 5.1, 2 H, CH<sub>2</sub>O), 6.99 (td app,  $J$  = 8.9; 1.9, 1 H, C<sub>5</sub>H), 7.23 (td app,  $J$  = 9.2; 5.2, 1 H, C<sub>4</sub>H).

$^{13}\text{C}$  NMR ( $\text{CD}_3\text{OD}$ , 125 MHz)  $\delta$ : 40.8 ( $\text{CH}_2\text{NH}_2$ ), 70.1 ( $\text{OCH}_2$ ), 112.1 (dd,  $J = 22.4$ ; 4.5,  $\text{C}_5\text{H}$ ), 117.1 (t,  $J = 23.8$ ,  $\text{C}_1$ ), 118.3 (dd,  $J = 9.4$ ; 2.4,  $\text{C}_4\text{H}$ ), 144.1 (dd,  $J = 11.0$ ; 3.3,  $\text{C}_3$ ), 150.7 (dd,  $J = 252.8$ ; 9.0, CF), 154.6 (dd,  $J = 244.0$ ; 5.8, CF), 165.1 ( $\text{CONH}_2$ ).

MS (ESI): 216.9  $[\text{M}+\text{H}]^+$ .

### 2,6-Difluoro-3-{2-[(7-nitro-2,1,3-benzoxadiazol-4-yl)amino]ethoxy}benzamide (1a)



To a solution of 3-(2-aminoethoxy)-2,6-difluorobenzamide **9** (101 mg, 0.47 mmol) and triethylamine (71.3  $\mu\text{L}$ , 1.51 mmol) in anhydrous dimethylformamide (3 mL), a solution of 4-chloro-7-nitro-1,2,3-benzoxadiazole (93 mg, 0.47 mmol) in anhydrous dimethylformamide (1 mL) was added under argon atmosphere. The mixture was stirred at room temperature protected from light for 22 hours. The solvent was evaporated under reduced pressure on a rotary evaporator. The crude was purified by silica gel column chromatography (dichloromethane  $\rightarrow$  dichloromethane/ethyl acetate 1:1), and 2,6-difluoro-3-{2-[(7-nitro-2,1,3-benzoxadiazol-4-yl)amino]ethoxy}benzamide **1a** was obtained as a brown solid in 18% yield.

Melting point: 169-172  $^{\circ}\text{C}$ .

IR (ATR): 3354 ( $\text{NH}_2$ ), 1676 (CO), 1586, 1491 (Ar).

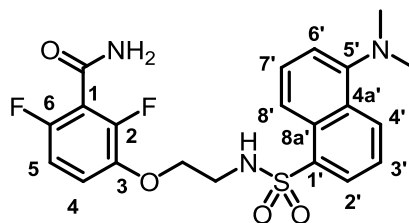
$^1\text{H}$  NMR ( $(\text{CD}_3)_2\text{CO}$ , 500 MHz)  $\delta$ : 4.16 (m, 2 H,  $\text{CH}_2\text{N}$ ), 4.54 (t,  $J = 5.2$ , 2 H,  $\text{CH}_2\text{O}$ ), 6.67 (d,  $J = 8.7$ , 1 H,  $\text{CH}_{\text{NBD}}$ ), 6.98 (td app,  $J = 8.9$ ; 2.1, 1 H,  $\text{C}_5\text{H}$ ), 7.17 (s br, 1 H, NH), 7.26 (td app,  $J = 9.1$ ; 5.1, 1 H,  $\text{C}_4\text{H}$ ), 7.41 (s br, 1 H, NH), 8.52 (d,  $J = 8.7$ , 1 H,  $\text{CH}_{\text{NBD}}$ ).

$^{13}\text{C}$  NMR ( $(\text{CD}_3)_2\text{CO}$ , 125 MHz)  $\delta$ : 43.8 ( $\text{CH}_2\text{NH}$ ), 68.5 ( $\text{OCH}_2$ ), 100.0 ( $\text{CH}_{\text{NBD}}$ ), 111.1 (dd,  $J = 23.2$ ; 4.1,  $\text{C}_5\text{H}$ ), 116.3 (d,  $J = 9.6$ ,  $\text{C}_4\text{H}$ ), 116.9 (t,  $J = 25.7$ ,  $\text{C}_1$ ), 123.5 ( $\text{C}_{\text{NBD}}$ ), 137.2 ( $\text{CH}_{\text{NBD}}$ ), 143.6 (dd,  $J = 11.2$ ; 3.4,  $\text{C}_3$ ), 144.7 ( $\text{C}_{\text{NBD}}$ ), 145.1 ( $\text{C}_{\text{NBD}}$ ), 145.4 ( $\text{C}_{\text{NBD}}$ ), 149.3 (dd,  $J = 248.6$ ; 8.3, CF), 153.3 (dd,  $J = 242.4$ ; 6.3, CF), 161.6 ( $\text{CONH}_2$ ).

Elemental Analysis of  $\text{C}_{17}\text{H}_{12}\text{F}_2\text{N}_2\text{O}_4$ : Calculated (%): C: 47.50; H: 2.92; N: 18.47. Observed (%): C: 47.40; H: 3.29; N: 18.13.

MS (ESI): 379.7  $[\text{M}+\text{H}]^+$ , 396.6  $[\text{M}+\text{Na}]^+$ .

### 3-[2-({[5-(Dimethylamino)-1-naphthyl]sulfonyl}amino)ethoxy]-2,6-difluorobenzamide (**1b**)



3-(2-aminoethoxy)-2,6-difluorobenzamide **9** (98 mg, 0.45 mmol) was dissolved in anhydrous dimethylformamide (3 mL) under an argon atmosphere. A solution of triethylamine (0.19 mL) and dansyl chloride (183 mg, 0.68 mmol) in anhydrous dimethylformamide (1 mL) was added, and the reaction mixture was stirred at room temperature for 22 hours. Afterward, the solvent was evaporated under reduced pressure and the crude was purified by silica gel column chromatography (dichloromethane) to afford 3-[2-({[5-(dimethylamino)-1-naphthyl]sulfonyl}amino)ethoxy]-2,6-difluorobenzamide **1b** in 10% yield.

Melting point: 130-132 °C.

IR (ATR): 3316 (NH<sub>2</sub>), 1744 (CO), 1582, 1502, 1459 (Ar).

<sup>1</sup>H NMR (CDCl<sub>3</sub>, 500 MHz) δ: 2.89 (s, 6 H, 2 CH<sub>3</sub>), 3.38 (q app, *J* = 5.5, 2 H, CH<sub>2</sub>N), 3.85 (t, *J* = 5.0, 2 H, CH<sub>2</sub>O), 5.25 (t, *J* = 6.0, 1 H, NH), 6.77-6.85 (m, 2 H, C<sub>4</sub>H, C<sub>5</sub>H), 7.17 (d, *J* = 7.2, 1 H, C<sub>6'</sub>H), 7.52 (t, *J* = 7.9, 1 H, C<sub>3'H</sub>/C<sub>7'H</sub>), 7.57 (t, *J* = 8.0, 1 H, C<sub>3'H</sub>/C<sub>7'H</sub>), 8.24-8.27 (m, 2 H, C<sub>4'H</sub>, C<sub>6'H</sub>), 8.54 (d, *J* = 7.2, 1 H, C<sub>2'H</sub>).

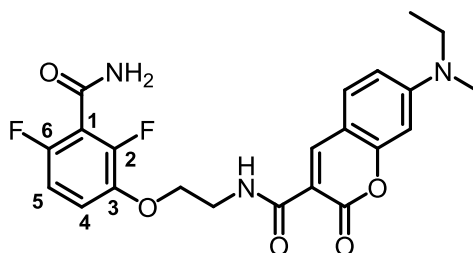
<sup>13</sup>C NMR (CDCl<sub>3</sub>, 125 MHz) δ: 43.2 (CH<sub>2</sub>N), 45.6 (2 CH<sub>3</sub>N), 68.9 (OCH<sub>2</sub>), 111.3 (dd, *J* = 20.6; 4.5, C<sub>5</sub>H), 115.5 (CH<sub>Ds</sub>), 118.6 (C<sub>1</sub>), 120.4 (dd, *J* = 9.1; 3.5, C<sub>4</sub>H), 123.4 (CH<sub>Ds</sub>), 128.8 (CH<sub>Ds</sub>), 129.5 (2 C<sub>Ds</sub>), 129.6 (2 CH<sub>Ds</sub>), 130.1 (C<sub>Ds</sub>), 130.8 (CH<sub>Ds</sub>), 135.1 (C<sub>Ds</sub>), 142.9 (dd, *J* = 9.3; 3.5, C<sub>3</sub>), 153.0 (dd, *J* = 262.9; 4.6, C<sub>2</sub>/C<sub>6</sub>), 156.7 (dd, *J* = 255.0; 2.9, C<sub>2</sub>/C<sub>6</sub>), 164.7 (CONH<sub>2</sub>).

Elemental Analysis of C<sub>17</sub>H<sub>12</sub>F<sub>2</sub>N<sub>2</sub>O<sub>4</sub>: Calculated (%): C: 56.12; H: 4.71; N: 9.35; S: 7.13. Observed (%): C: 57.17; H: 5.16; N: 8.29; S: 6.43.

MS (EI): 432.1 [M+H]<sup>+</sup>.

HPLC t<sub>r</sub> (min): 20.71.

***N*-{2-[3-(aminocarbonyl)-2,4-difluorophenoxy]ethyl}-7-(diethylamino)-2-oxo-2*H*-chromene-3-carboxamide (1c)**



To a solution of 3-(2-aminoethoxy)-2,6-difluorobenzamide **9** (80 mg, 0.37 mmol) in anhydrous dimethylformamide (5 mL), *N,N*-diisopropylethylamine (DIPEA) (129  $\mu$ L, 0.74 mmol), bromo-trispyrrolidino-phosphoniumhexafluorophosphate (PyBrOP) (310.5 mg, 0.66 mmol) and 7-(diethylamino)coumarin-3-carboxylic acid (100 mg, 0.38 mmol) were added under an argon atmosphere. The reaction mixture was stirred at room temperature for 4 hours. The solvent was evaporated under reduced pressure and the crude was purified by silica gel column chromatography (dichloromethane  $\rightarrow$  dichloromethane/ethyl acetate 9:1) to afford *N*-{2-[3-(aminocarbonyl)-2,4-difluorophenoxy]ethyl}-7-(diethylamino)-2-oxo-2*H*-chromene-3-carboxamide **1c** in 27% yield.

Melting point: 155-158  $^{\circ}$ C.

IR (ATR): 3366 (NH<sub>2</sub>), 1704, 1663 (CO), 1618, 1583, 1537 (Ar).

<sup>1</sup>H NMR (DMSO-*d*<sub>6</sub>, 700 MHz)  $\delta$ : 1.14 (t, *J* = 7.0, 6 H, 2 CH<sub>3</sub>), 3.48 (q, *J* = 7.0, 4 H, 2 CH<sub>2</sub>), 3.70 (q, *J* = 5.7, 2 H, CH<sub>2</sub>N), 4.18 (t, *J* = 5.7, 2 H, CH<sub>2</sub>O), 6.61 (d, *J* = 2.0, 1 H, CH<sub>Coum</sub>), 6.81 (dd, *J* = 9.0; 2.2, 1 H, CH<sub>Coum</sub>), 7.07 (t app, *J* = 8.8, 1 H, C<sub>5</sub>H), 7.29 (td app, *J* = 9.3; 5.3, 1 H, C<sub>4</sub>H), 7.69 (d, *J* = 9.0, 1 H, CH<sub>Coum</sub>), 7.85 (s br, 1 H, NH), 8.13 br (s, 1 H, NH), 8.69 (s, 1 H, CH<sub>Coum</sub>), 8.93 (t, *J* = 5.7, 1 H, NH).

<sup>13</sup>C NMR (DMSO-*d*<sub>6</sub>, 175 MHz)  $\delta$ : 12.3 (2 CH<sub>3</sub>), 38.3 (CH<sub>2</sub>N), 44.3 (CH<sub>2</sub>NH), 68.3 (OCH<sub>2</sub>), 95.9 (CH<sub>Coum</sub>), 107.7 (C<sub>Coum</sub>), 109.0 (C<sub>Coum</sub>), 110.2 (CH<sub>Coum</sub>), 111.0 (dd, *J* = 22.6; 4.0, C<sub>5</sub>H), 115.6 (d, *J* = 9.4, C<sub>4</sub>H), 116.7 (dd, *J* = 25.1; 20.3, C<sub>1</sub>), 131.7 (CH<sub>Coum</sub>), 142.8 (dd, *J* = 10.6; 2.7, C<sub>3</sub>), 147.9 (CH<sub>Coum</sub>), 148.0 (dd, *J* = 248.5; 9.0, CF), 152.0 (dd, *J* = 241.7; 7.2, CF), 152.5 (C<sub>Coum</sub>), 157.3 (C<sub>Coum</sub>), 161.3 (CONH<sub>2</sub>), 161.8 (CO), 162.6 (CO).

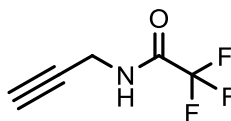
Elemental Analysis of C<sub>23</sub>H<sub>23</sub>F<sub>2</sub>N<sub>3</sub>O<sub>5</sub>: Calculated (%): C: 60.13; H: 5.05; N: 9.15. Observed (%): C: 60.23; H: 5.41; N: 8.44.

MS (EI): 459.6 [M+H]<sup>+</sup>.

HPLC *t*<sub>r</sub> (min): 18.86.

## 4.2 Set II

### 2,2,2-Trifluoro-*N*-(prop-2-ynyl)acetamide (**12**)



To a solution of propargylamine **10** (2 g, 36.3 mmol) in anhydrous methanol (5 mL) at 0 °C stirring under an argon atmosphere, ethyl trifluoroacetate (3.82 mL, 36.3 mmol) was added dropwise. The mixture was stirred at room temperature for 17 hours. The solvent was evaporated under reduced pressure on a rotary evaporator and the crude was purified by silica gel column chromatography (dichloromethane) to obtain 2,2,2-trifluoro-*N*-(prop-2-ynyl)acetamide **12** in 60% yield.

Melting point: liquid.

IR (ATR): 3305 (NH), 1711 (CO), 1553 (NH).

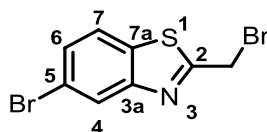
<sup>1</sup>H NMR (CDCl<sub>3</sub>, 300 MHz) δ: 2.32 (d, *J* = 2.6, 1 H, CH), 4.13 (dd, *J* = 5.3; 2.5, 2 H, CH<sub>2</sub>), 6.80 (s br, 1 H, NH).

<sup>13</sup>C NMR (CDCl<sub>3</sub>, 75 MHz) δ: 29.8 (CH<sub>2</sub>), 73.3 (CH), 77.4 (C), 115.7 (q, *J* = 288.0, CF<sub>3</sub>), 157.1 (q, *J* = 37.4, CO).

MS (EI): 150.0 [M+H]<sup>+</sup>.

HPLC *t*<sub>r</sub> (min): 11.39.

### 5-Bromo-2-(bromomethyl)benzo[*d*]thiazole (**14**)



To a solution of 2-methyl-5-bromobenzothiazole **13** (5.00 g, 22.04 mmol) in CCl<sub>4</sub> (90 mL), *N*-bromosuccinimide (8.00 g, 44.94 mmol) and azobisisobutyronitrile (0.75 g, 4.57 mmol) were added under an argon atmosphere, and the reaction was stirred at 90 °C for 3 hours. Afterwards, the solvent was evaporated under reduced pressure. The crude was purified by silica gel column chromatography (hexane → hexane/ethyl acetate 95:5) to afford 5-bromo-2-(bromomethyl)benzo[*d*]thiazole **14** in 13% yield.

IR (ATR): 1730, 1583, 1542, 1507, 1435 (Ar).

<sup>1</sup>H NMR (CDCl<sub>3</sub>, 300 MHz) δ: 4.79 (s, 2 H, CH<sub>2</sub>), 7.54 (dd, *J* = 8.6; 1.8, 1 H, C<sub>6</sub>H), 7.74 (d, *J* = 8.6, 1 H, C<sub>7</sub>H), 8.17 (d, *J* = 1.8, 1 H, C<sub>4</sub>H).

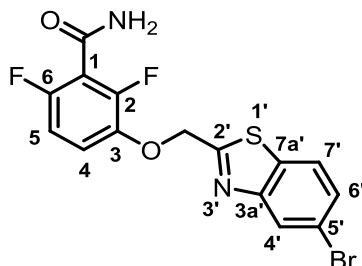


$^{13}\text{C}$  NMR ( $\text{CDCl}_3$ , 75 MHz)  $\delta$ : 27.0 ( $\text{CH}_2$ ), 120.3 ( $\text{C}_5$ ), 123.0 ( $\text{C}_7\text{H}$ ), 126.6 ( $\text{C}_4\text{H}$ ), 129.1 ( $\text{C}_6\text{H}$ ), 135.3 ( $\text{C}_{7a}$ ), 154.2 ( $\text{C}_{3a}$ ), 168.3 ( $\text{C}_2$ ).

MS (ESI): 307.8 [ $\text{M}+\text{H}$ ] $^+$ .

HPLC  $t_r$  (min): 22.97.

### 3-((5-Bromobenzo[*d*]thiazol-2-yl)methoxy)-2,6-difluorobenzamide (**15**)



5-Bromo-2-(bromomethyl)benzo[*d*]thiazole **14** (943 mg, 3.07 mmol) was dissolved in dry dimethylformamide (15 mL) in a round-bottomed flask and 2,6-difluoro-3-hydroxybenzamide **7** (532 mg, 3.07 mmol) and potassium carbonate (1274 mg, 9.21 mmol) were added under an argon atmosphere. The mixture was stirred at room temperature overnight. Then, the solvents were evaporated under reduced pressure. The brown solid was purified by silica gel column chromatography (hexane  $\rightarrow$  ethyl acetate  $\rightarrow$  methanol) to obtain 3-((5-bromobenzo[*d*]thiazol-2-yl)methoxy)-2,6-difluorobenzamide **15** in 94% yield.

IR (ATR): 3373 ( $\text{NH}_2$ ), 3189, 1669 ( $\text{CO}$ ), 1591, 1524, 1490 ( $\text{Ar}$ ).

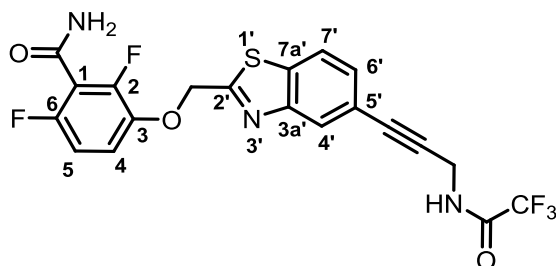
$^1\text{H}$  NMR ( $\text{DMSO}$ , 300 MHz)  $\delta$ : 5.70 (s, 2 H,  $\text{CH}_2$ ), 7.10 (td app,  $J = 9.0$ ; 1.8, 1 H,  $\text{C}_5\text{H}$ ), 7.39 (td app,  $J = 9.4$ ; 5.2, 1 H,  $\text{C}_4\text{H}$ ), 7.64 (dd,  $J = 8.6$ ; 1.9, 1 H,  $\text{C}_6\text{H}$ ), 7.87 (s br, 1 H,  $\text{NH}$ ), 8.13 (d,  $J = 8.6$ , 1 H,  $\text{C}_7\text{H}$ ), 8.15 (s br, 1 H,  $\text{NH}_2$ ), 8.25 (d,  $J = 1.9$ , 1 H,  $\text{C}_4\text{H}$ ).

$^{13}\text{C}$  NMR ( $\text{DMSO}$ , 75 MHz)  $\delta$ : 68.6 ( $\text{CH}_2$ ), 111.1 (dd,  $J = 23.4$ ; 4.1,  $\text{C}_5\text{H}$ ), 116.3 (dd,  $J = 9.4$ ; 1.9,  $\text{C}_4\text{H}$ ), 116.8 (dd,  $J = 24.8$ ; 20.3,  $\text{C}_1$ ), 119.2 ( $\text{C}_5'$ ), 124.4 ( $\text{C}_7\text{H}$ ), 125.3 ( $\text{C}_4'\text{H}$ ), 128.3 ( $\text{C}_6\text{H}$ ), 133.7 ( $\text{C}_{7a}'$ ), 141.9 (dd,  $J = 11.0$ ; 3.3,  $\text{C}_3$ ), 148.1 (dd,  $J = 248.9$ ; 9.1,  $\text{CF}$ ), 152.5 (dd,  $J = 242.2$ ; 7.1,  $\text{CF}$ ), 153.7 ( $\text{C}_{3a}'$ ), 161.1 ( $\text{C}_2'$ ), 169.9 ( $\text{CONH}_2$ ).

MS (ESI): 400.8 [ $\text{M}+\text{H}$ ] $^+$ .

HPLC  $t_r$  (min): 19.75.

**2,6-Difluoro-3-((5-(3-(2,2,2-trifluoroacetamido)prop-1-ynyl)benzo[d]thiazol-2-yl)methoxy)benzamide (16):**



a) Pd(PPh<sub>3</sub>)<sub>4</sub> as catalyst:

2,2,2-Trifluoro-*N*-(prop-2-ynyl)acetamide **12** (397 mg, 2.63 mmol), 3-((5-bromobenzo[d]thiazol-2-yl)methoxy)-2,6-difluorobenzamide **15** (350 mg, 0.88 mmol), tetrakis(triphenylphosphine)palladium(0) (101 mg, 0.09 mmol) and copper(I) iodide (87 mg, 0.46 mmol) were mixed in a microwave vial and purged with argon. Anhydrous dimethylformamide (15 mL) and triethylamine (0.2 mL, 1.13 mmol) were added and the mixture was heated at 100 °C under MW radiation for 45 minutes. The solvent was evaporated under reduced pressure and the brown residue was purified by silica gel column chromatography (hexane → ethyl acetate) to afford 2,6-difluoro-3-((5-(3-(2,2,2-trifluoroacetamido)prop-1-ynyl)benzo[d]thiazol-2-yl)methoxy) benzamide **16** in 86% yield.

IR (ATR): 3301 (NH<sub>2</sub>), 1716 (CO), 1679 (CO), 1553, 1489, 1439 (Ar).

<sup>1</sup>H NMR (DMSO, 300 MHz) δ: 4.32 (d, *J* = 5.6, 2 H, CH<sub>2</sub>NH), 5.70 (s, 2 H, CH<sub>2</sub>O), 7.11 (td app, *J* = 8.9; 1.8, 1 H, C<sub>5</sub>H), 7.39 (td app, *J* = 9.3; 5.2, 1 H, C<sub>4</sub>H), 7.51 (dd, *J* = 8.4; 1.5, 1 H, C<sub>6</sub>H), 7.88 (s br, 1 H, NH), 8.07 (d, *J* = 1.1, 1 H, C<sub>4</sub>H), 8.16 (d, *J* = 8.3, 1 H, C<sub>7</sub>H), 8.17 (s br, 1 H, NH), 10.10 (t, *J* = 5.3, 1 H, NHCH<sub>2</sub>).

<sup>13</sup>C NMR (DMSO, 175 MHz) δ: 29.4 (CH<sub>2</sub>NH), 68.6 (CH<sub>2</sub>O), 82.1 (C≡C), 85.3 (C≡C), 111.1 (dd, *J* = 23.2; 4.0, C<sub>5</sub>H), 116.2 (d, *J* = 9.3, C<sub>4</sub>H), 116.6-117.0 (m, C<sub>1</sub>, CF<sub>3</sub>), 119.9 (C<sub>5</sub>'), 123.1 (C<sub>7</sub>H), 125.5 (C<sub>4</sub>H), 128.3 (C<sub>6</sub>H), 135.1 (C<sub>7a</sub>'), 141.9 (dd, *J* = 11.0; 3.2, 1 C, C<sub>3</sub>), 148.3 (dd, *J* = 248.7; 8.4, CF), 152.3 (dd, *J* = 242.2; 7.1, CF), 152.7 (C<sub>3a</sub>'), 156.2 (d, *J* = 37.0, COCF<sub>3</sub>), 161.1 (C<sub>2</sub>'), 169.3 (CONH<sub>2</sub>).

MS (ESI): 469.6 [M+H]<sup>+</sup>.

HPLC t<sub>r</sub> (min): 17.64.

b) Pd/C as catalyst:

3-((5-Bromobenzo[d]thiazol-2-yl)methoxy)-2,6-difluorobenzamide **15** (101.7 g, 0.25 mmol), cesium carbonate (191.4 mg, 0.57 mmol), 4-diphenylphosphinobenzoic acid (16.5 mg, 46 μmol), 10%

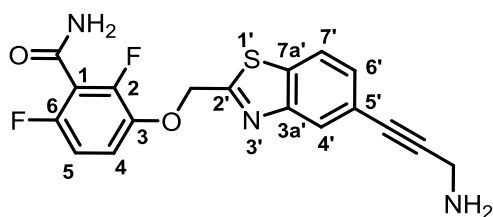
palladium/carbon (1.7 mg, 11  $\mu\text{mol}$ ), copper(I) iodide (10.1 mg, 46  $\mu\text{mol}$ ), dimethylformamide (3 mL) and water (4 mL) were mixed in a microwave vial and purged with argon for 30 minutes. 2,2,2-Trifluoro-*N*-(prop-2-ynyl)acetamide **12** (36 mg, 228  $\mu\text{mol}$ ) in 1 mL of dimethylformamide was added. The mixture was heated in the microwave at 120 °C for 15 minutes. The mixture was filtered through Celite, and the organic and aqueous layers were separated. According to the HPLC-MS analysis, there was no product in either of the two phases.

b)  $\text{Pd}_2(\text{dba})_3 \cdot \text{CHCl}_3$  and PS- $\text{PPh}_3$  as catalyst:

Polystyrene-supported triphenylphosphine (19 mg, 38  $\mu\text{mol}$ ), copper(I) iodide (4 mg, 38  $\mu\text{mol}$ ) and tris(dibenzylideneacetone)dipalladium(0)-chloroform adduct (5 mg, 38  $\mu\text{mol}$ ) were mixed in a microwave vial and purged with argon. 3-((5-Bromobenzo[*d*]thiazol-2-yl)methoxy)-2,6-difluorobenzamide **15** (76 mg, 0.19 mmol), triethylamine (1 mL), 2,2,2-trifluoro-*N*-(prop-2-ynyl)acetamide **12** (150 mg, 0.95 mmol) and anhydrous dimethylformamide (2 mL) were added and the mixture was purged with argon. The reaction was heated at 120 °C in the microwave for 1 hour. After that, there was still some starting material left, and the heating was repeated. The mixture was filtered through Celite and solvents were evaporated. The product was dried under vacuum overnight and the dark brown liquid was purified by silica gel column chromatography (hexane  $\rightarrow$  ethyl acetate) to afford 2,6-difluoro-3-((5-(3-(2,2,2-trifluoroacetamido)prop-1-ynyl)benzo[*d*]thiazol-2-yl)methoxy)benzamide **16** in 54% yield.

Spectroscopic data as earlier.

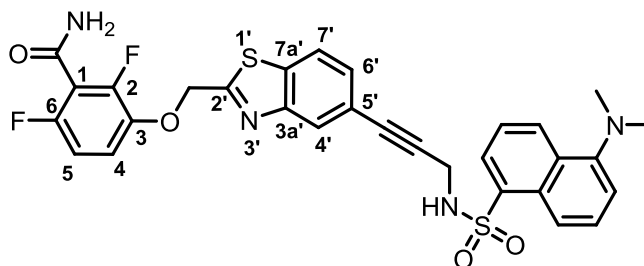
### 3-((5-(3-Aminoprop-1-yn-1-yl)benzo[*d*]thiazol-2-yl)methoxy)-2,6-difluorobenzamide (**17**)



2,6-Difluoro-3-((5-(3-(2,2,2-trifluoroacetamido)prop-1-ynyl)benzo[*d*]thiazol-2-yl)methoxy)benzamide **16** (150 mg, 0.32 mmol) was dissolved in methanol (30 mL) and 28% aqueous ammonia solution (22 mL) was added. The light green solution was stirred at room temperature overnight. Afterward, solvents were evaporated under reduced pressure and the crude was triturated with diethyl ether to afford 3-((5-(3-aminoprop-1-ynyl)benzo[*d*]thiazol-2-

yl)methoxy)-2,6-difluorobenzamide **17** in 92% yield, which was used in the next step without purification. MS (EI): 374.1 [M+H]<sup>+</sup>.

**3-((5-(3-(5-(Dimethylamino)naphthalene-1-sulfonamido)prop-1-ynyl)benzo[d]thiazol-2-yl)methoxy)-2,6-difluorobenzamide (2a)**



3-((5-(3-Aminoprop-1-ynyl)benzo[d]thiazol-2-yl)methoxy)-2,6-difluorobenzamide **17** was dissolved in a mixture of anhydrous dimethylformamide (1 mL) and dichloromethane (2 mL), and triethylamine (62  $\mu$ L, 0.442 mmol) was added under an argon atmosphere. Then, a solution of dansyl chloride (60 mg, 0.221 mmol) in anhydrous dichloromethane (1 mL) was added. The reaction mixture was stirred at room temperature for 20 hours. The solvents were evaporated under reduced pressure. The residue was dissolved in dichloromethane and washed with saturated aqueous sodium bicarbonate. The organic layer was dried with sodium sulfate, filtered and concentrated. The crude was purified by silica gel column chromatography (dichloromethane  $\rightarrow$  ethyl acetate) to afford 3-((5-(3-(5-(dimethylamino)naphthalene-1-sulfonamido)prop-1-ynyl)benzo[d]thiazol-2-yl)methoxy)-2,6-difluorobenzamide **2a** as a yellow solid in 28% yield.

Melting point: 194-196  $^{\circ}$ C.

IR (ATR): 1739, 1681 (CO), 1489, 1461 (Ar)

<sup>1</sup>H NMR (DMSO, 700 MHz)  $\delta$ : 2.67 (s, 6 H, 2 CH<sub>3</sub>), 4.04 (d,  $J$  = 4.9, 2 H, CH<sub>2</sub>N), 5.67 (s, 2 H, CH<sub>2</sub>O), 6.79 (dd,  $J$  = 8.3; 1.4, 1 H, CH<sub>Ds</sub>), 7.12 (t app,  $J$  = 9.0, 1 H, C<sub>5</sub>H), 7.21 (d,  $J$  = 7.4, 1 H, CH<sub>Ds</sub>), 7.27 (d,  $J$  = 0.8, 1 H, C<sub>4'</sub>H), 7.38 (td app,  $J$  = 9.2; 5.1, 1 H, C<sub>4</sub>H), 7.58-7.63 (m, 2 H, C<sub>6</sub>H, CH<sub>Ds</sub>), 7.90 (s br, 1 H, NH), 7.96 (d,  $J$  = 8.3, 1 H, C<sub>7</sub>H), 8.17 (s br, 1 H, NH), 8.22 (dd,  $J$  = 7.2; 1.0, 1 H, CH<sub>Ds</sub>), 8.32 (d,  $J$  = 8.6, 1 H, CH<sub>Ds</sub>), 8.36 (d,  $J$  = 8.6, 1 H, CH<sub>Ds</sub>), 8.53 (t,  $J$  = 5.0, 1 H, NHSO<sub>2</sub>).

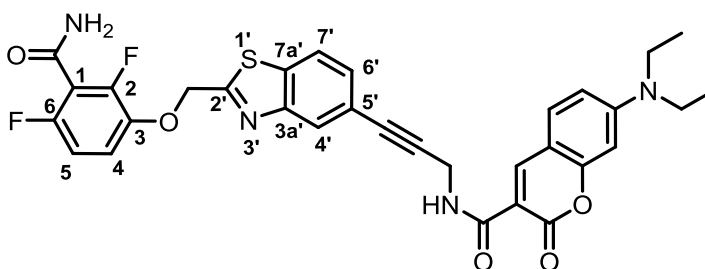
<sup>13</sup>C NMR (DMSO, 175 MHz)  $\delta$ : 32.4 (CH<sub>2</sub>N), 44.9 (2 CH<sub>3</sub>), 68.5 (CH<sub>2</sub>O), 82.2 (C $\equiv$ C), 86.3 (C $\equiv$ C), 111.2 (dd,  $J$  = 25.0; 2.9, C<sub>5</sub>H), 115.0 (CH<sub>Ds</sub>), 116.2 (d,  $J$  = 8.7, C<sub>4</sub>H), 116.9 (dd,  $J$  = 25.5; 20.0, C<sub>1</sub>), 119.2 (CH<sub>Ds</sub>), 119.6 (C<sub>5'</sub>), 122.6 (C<sub>7</sub>H), 123.6 (C<sub>4'</sub>H), 124.9 (C<sub>6'</sub>H), 127.7 (CH<sub>Ds</sub>), 127.8 (CH<sub>Ds</sub>), 129.0 (CH<sub>Ds</sub>), 129.4 (C<sub>Ds</sub>), 129.8 (CH<sub>Ds</sub>), 132.1 (C<sub>7a</sub>), 134.7 (C<sub>Ds</sub>), 136.0 (C<sub>Ds</sub>), 142.3 (dd,  $J$  = 10.8; 2.4, C<sub>3</sub>), 148.0 (dd,  $J$  = 248.8; 8.4, CF), 151.4 (C<sub>Ds</sub>), 152.1 (C<sub>3a'</sub>), 152.5 (dd,  $J$  = 243.1; 6.7, CF), 161.1 (C<sub>2'</sub>), 169.0 (CONH<sub>2</sub>).

Elemental Analysis of C<sub>30</sub>H<sub>24</sub>F<sub>2</sub>N<sub>4</sub>O<sub>4</sub>S<sub>2</sub>: Calculated (%): C: 59.39; H: 3.99; N: 9.24; S: 10.57. Observed (%): C: 60.57; H: 4.27; N: 7.93; S: 8.77 (impurity Ph<sub>3</sub>PO).

MS (EI): 607.1 [M+H]<sup>+</sup>.

HPLC t<sub>r</sub> (min): 14.78.

***N*-(3-(2-((3-carbamoyl-2,4-difluorophenoxy)methyl)benzo[d]thiazol-5-yl)prop-2-ynyl)-7-(diethylamino)-2-oxo-2*H*-chromene-3-carboxamide (2b)**



To a solution of 3-((5-(3-aminoprop-1-ynyl)benzo[d]thiazol-2-yl)methoxy)-2,6-difluorobenzamide **17** (119 mg, 0.32 mmol) in anhydrous dimethylformamide (5 mL), DIPEA (0.1 mL, 0.64 mmol), PyBrOP (268 mg, 0.57 mmol) and 7-(diethylamino)coumarin-3-carboxylic acid (100 mg, 0.38 mmol) were added under an argon atmosphere. The mixture was stirred at room temperature for 4 hours. The solvent was evaporated under vacuum, and the crude was purified by silica gel column chromatography (dichloromethane/ethyl acetate 1:1) to obtain *N*-(3-(2-((3-carbamoyl-2,4-difluorophenoxy)methyl)benzo[d]thiazol-5-yl)prop-2-ynyl)-7-(diethylamino)-2-oxo-2*H*-chromene-3-carboxamide **2b** in 5% yield.

Melting point: 248-249 °C.

<sup>1</sup>H NMR (DMSO, 700 MHz) δ: 1.17 (t, *J* = 7.0, 6 H, 2 CH<sub>3</sub>), 3.50 (q, *J* = 6.9, 4 H, 2 CH<sub>2</sub><sub>coum</sub>), 4.43 (d, *J* = 5.5, 2 H, CH<sub>2</sub>NH), 5.71 (s, 2 H, CH<sub>2</sub>O), 6.64 (d, *J* = 2.0, 1 H, CH<sub>coum</sub>), 6.83 (dd, *J* = 8.9; 2.1, 1 H, CH<sub>coum</sub>), 7.13 (t app, *J* = 8.8, 1 H, C<sub>5</sub>H), 7.40 (td app, *J* = 9.1; 5.1, 1 H, C<sub>4</sub>H), 7.52 (dd, *J* = 8.3; 1.1, 1 H, C<sub>6</sub>H), 7.72 (d, *J* = 9.1, 1 H, CH<sub>coum</sub>), 7.90 (s br, 2 H, NH<sub>2</sub>), 8.08 (s, 1 H, CH<sub>4'</sub>), 8.16 (d, *J* = 8.4, 1 H, C<sub>7</sub>H), 8.18 (s br, 2 H, NH<sub>2</sub>), 8.72 (s, 1 H, CH<sub>coum</sub>), 9.00 (t, *J* = 5.5, 1 H, NH).

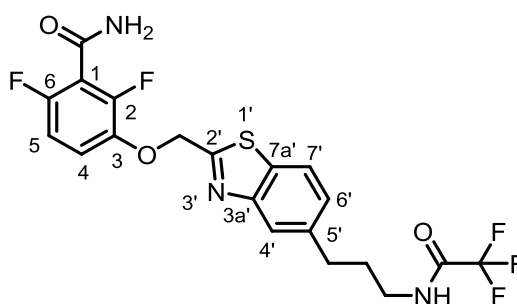
<sup>13</sup>C NMR (DMSO, 175 MHz) δ: 12.3 (2 CH<sub>3</sub>), 29.2 (CH<sub>2</sub>NH), 44.4 (2 CH<sub>2</sub>N), 68.8 (CH<sub>2</sub>O), 81.1 (C≡C), 87.5 (C≡C), 95.9 (CH<sub>coum</sub>), 107.7 (C<sub>coum</sub>), 108.8 (C<sub>coum</sub>), 110.2 (CH<sub>coum</sub>), 111.1 (dd, *J* = 24.3; 4.2, C<sub>5</sub>H), 116.2 (d, *J* = 9.9, C<sub>4</sub>H), 117.6-118.0 (m, C<sub>1</sub>), 120.4 (C<sub>5'</sub>), 123.0 (C<sub>7</sub>H), 125.4 (C<sub>4</sub>H), 128.4 (CH<sub>coum</sub>), 132.0 (C<sub>6</sub>H), 134.8 (C<sub>7a'</sub>), 141.8-142.1 (m, C<sub>3</sub>), 148.2 (CH<sub>coum</sub>), 149.2 (d, *J* = 265.5, CF), 152.5 (d, *J* = 242.0, CF), 152.5 (C<sub>3a'</sub>), 152.6 (C<sub>coum</sub>), 157.4 (C<sub>coum</sub>), 161.1 (CONH<sub>2</sub>), 161.7 (CONH), 162.2 (CO<sub>coum</sub>), 169.2 (C<sub>2</sub>).

Elemental Analysis of  $C_{32}H_{26}F_2N_4O_5S$ : Calculated (%): C: 57.31; H: 4.81; N: 8.35 S: 4.78. Observed (%): C: 57.21; H: 4.55; N: 7.96; S: 4.58.

MS (EI): 617.2  $[M+H]^+$ .

HPLC  $t_r$  (min): 23.27.

**2,6-Difluoro-3-((5-(3-(2,2,2-trifluoroacetamido)propyl)benzo[d]thiazol-2-yl)methoxy)benzamide (18)**



Raney-Ni was added to a solution of 2,6-difluoro-3-((5-(3-(2,2,2-trifluoroacetamido)prop-1-ynyl)benzo[d]thiazol-2-yl)methoxy)benzamide **16** (250 mg, 0.53 mmol) in a mixture of anhydrous tetrahydrofuran (20 mL) and methanol (40 mL) under an argon atmosphere, and the mixture was hydrogenated for 3 hours (1 bar). Then, the mixture was filtered through Celite and concentrated under reduced pressure. The crude was purified by silica gel column chromatography (hexane → ethyl acetate) to afford 2,6-difluoro-3-((5-(3-(2,2,2-trifluoroacetamido)propyl)benzo[d]thiazol-2-yl)methoxy)benzamide **18** in 22% yield.

IR (ATR): 3303 (NH), 1710, 1680 (CO), 1490 (Ar).

$^1H$  NMR (MeOD, 300 MHz)  $\delta$ : 1.96 (q app,  $J = 7.5$ , 2 H,  $CH_2CH_2CH_2$ ), 2.82 (t,  $J = 7.7$ , 2 H,  $CH_2Ar$ ), 3.34 (t,  $J = 7.2$ , 2 H,  $CH_2N$ ), 5.57 (s, 2 H,  $CH_2O$ ), 6.97 (td app,  $J = 8.9$ ; 1.8, 1 H,  $C_5H$ ), 7.32 (td app,  $J = 9.2$ ; 5.0, 1 H,  $C_4H$ ), 7.35 (dd,  $J = 8.3$ ; 1.3, 1 H,  $C_6H$ ), 7.57 (s, 1 H,  $NHCO$ ), 7.84 (s, 1 H,  $C_4'H$ ), 7.92 (d,  $J = 8.3$ , 1 H,  $C_7'H$ ).

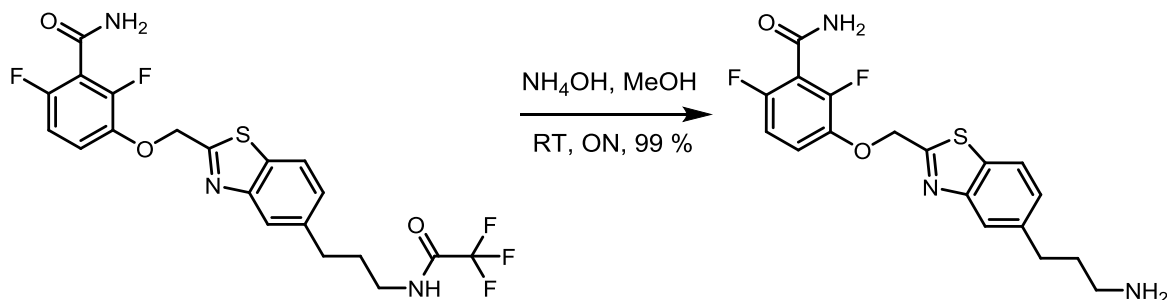
$^{13}C$  NMR (MeOD, 75 MHz)  $\delta$ : 31.7 ( $CH_2$ ), 33.8 ( $CH_2Ar$ ), 40.3 ( $CH_2NH$ ), 70.4 ( $CH_2O$ ), 112.1 (dd,  $J = 23.7$ , 3.7,  $C_5H$ ), 117.0-117.2 (m,  $C_1$ ), 117.6 (q,  $J = 286$ ,  $CF_3$ ), 118.7 (d,  $J = 9.2$ ,  $C_4H$ ), 123.2 ( $C_7'H$ ), 127.8 ( $C_4'H$ ), 130.0 ( $C_6'H$ ), 133.9 ( $C_5'$ ), 141.7 ( $C_7'a$ ), 143.8 (dd,  $J = 11.2$ ; 2.4,  $C_3$ ), 150.7 (dd,  $J = 252$ ; 8.2, CF), 154.2 ( $C_{3'a}$ ), 154.9 (dd,  $J = 250$ ; 6.6, CF), 159.0 (d,  $J = 36.8$ ,  $COCF_3$ ), 165.0 ( $C_2'$ ), 169.7 ( $CONH_2$ ).

MS (EI): 473.7  $[M+H]^+$ .

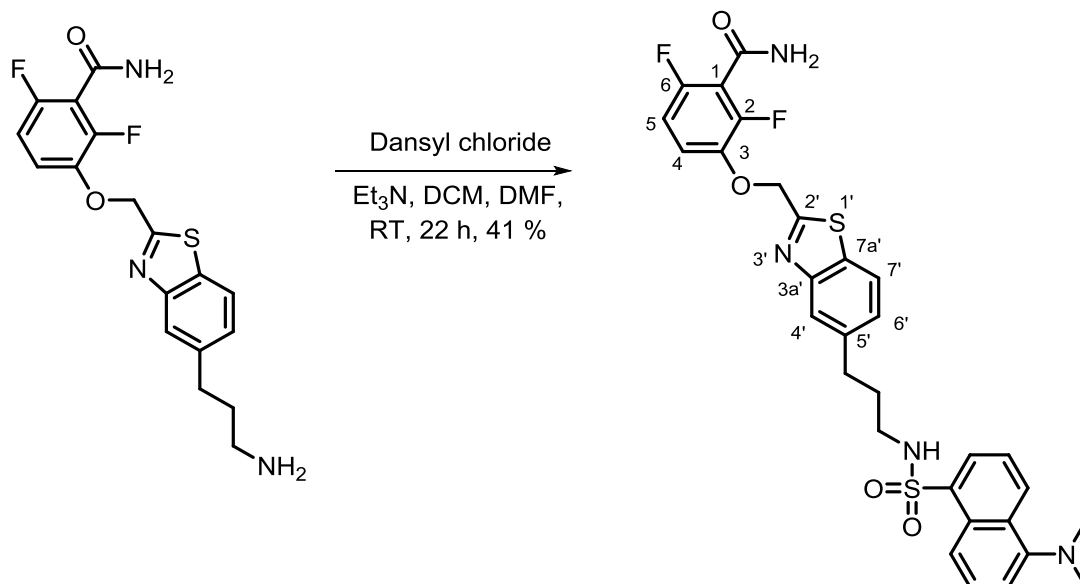
HPLC  $t_r$  (min): 20.27.

**3-((5-(3-((5-(Dimethylamino)naphthalene)-1-sulfonamido)propyl)benzo[d]thiazol-2-yl)methoxy)-2,6-difluorobenzamide (3)**

via 3-((5-(3-Aminopropyl)benzo[d]thiazol-2-yl)methoxy)-2,6-difluorobenzamide:



To a solution of 2,6-difluoro-3-((5-(3-(2,2,2-trifluoroacetamido)propyl)benzo[d]thiazol-2-yl)methoxy)benzamide **18** (61 mg, 0.13 mmol) in methanol (16 mL), 28% aqueous ammonia solution (7.8 mL) was added, and the reaction was stirred at room temperature overnight. Then, the solvent was evaporated under vacuum to afford 3-((5-(3-aminopropyl)benzo[d]thiazol-2-yl)methoxy)-2,6-difluorobenzamide in 99% yield, which was used without purification. MS (EI): 378.1  $[\text{M}+\text{H}]^+$ .



To a solution of 3-((5-(3-aminopropyl)benzo[d]thiazol-2-yl)methoxy)-2,6-difluorobenzamide (52 mg, 0.14 mmol) in a mixture of anhydrous dimethylformamide (1 mL) and dichloromethane (2 mL), triethylamine (58  $\mu\text{L}$ , 0.41 mmol) was added under an argon atmosphere. Then, a solution of dansyl chloride (56 mg, 0.21 mmol) in anhydrous dichloromethane (1 mL) was added dropwise, and the

mixture was stirred at room temperature for 22 hours. After this time, the solvent was evaporated under reduced pressure, and the crude was purified by silica gel column chromatography (dichloromethane → ethyl acetate) to afford 3-((5-(3-((5-(dimethylamino)naphthalene)-1-sulfonamido)propyl)benzo[d]thiazol-2-yl)methoxy)-2,6-difluorobenzamide **3** in 13% yield.

Melting point: 185-186 °C.

IR (ATR): 3435 (NH), 1670 (C=O), 1604, 1486, 1450 (Ar).

<sup>1</sup>H NMR (DMSO, 700) δ: 1.58 (qt app, *J* = 7.2, 2 H, CH<sub>2</sub>CH<sub>2</sub>CH<sub>2</sub>), 2.55 (t, *J* = 7.7, 2 H, CH<sub>2</sub>Ar), 2.82 (s, 6 H, 2 CH<sub>3</sub>), 2.83 (t, *J* = 7.3, 2 H, CH<sub>2</sub>N), 5.66 (s, 2 H, CH<sub>2</sub>O), 7.02 (dd, *J* = 8.2; 1.5, 1 H, CH<sub>Ds</sub>), 7.10 (t app, *J* = 9.0, 1 H, C<sub>5</sub>H), 7.26 (d, *J* = 7.3, 1 H, CH<sub>Ds</sub>), 7.38 (td app, *J* = 9.2; 5.1, 1 H, C<sub>4</sub>H), 7.57-7.62 (m, 3 H, CH<sub>Ds</sub>, C<sub>4</sub>H, C<sub>6</sub>H), 7.89 (s br, 1 H, NH), 7.92 (d, *J* = 8.2, 1 H, C<sub>7</sub>H), 8.01 (t, *J* = 5.9, 1 H, NHSO<sub>2</sub>), 8.07 (dd, *J* = 7.1; 1.1, 1 H, CH<sub>Ds</sub>), 8.18 (s br, 1 H, NH), 8.33 (d, *J* = 8.7, 1 H, CH<sub>Ds</sub>), 8.45 (d, *J* = 8.44, 1 H, CH<sub>Ds</sub>).

<sup>13</sup>C-RMN (DMSO, 175 MHz) δ: 31.1, 31.8 (CH<sub>2</sub>CH<sub>2</sub>Ar), 41.8 (CH<sub>2</sub>N), 45.1 (2 CH<sub>3</sub>), 68.5 (CH<sub>2</sub>O), 111.1 (d, *J* = 21.6, C<sub>5</sub>H), 115.1 (CH<sub>Ds</sub>), 116.2 (d, *J* = 21.6, C<sub>4</sub>H), 116.8 (t, *J* = 23.4, C<sub>1</sub>), 119.1 (CH<sub>Ds</sub>), 122.0 (C<sub>7</sub>H), 123.6 (C<sub>4</sub>H), 126.2 (C<sub>6</sub>H), 127.9 (2 CH<sub>Ds</sub>), 128.3 (CH<sub>Ds</sub>), 129.1 (C<sub>Ds</sub>, C<sub>5'</sub>), 129.4 (CH<sub>Ds</sub>), 131.9 (C<sub>7a'</sub>), 136.1 (C<sub>Ds</sub>), 140.1 (C<sub>Ds</sub>), 142.0 (d, *J* = 9.0, C<sub>3</sub>), 148.0 (dd, *J* = 249.5; 7.7, CF), 151.4 (C<sub>Ds</sub>), 152.9 (C<sub>3a'</sub>), 152.4 (d, *J* = 240.4, CF), 161.1 (C<sub>2'</sub>), 167.4 (CON).

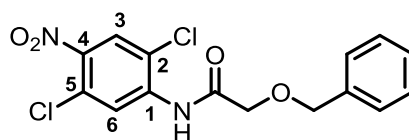
Elemental Analysis of C<sub>30</sub>H<sub>28</sub>F<sub>2</sub>N<sub>4</sub>O<sub>4</sub>S<sub>2</sub>: Calculated (%): C: 59.00; H: 4.62; N: 9.17; S: 10.50. Observed (%): C: 58.41; H: 4.63; N: 9.17; S: 10.19.

MS (EI): 611.2 [M+H]<sup>+</sup>.

HPLC t<sub>r</sub> (min): 21.13.

### 4.3 Set III

#### 2-(Benzyloxy)-*N*-(2,5-dichloro-4-nitrophenyl)acetamide (**21**)



A solution of 2,5-dichloro-4-nitroaniline **19** (7.32 g, 35.4 mmol) in anhydrous dichloromethane (100 mL) was cooled in an ice bath and triethylamine (7.5 mL, 53.8 mmol) was added under an argon atmosphere. Then, a solution of benzyloxyacetyl chloride (5 mL, 31.7 mmol) in anhydrous dichloromethane (35 mL) was added dropwise to the former, and the reaction mixture was stirred at room temperature for 22 hours. Afterward, the mixture was washed with water (50 mL) and



brine (50 mL). The organic phase was dried with sodium sulfate, filtered and concentrated under vacuum to yield a yellow solid, which was purified by silica gel column chromatography (hexane → hexane/ethyl acetate 95:5 → ethyl acetate) to afford 2-(benzyloxy)-*N*-(2,5-dichloro-4-nitrophenyl)acetamide **21** in 26% yield.

IR (ATR): 3362 (NH), 1705 (CO), 1574-1506 (Ar).

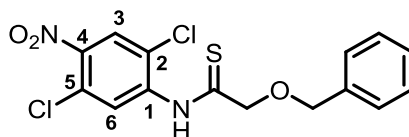
<sup>1</sup>H NMR (CDCl<sub>3</sub>, 300 MHz) δ: 4.10 (s, 2 H, COCH<sub>2</sub>), 4.64 (s, 2 H, CH<sub>2</sub>Ph), 7.27-7.36 (m, 5 H, CH<sub>Ph</sub>), 8.01 (s, 1 H, C<sub>6</sub>H), 8.77 (s, 1 H, C<sub>3</sub>H), 9.22 (s, 1 H, NH).

<sup>13</sup>C NMR (CDCl<sub>3</sub>, 75 MHz) δ: 69.4, 74.0 (2 CH<sub>2</sub>), 120.8 (CCl), 122.4, 126.6 (C<sub>3</sub>H, C<sub>6</sub>H), 127.9 (2 CH<sub>Bn</sub>), 128.6 (CCl), 128.7 (CH<sub>Ph</sub>), 128.8 (2 CH<sub>Bn</sub>), 136.1 (CNH), 138.3 (C<sub>Ph</sub>), 142.3 (CNO<sub>2</sub>), 168.2 (CO).

MS (EI): 378 [M+Na]<sup>+</sup>.

HPLC t<sub>r</sub> (min): 24.08.

### 2-(Benzyloxy)-*N*-(2,5-dichloro-4-nitrophenyl)ethanethioamide (**22**)



2-(Benzyloxy)-*N*-(2,5-dichloro-4-nitrophenyl)acetamide **21** (1.15 g, 3.24 mmol) was dissolved in anhydrous toluene (30 mL) and Lawesson's reagent (1.31 g, 3.24 mmol) was added under an argon atmosphere. The mixture was refluxed for 13.5 hours, and after that stirred at room temperature for 6 hours. Then, it was filtered through a short path of silica gel, washing with dichloromethane. The solvents were evaporated under reduced pressure to obtain a brown liquid, which was purified by silica gel column chromatography (hexane → hexane/ethyl acetate 7:3 → ethyl acetate) to obtain 2-(benzyloxy)-*N*-(2,5-dichloro-4-nitrophenyl)ethanethioamide **22** in 71% yield.

IR (ATR): 3263 (NH), 1575, 1514, 1513 (Ar).

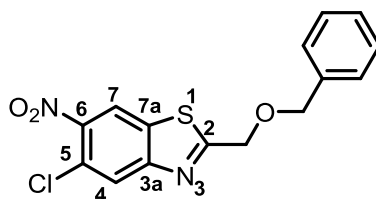
<sup>1</sup>H NMR (CDCl<sub>3</sub>, 300 MHz) δ: 4.47 (s, 2 H, CSCH<sub>2</sub>), 4.72 (s, 2 H, CH<sub>2</sub>Ph), 7.30-7.39 (m, 5 H, CH<sub>Ph</sub>), 8.08 (s, 1 H, C<sub>3</sub>H), 9.71 (s, 1 H, C<sub>6</sub>H), 10.58 (s, 1 H, NH).

<sup>13</sup>C NMR (CDCl<sub>3</sub>, 75 MHz) δ: 73.8, 77.3 (2 CH<sub>2</sub>), 123.5 (CCl), 124.0 (C<sub>6</sub>H), 126.7 (C<sub>3</sub>H), 127.2 (CCl), 128.1 (2 CH<sub>Ph</sub>), 128.8 (CH<sub>Ph</sub>), 128.9 (2 CH<sub>Ph</sub>), 136.2 (C<sub>Ph</sub>), 138.5 (CNH), 143.5 (CNO<sub>2</sub>), 198.3 (CS).

EM (ESI): 370.7 [M+H]<sup>+</sup>.

HPLC t<sub>r</sub> (min): 25.51.

### 2-((Benzyloxy)methyl)-5-chloro-6-nitrobenzo[*d*]thiazole (**23**)



2-(Benzyloxy)-*N*-(2,5-dichloro-4-nitrophenyl)ethanethioamide **22** (670 mg, 1.81 mmol) was dissolved in *N*-methyl-2-pyrrolidone (14 mL) under an argon atmosphere, and 60% sodium hydride in mineral oil (50 mg, 1.25 mmol) was added slowly. The mixture was refluxed for 1 hour, and then 20 mg of sodium hydride were added and reflux was continued for 0.5 hours. After cooling down the reaction to room temperature, ice-water was added, and the aqueous phase was extracted four times with ethyl acetate. The combined organic phases were washed with brine, dried with sodium sulfate, filtered and evaporated under reduced pressure to obtain dark brown crude, which was purified by silica gel column chromatography (hexane → hexane/ethyl acetate 86:14 → ethyl acetate) to afford 2-((benzyloxy)methyl)-5-chloro-6-nitrobenzo[*d*]thiazole **23** in 17% yield.

IR (ATR): 1727 (CN), 1545, 1461 (Ar).

<sup>1</sup>H NMR (CDCl<sub>3</sub>, 300 MHz) δ: 4.76, 4.94 (s, 4 H, 2 CH<sub>2</sub>), 7.33-7.42 (m, 5 H, CH<sub>Ph</sub>), 8.11 (s, 1 H, C<sub>3</sub>H), 8.47 (s, 1 H, C<sub>6</sub>H).

<sup>13</sup>C NMR (CDCl<sub>3</sub>, 75 MHz) δ: 69.4, 73.9 (2 CH<sub>2</sub>), 119.8 (C<sub>7</sub>H), 125.1 (C<sub>Cl</sub>), 125.6 (C<sub>4</sub>H), 128.1 (2 CH<sub>Ph</sub>), 128.5 (CH<sub>Ph</sub>), 128.8 (2 CH<sub>Ph</sub>), 133.6 (C<sub>7a</sub>), 136.7 (C<sub>Ph</sub>), 144.9 (CNO<sub>2</sub>), 155.7 (C<sub>3a</sub>), 178.2 (C<sub>2</sub>).

### 3.4 Biological evaluation

Expression and purification of Bs-FtsZ and polymer pelleting assays were carried out as described by Andreu et al. (2010).<sup>11</sup> Fluorescence measurements were performed with Horiba-Jovin-Yvon Fluoromax-4 spectrofluorometer at 25 °C with sample volumes of 500 μL in cuvettes of 10 x 2 mm. The excitation wavelengths were selected according to absorption spectra previously registered. The measurements were made with concentrations of 10 μM for the compound of interest (except 20 μM for **1a**), 10 μM Bs-FtsZ, 10 μM MgCl<sub>2</sub>, 10 μM PC190723 or 8J, 0.1 mM GMPCCP or GTP in 50 mM HEPES, pH 6.8 in the presence of 2% DMSO.

## 5. References

1. Nogales, E., Downing, K. H., Amos, L. A. and Löwe, J. *Nat. Struct. Biol.* **1998**, 5 (6), 451.
2. Errington, J., Daniel, R. and Scheffers, D. *Microbiol. Mol. Biol. Rev.* **2003**, 67 (1), 52-65.
3. Lutkenhaus, J., Pichoff, S. and Du, S. *Cytoskeleton* **2012**, 69, 778-790.
4. Schaffner-Barbero, C., Martín-Fontecha, M., Chacón, P. and Andreu, J. M. *ACS Chem. Biol.* **2012**, 7 (2), 269-277.
5. Li, X. and Ma, S. *Eur. J. Med. Chem.* **2015**, 1-15.
6. Ohashi, Y., Chijiwa, Y., Suzuki, K., Takahashi, K., Nanamiya, H., Sato, T., Hosoya, Y., Ochi, K. and Kawamura, F. *J. Bacteriol.* **1999**, 181 (4), 1348-1351.
7. Haydon, D. J., Stokes, N. R., Ure, R., Galbraith, G., Bennett, J. M., Brown, D. R., Baker, P. J., Barynin, V. V., Rice, D. W., Sedelnikova, S. E., Heal, J. R., Sheridan, J. M., Aiwale, S. T., Chauhan, P. K., Srivastava, A., Taneja, A., Collins, I., Errington, J. and Czaplewski, L. G. *Science* **2008**, 321 (5896), 1673-1675.
8. Haydon, D. J., Bennett, J. M., Brown, D., Collins, I., Galbraith, G., Lancett, P., Macdonald, R., Stokes, N. R., Chauhan, P. K., Sutariya, J. K., Nayal, N., Srivastava, A., Beanland, J., Hall, R., Henstock, V., Noula, C., Rockley, C. and Czaplewski, L. *J. Med. Chem.* **2010**, 53 (10), 3927-3936.
9. Tan, C. M., Therien, A. G., Lu, J., Lee, S. H., Caron, A., Gill, C. J., Lebeau-Jacob, C., Benton-Perdomo, L., Monteiro, J. M., Pereira, P. M., Elsen, N. L., Wu, J., Deschamps, K., Petcu, M., Wong, S., Daigneault, E., Kramer, S., Liang, L., Maxwell, E., Claveau, D., Vaillancourt, J., Skorey, K., Tam, J., Wang, H., Meredith, T. C., Sillaots, S., Wang-Jarantow, L., Ramtohl, Y., Langlois, E., Landry, F., Reid, J. C., Parthasarathy, G., Sharma, S., Baryshnikova, A., Lumb, K. J., Pinho, M. G., Soisson, S. M. and Roemer, T. *Sci. Transl. Med.* **2012**, 4 (126), 126ra35.
10. Elsen, N. L., Lu, J., Parthasarathy, G., Reid, J. C., Sharma, S., Soisson, S. M. and Lumb, K. J. *J. Am. Chem. Soc.* **2012**, 134 (30), 12342-12345.
11. Andreu, J. M., Schaffner-Barbero, C., Huecas, S., Alonso, D., López-Rodríguez, M. L., Ruíz-Ávila, L. B., Núñez-Ramírez, R., Llorca, O. and Martín-Galiano, A. J. *J. Biol. Chem.* **2010**, 285 (19), 14239-14246.
12. Sorto, N. A., Olmstead, M. M. and Shaw, J. T. *J. Org. Chem.* **2010**, 75 (22), 7946-7949.
13. Miguel, A., Hsin, J., Liu, T., Tang, G., Altman, R. B. and Huang, K. C. *PLoS Comp. Biol.* **2015**, 11 (3), e1004117.

## 6. Appendix

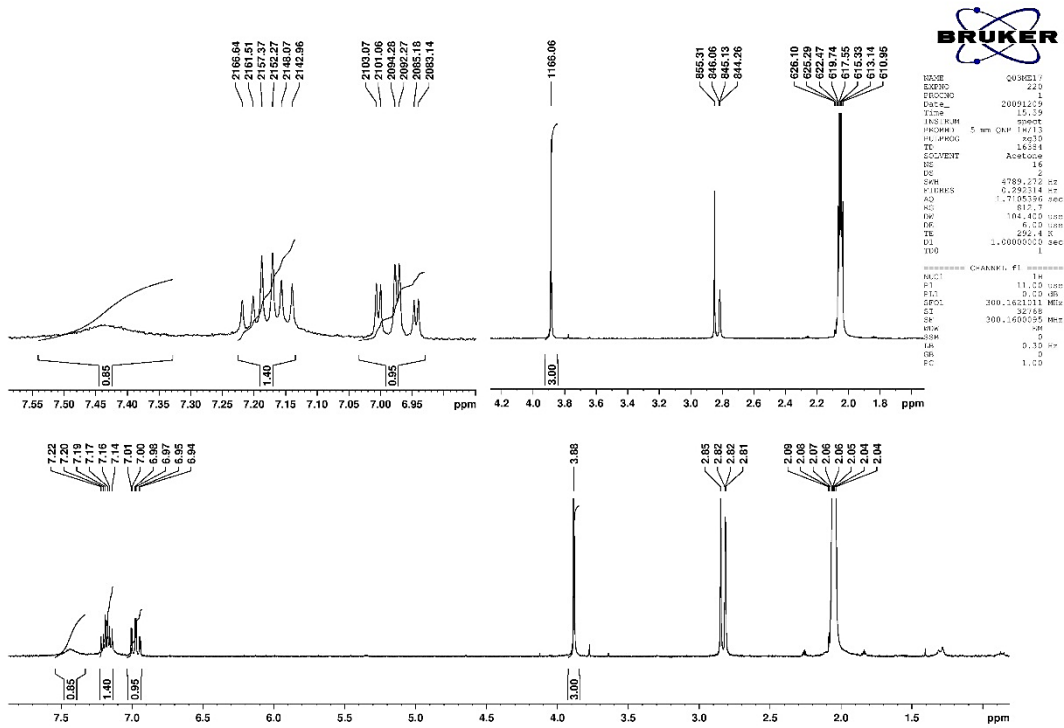


Figure A 1.  $^1\text{H}$  NMR spectrum of 6.

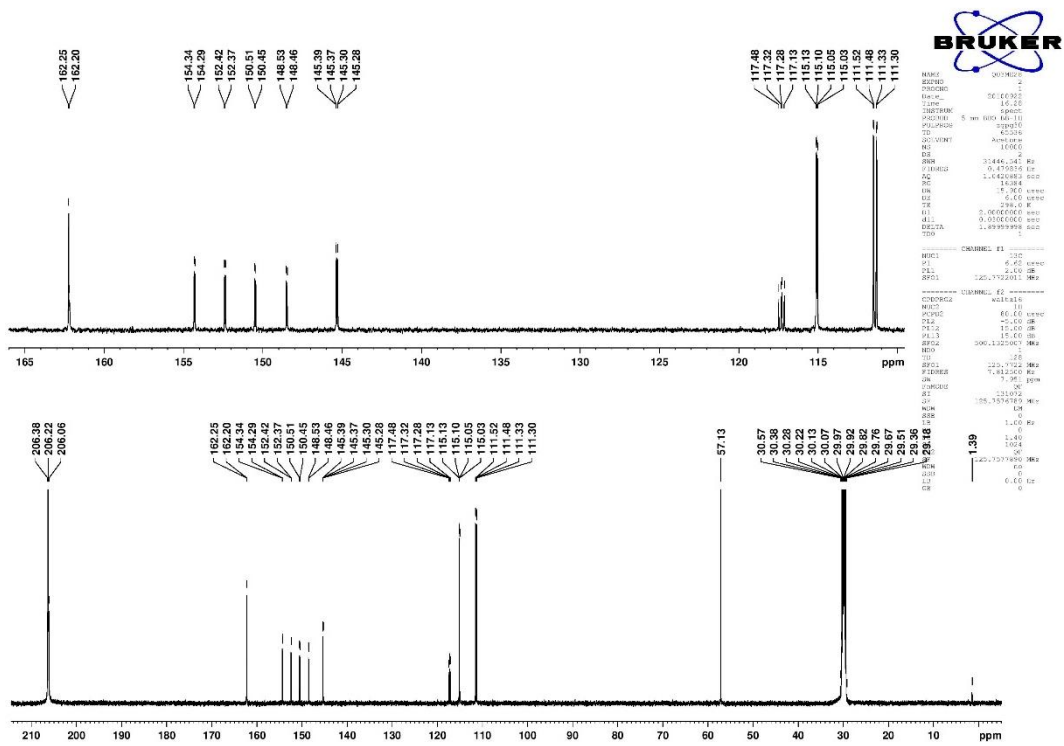


Figure A 2.  $^{13}\text{C}$  NMR spectrum of 6.

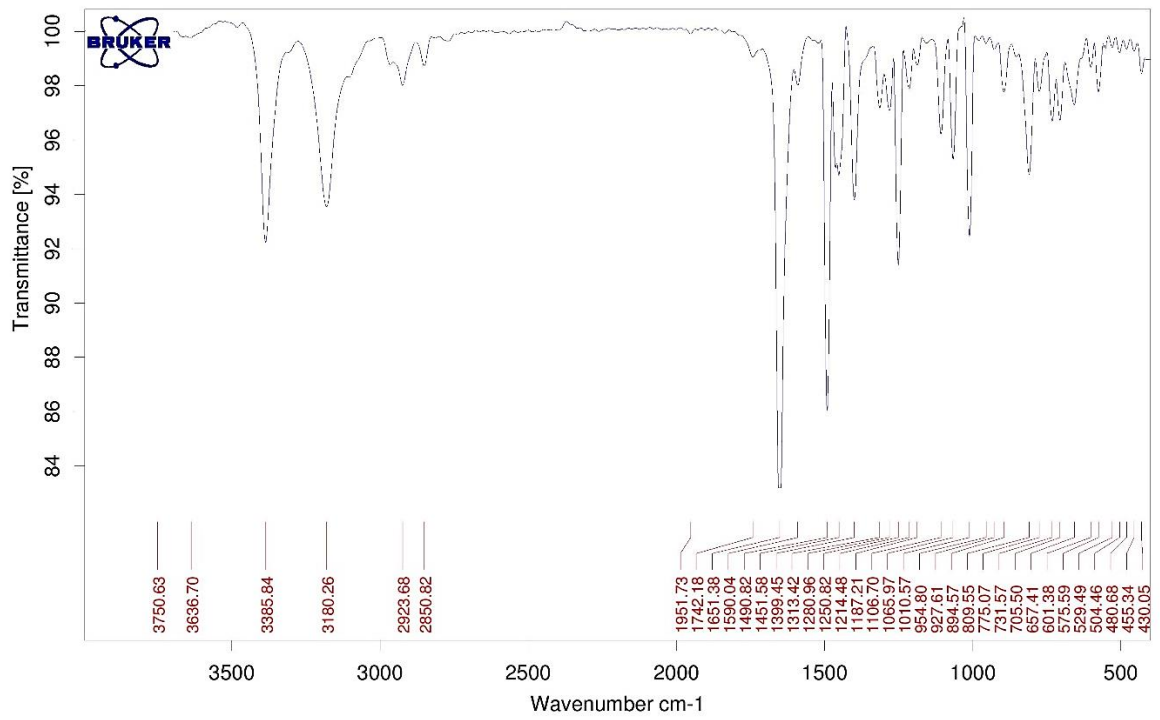


Figure A 3. IR spectrum of 6.

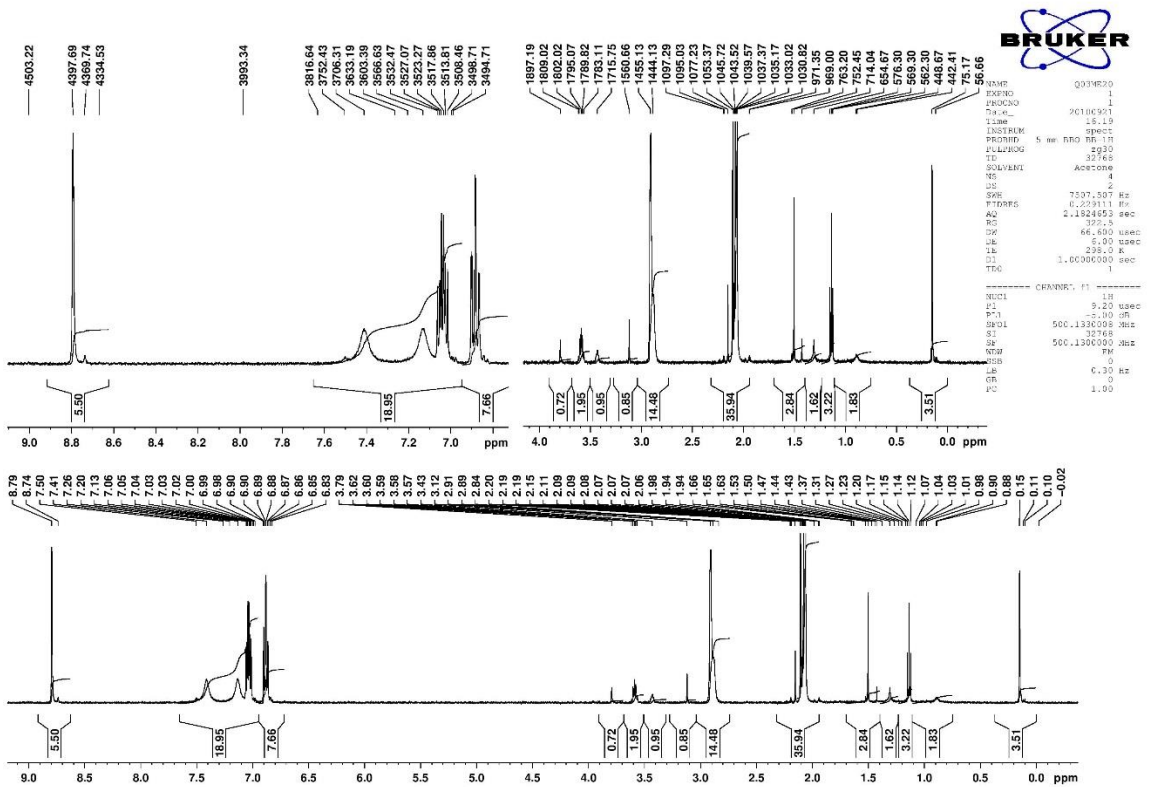


Figure A 4. <sup>1</sup>H NMR spectrum of 7.

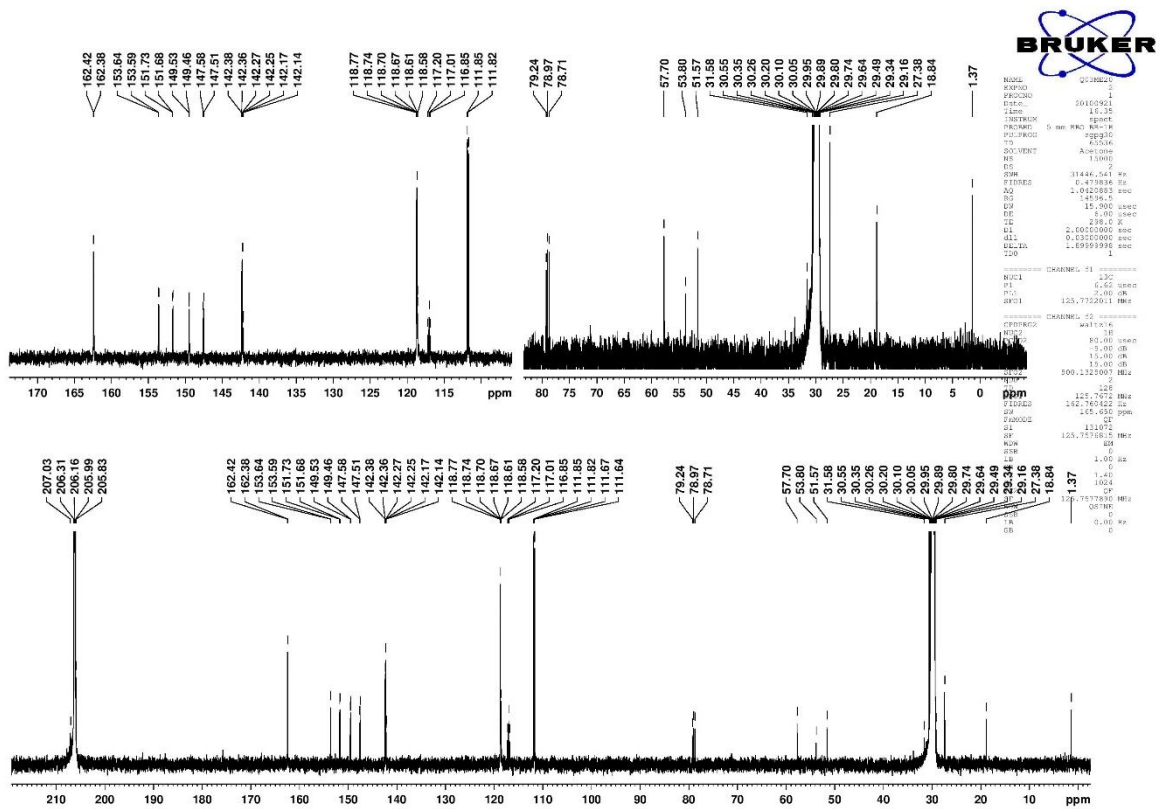


Figure A 5. <sup>13</sup>C NMR spectrum of 7.

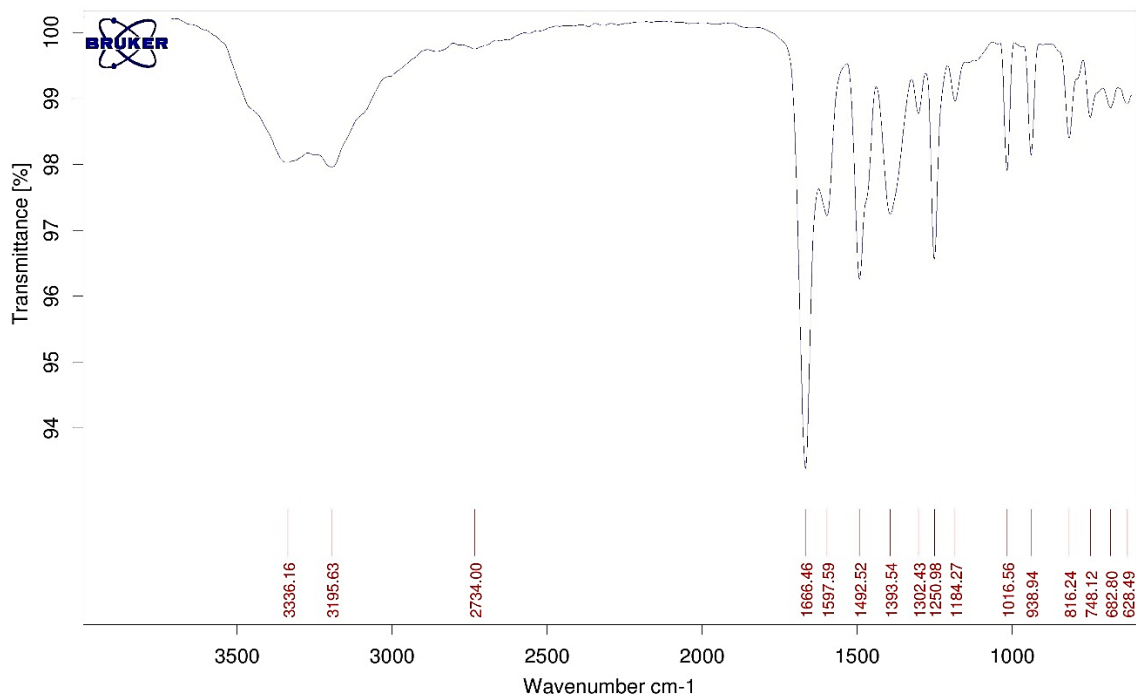


Figure A 6. IR spectrum of 7.

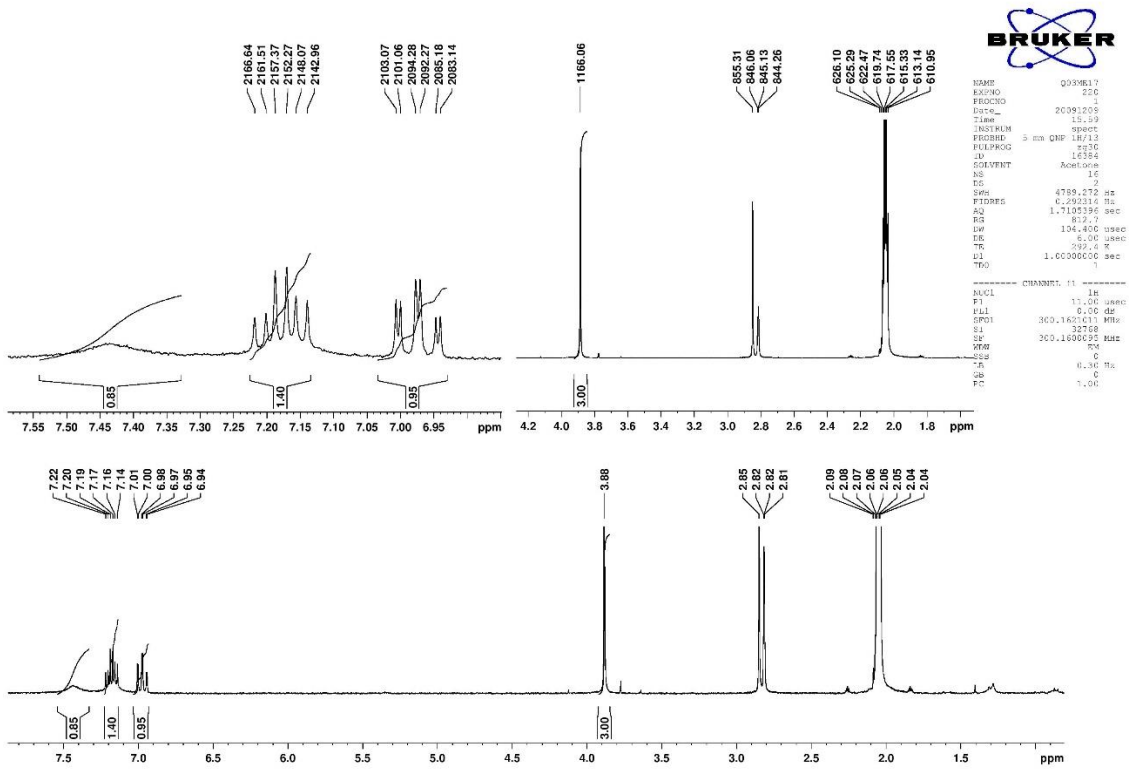


Figure A 7. <sup>1</sup>H NMR spectrum of 8.

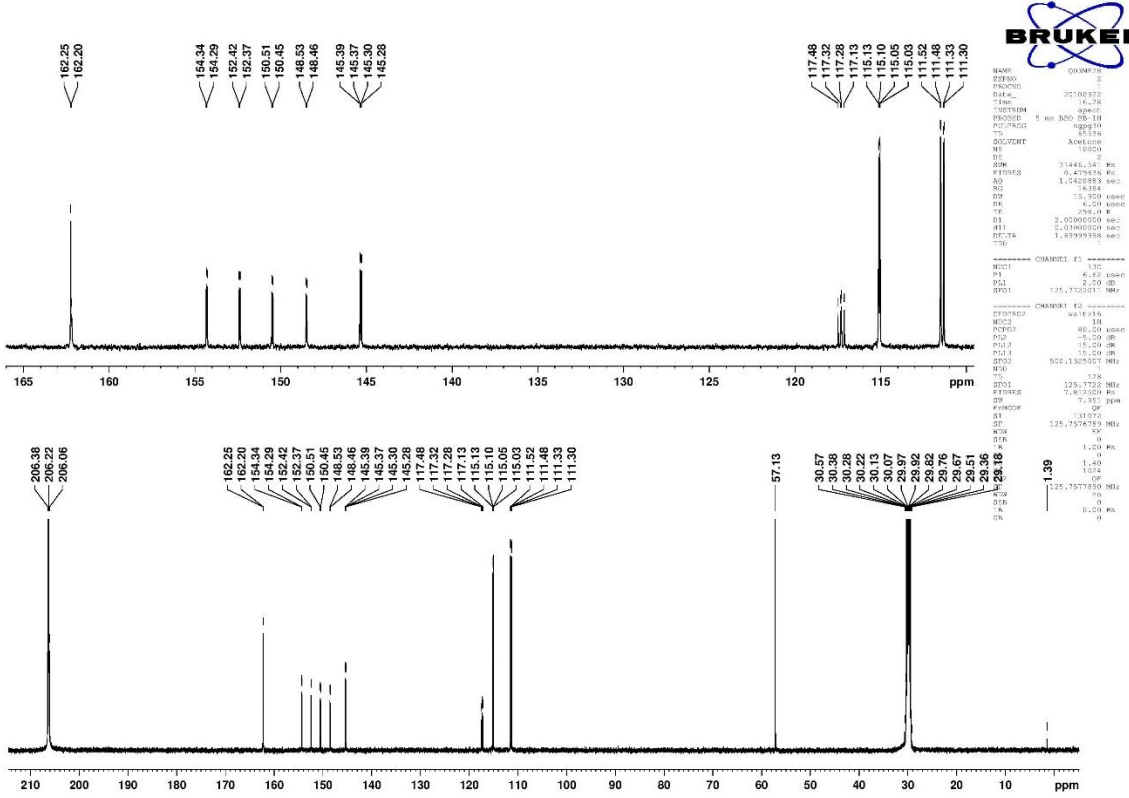


Figure A 8. <sup>13</sup>C NMR spectrum of 8.

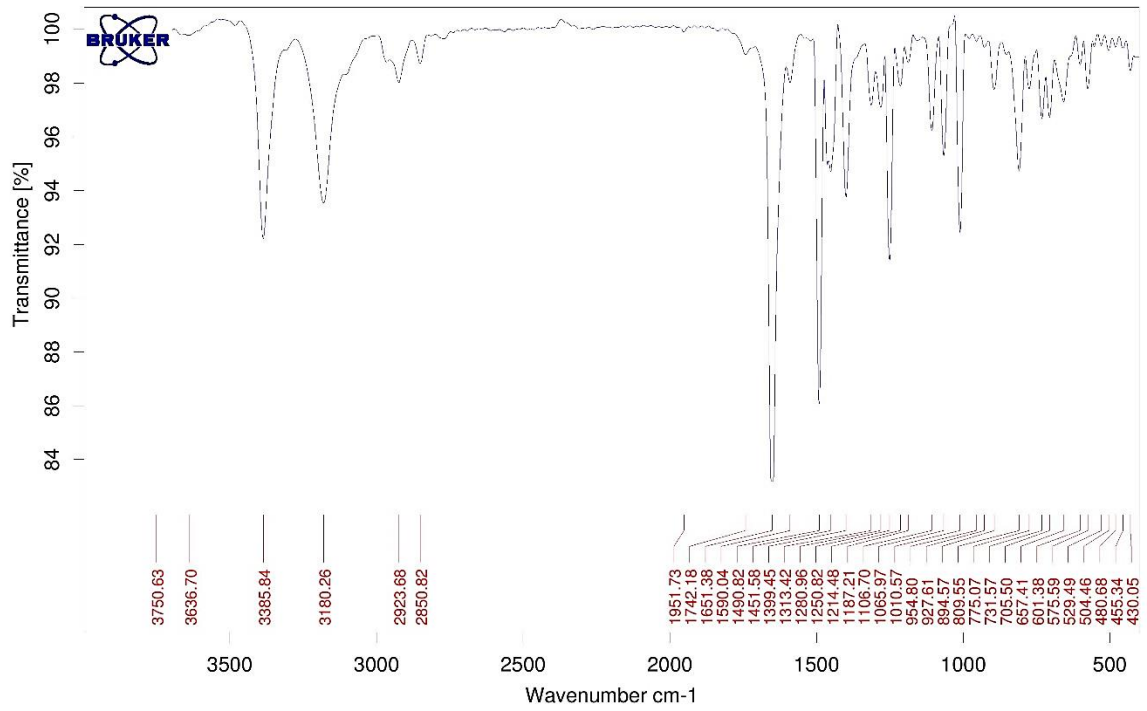


Figure A 9. IR spectrum of 8.

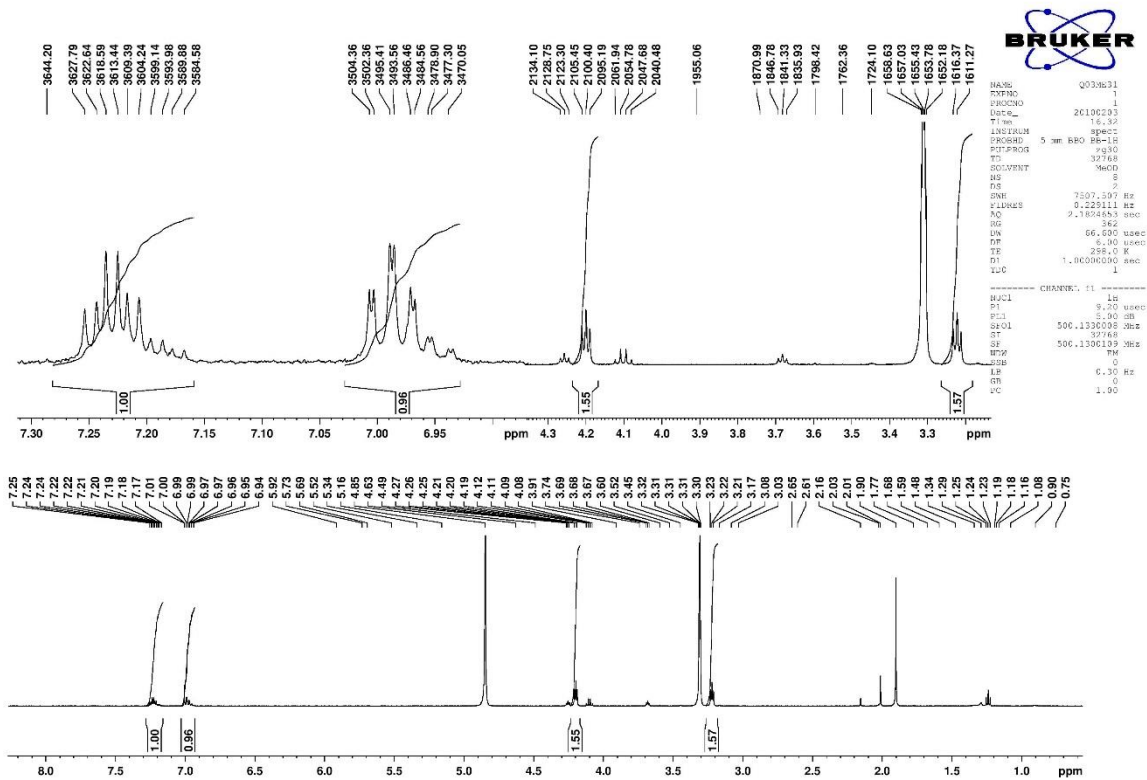


Figure A 10. <sup>1</sup>H NMR spectrum of 9.



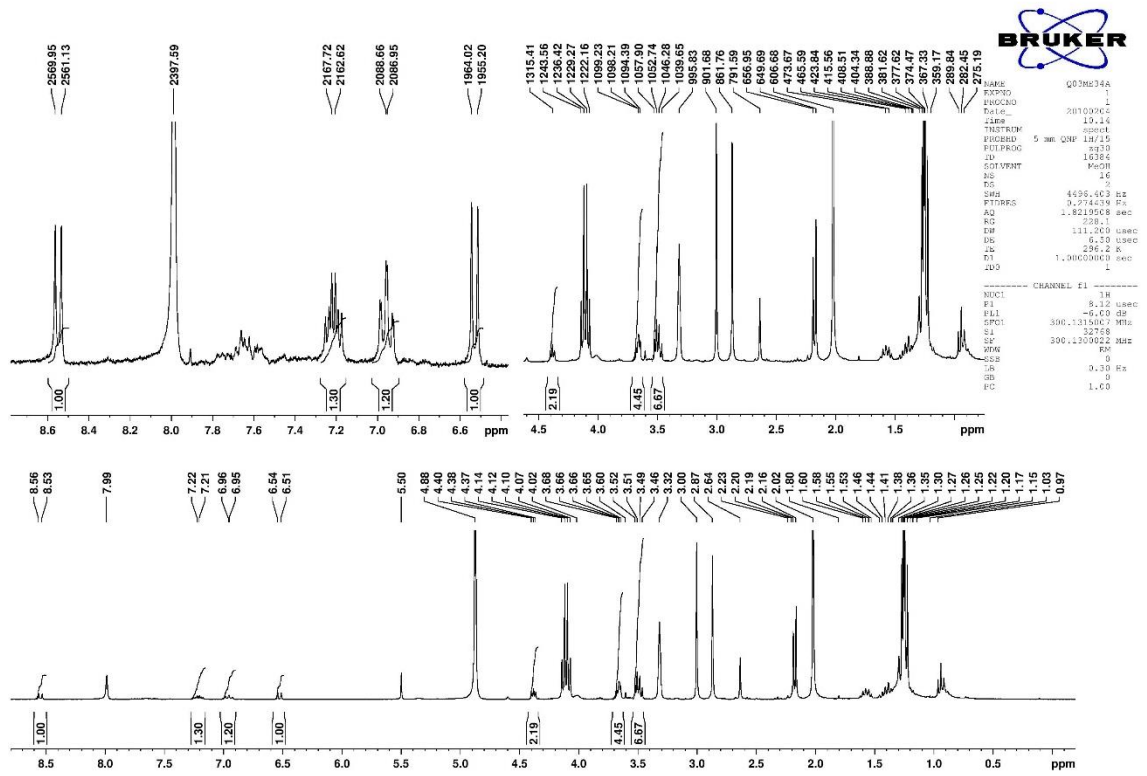


Figure A 11. <sup>1</sup>H NMR spectrum of 1a.

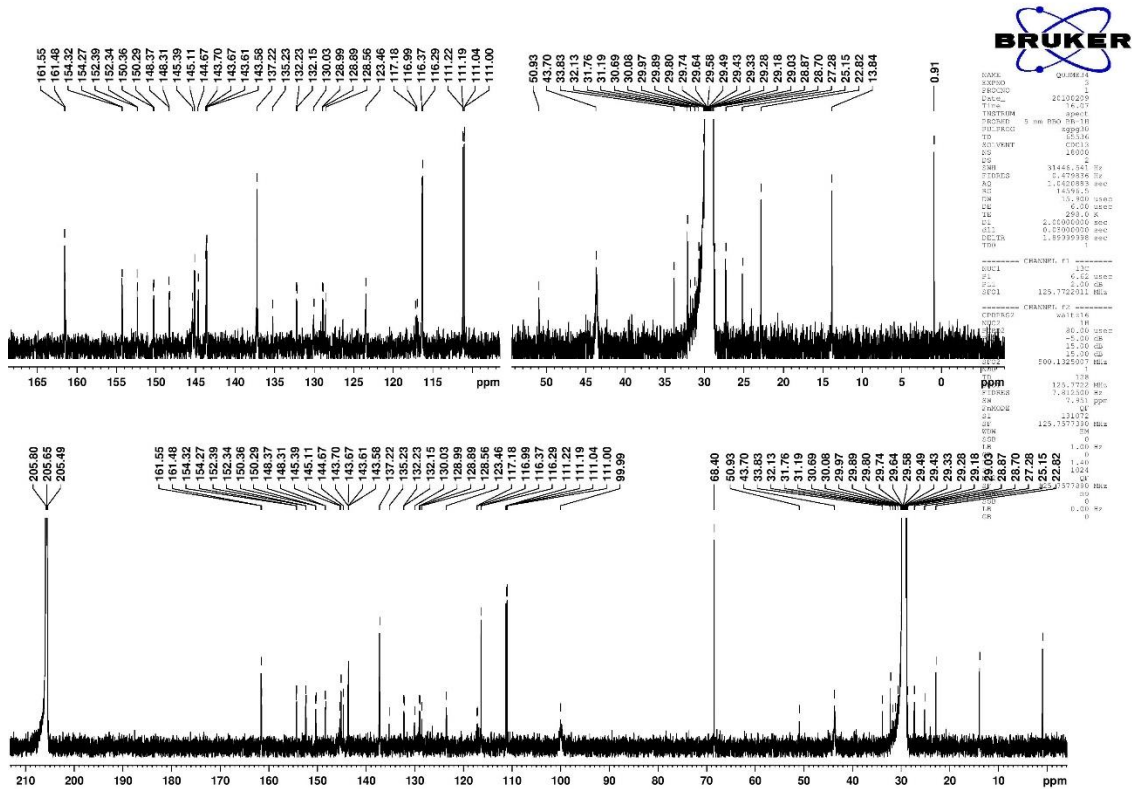


Figure A 12. <sup>13</sup>C NMR spectrum of 1a.

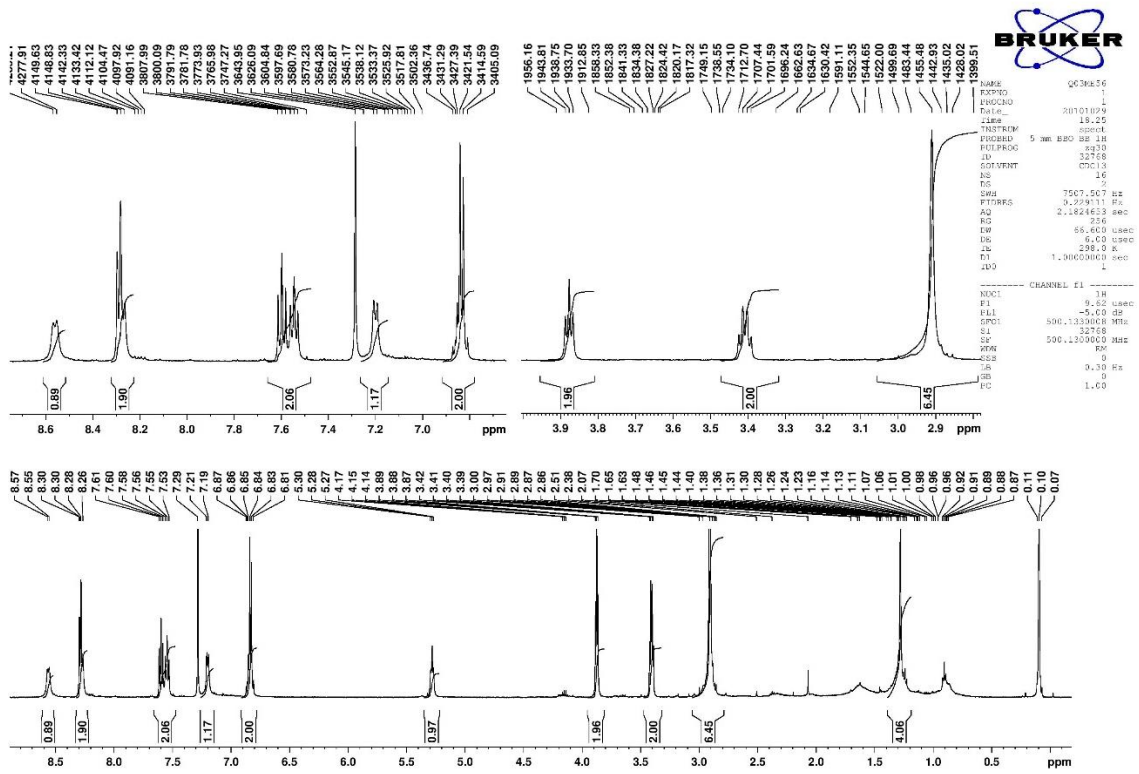


Figure A 13.  $^1\text{H}$  NMR spectrum of **1b**.

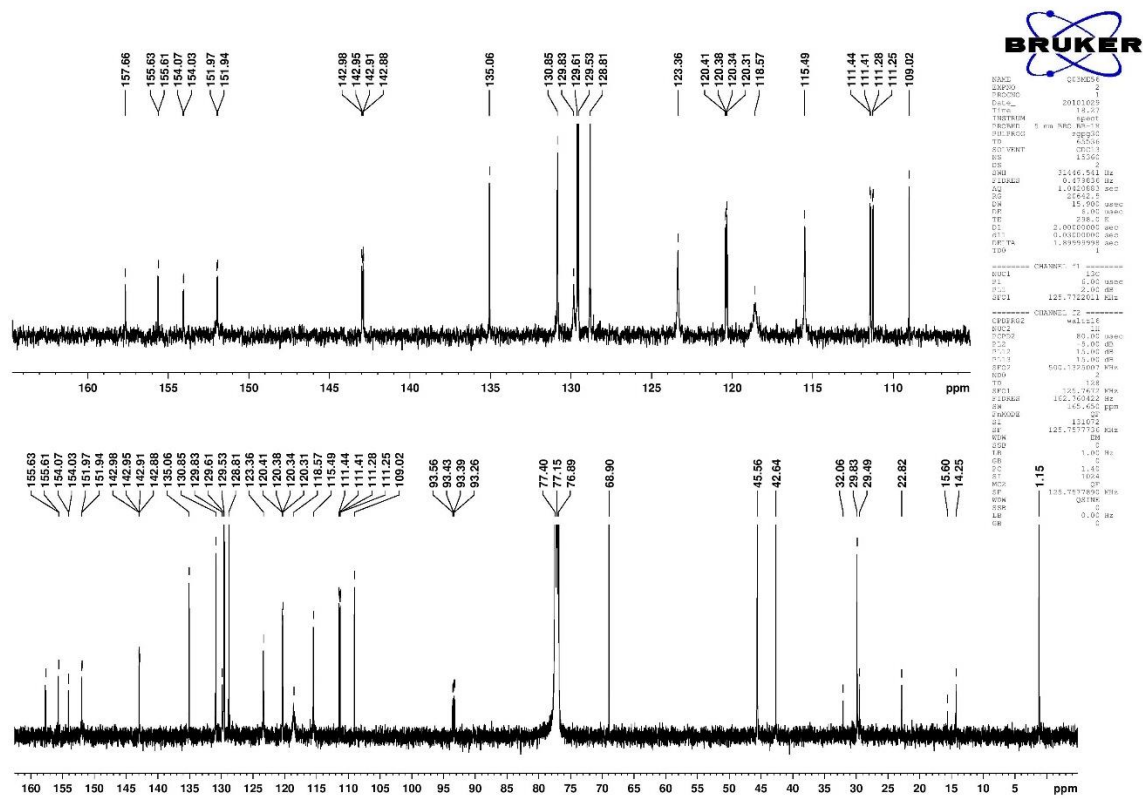


Figure A 14.  $^{13}\text{C}$  NMR spectrum of **1b**.

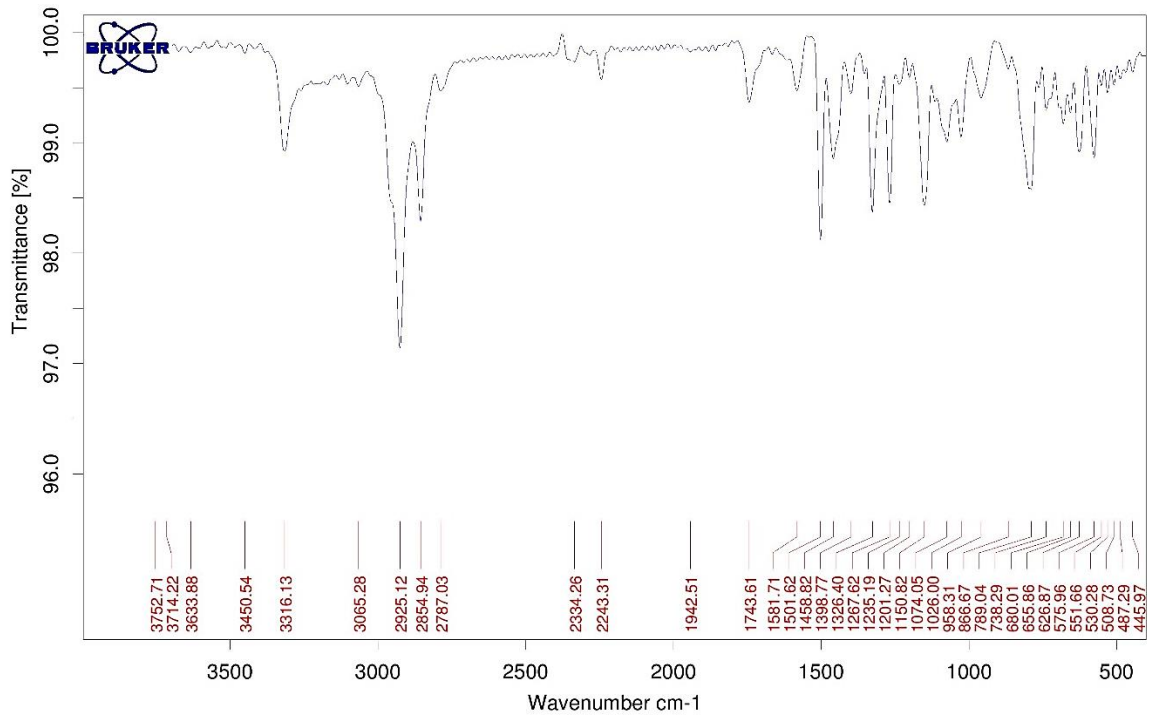
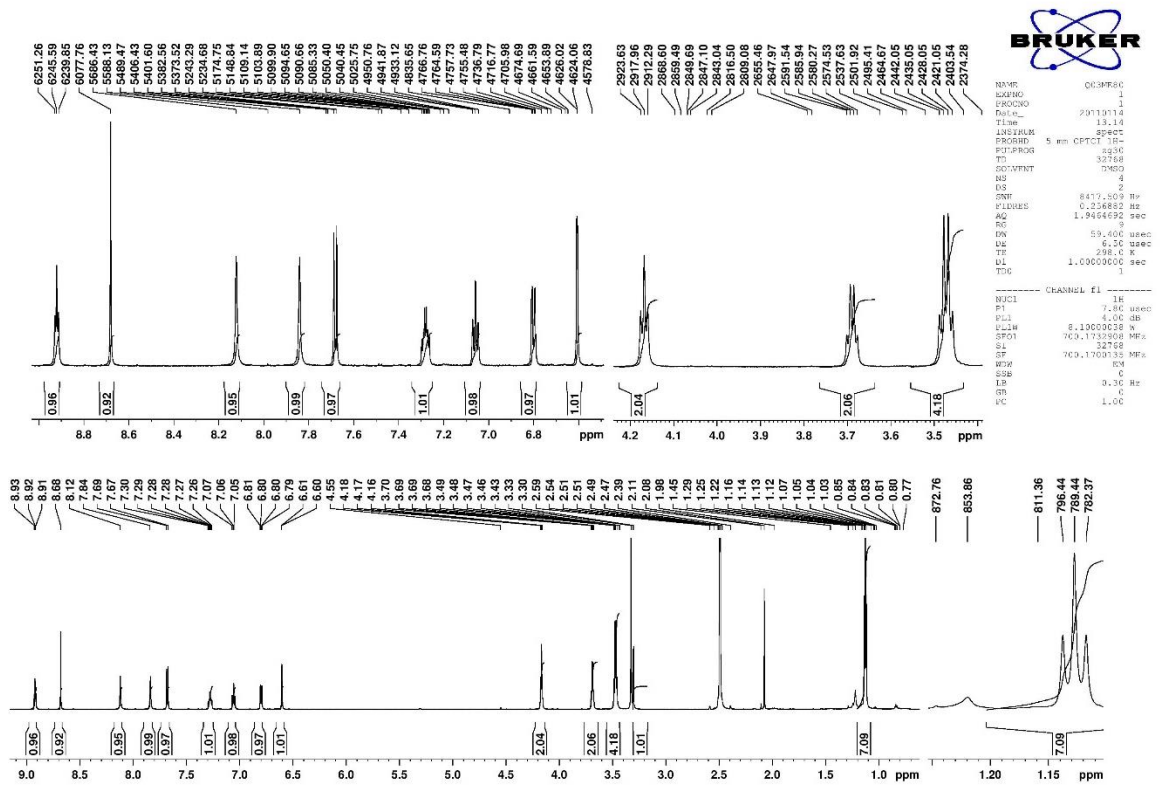


Figure A 15. IR spectrum of 1b.



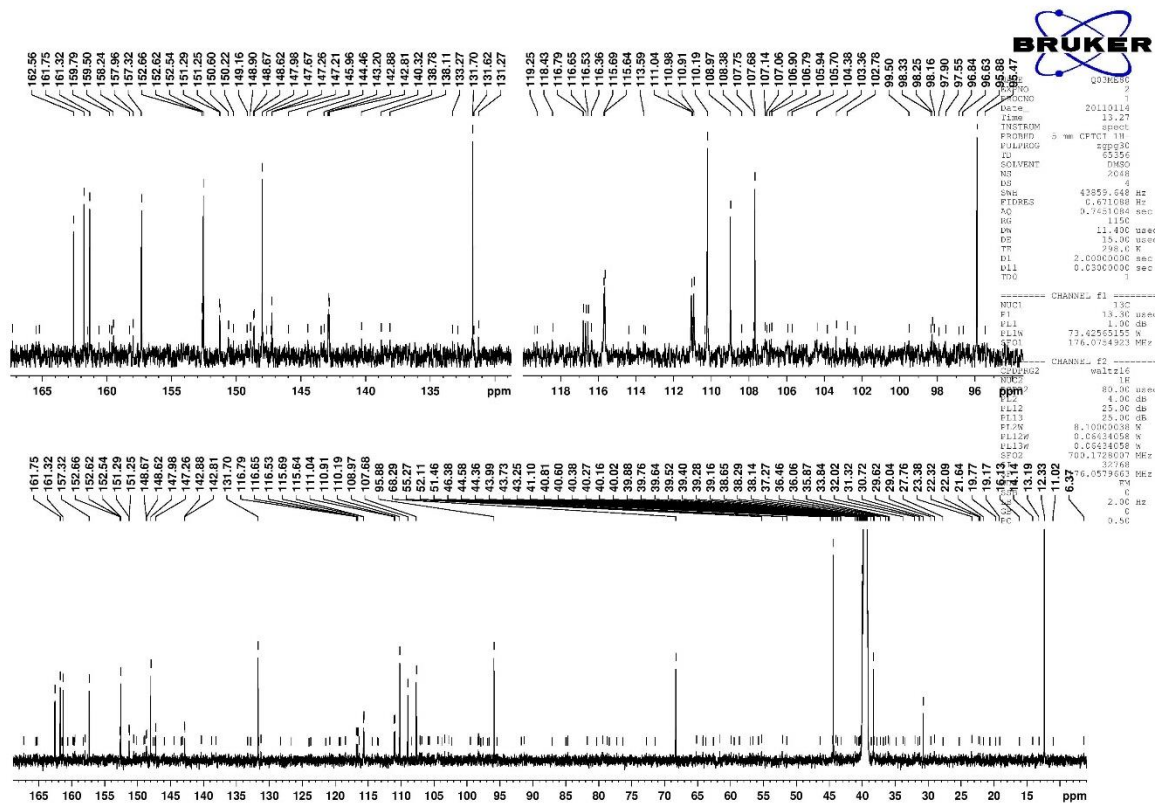


Figure A 17.  $^{13}\text{C}$  NMR spectrum of 1c.

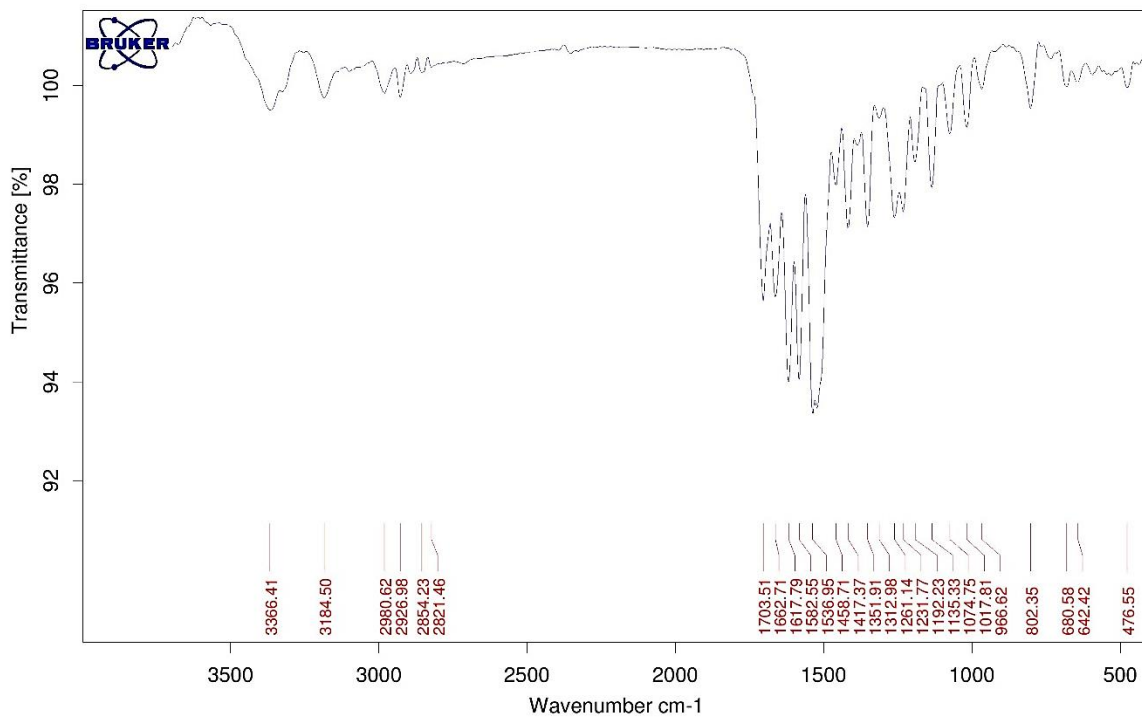


Figure A 18. IR spectrum of 1c.

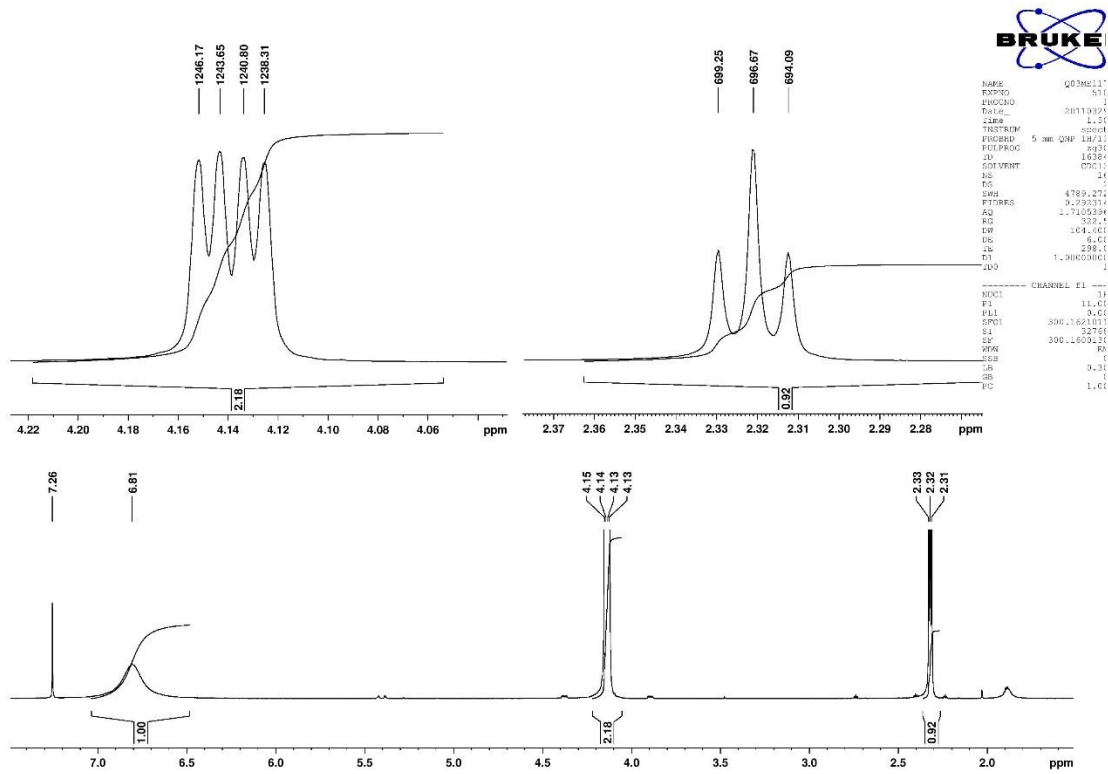


Figure A 19. <sup>1</sup>H NMR spectrum of 12.

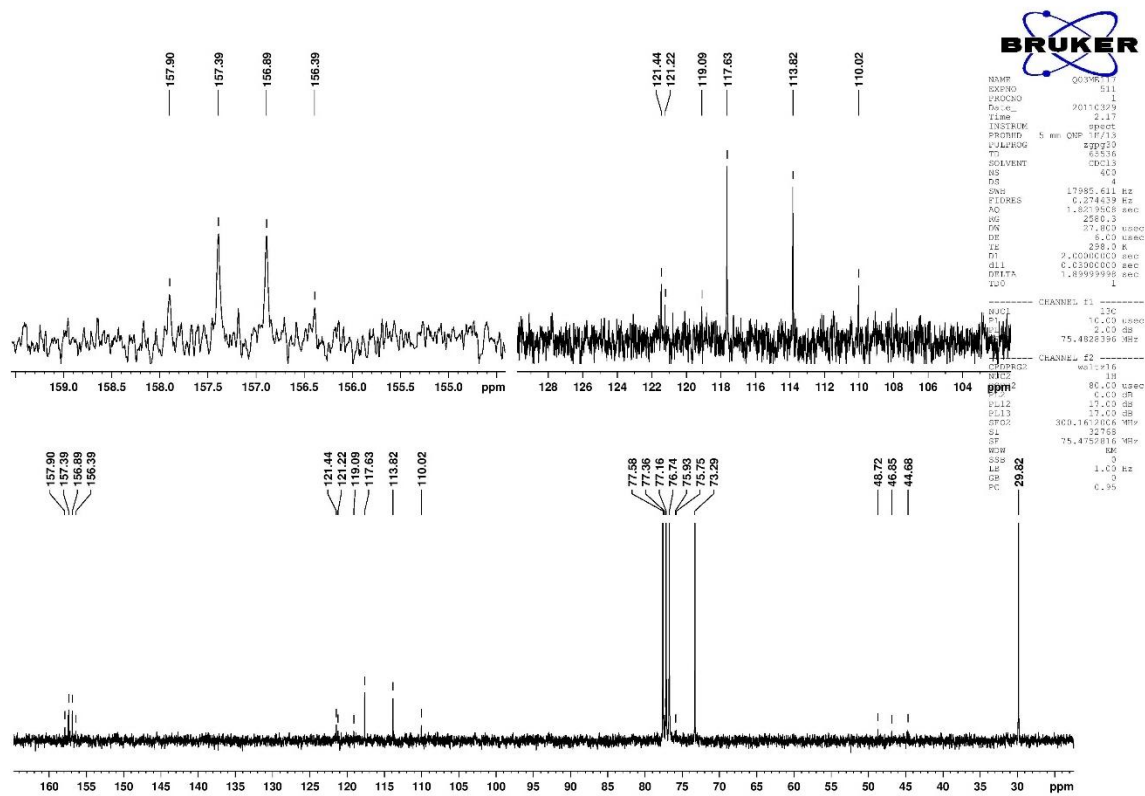


Figure A 20. <sup>13</sup>C NMR spectrum of 12.

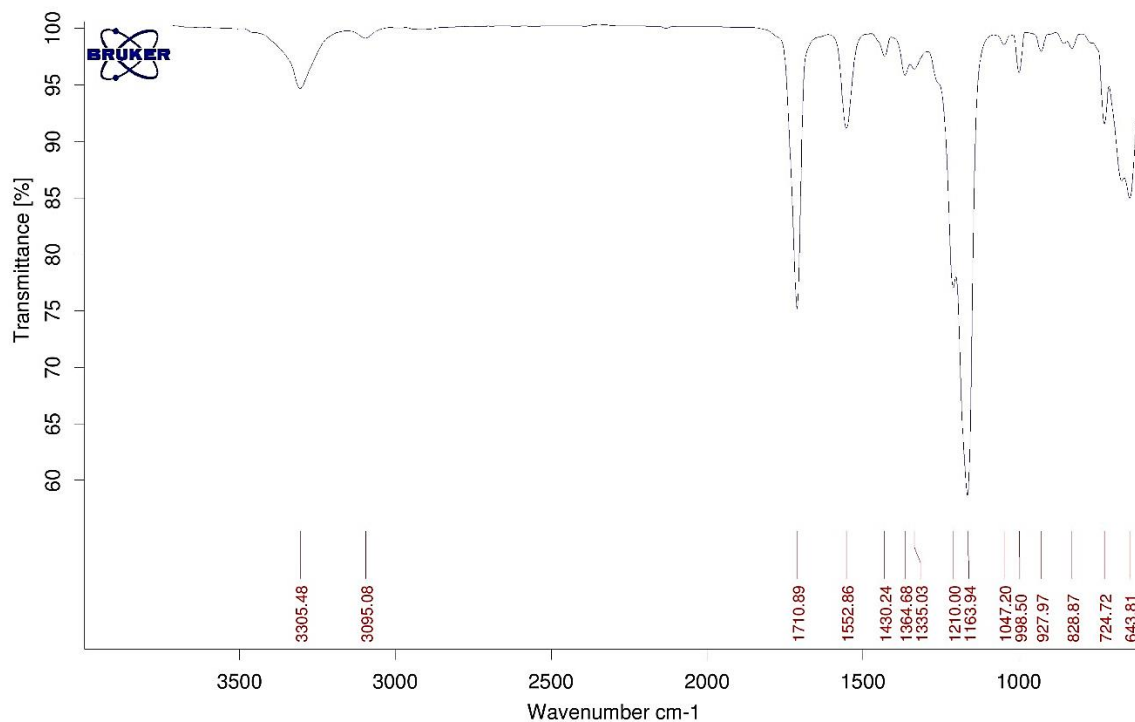


Figure A 21. IR spectrum of 12.

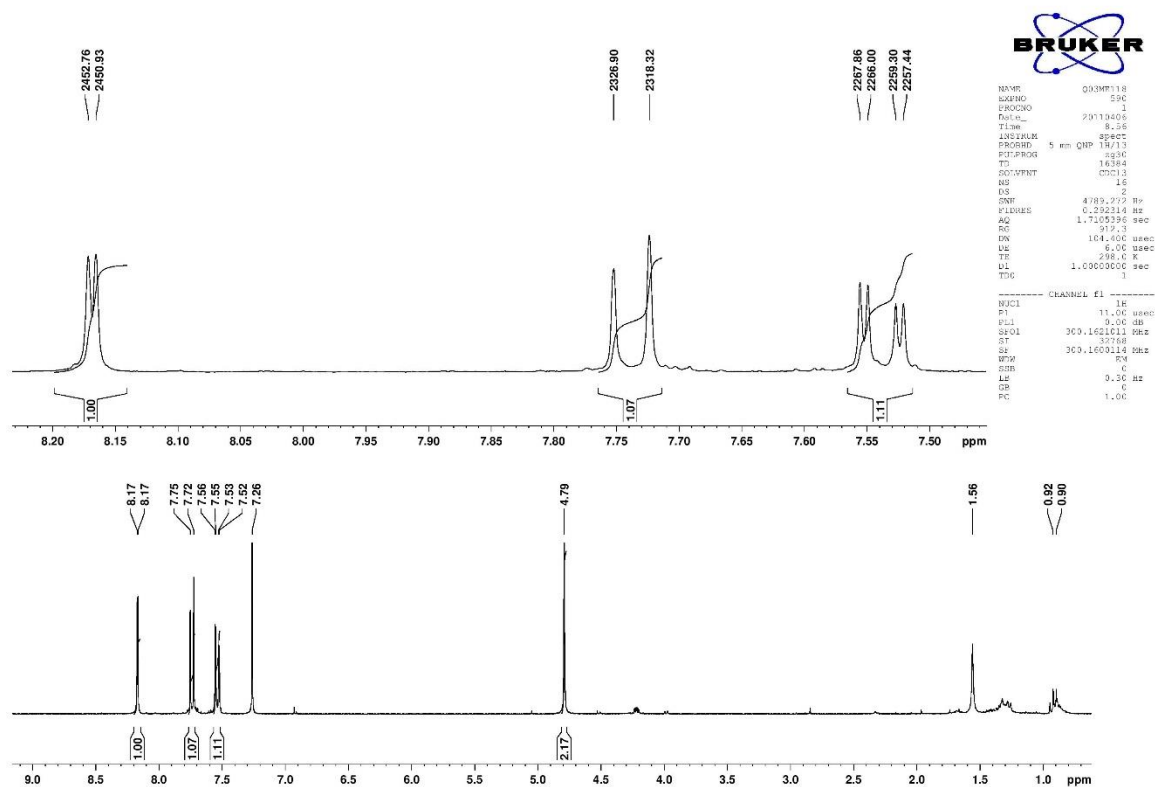


Figure A 22. <sup>1</sup>H NMR spectrum of 14.

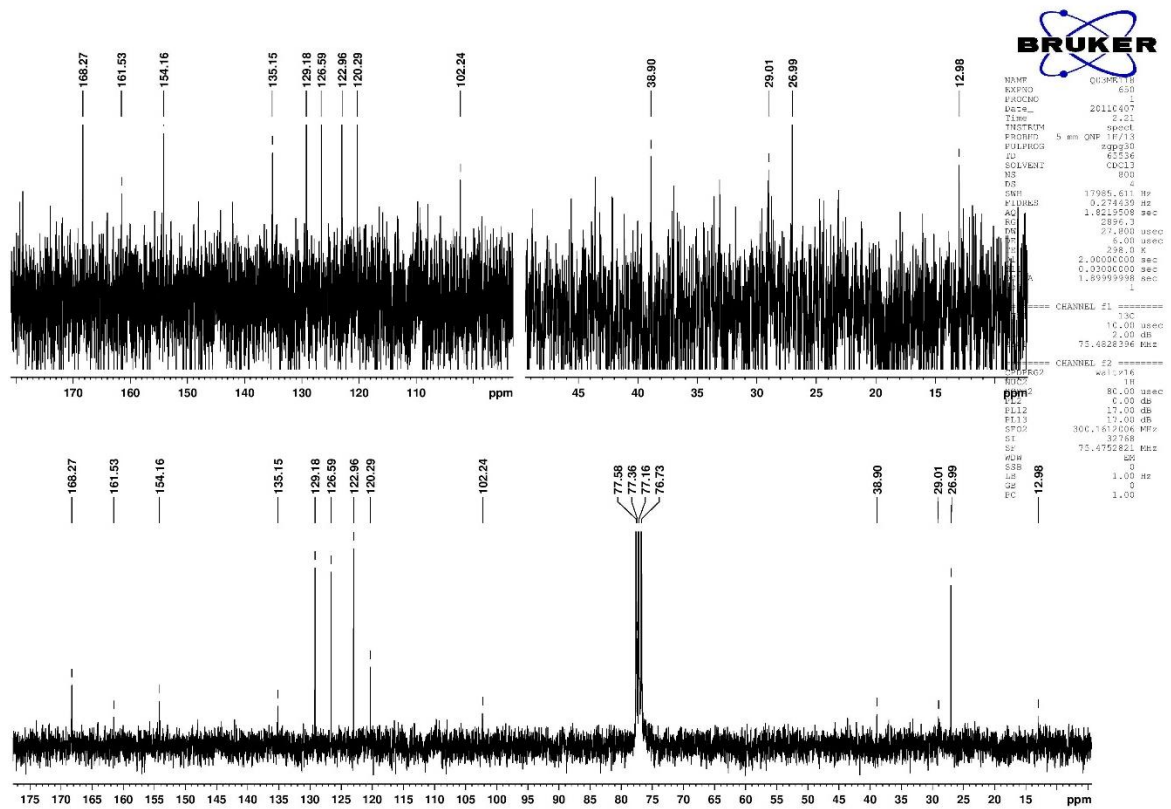


Figure A 23. <sup>13</sup>C NMR spectrum of 14.

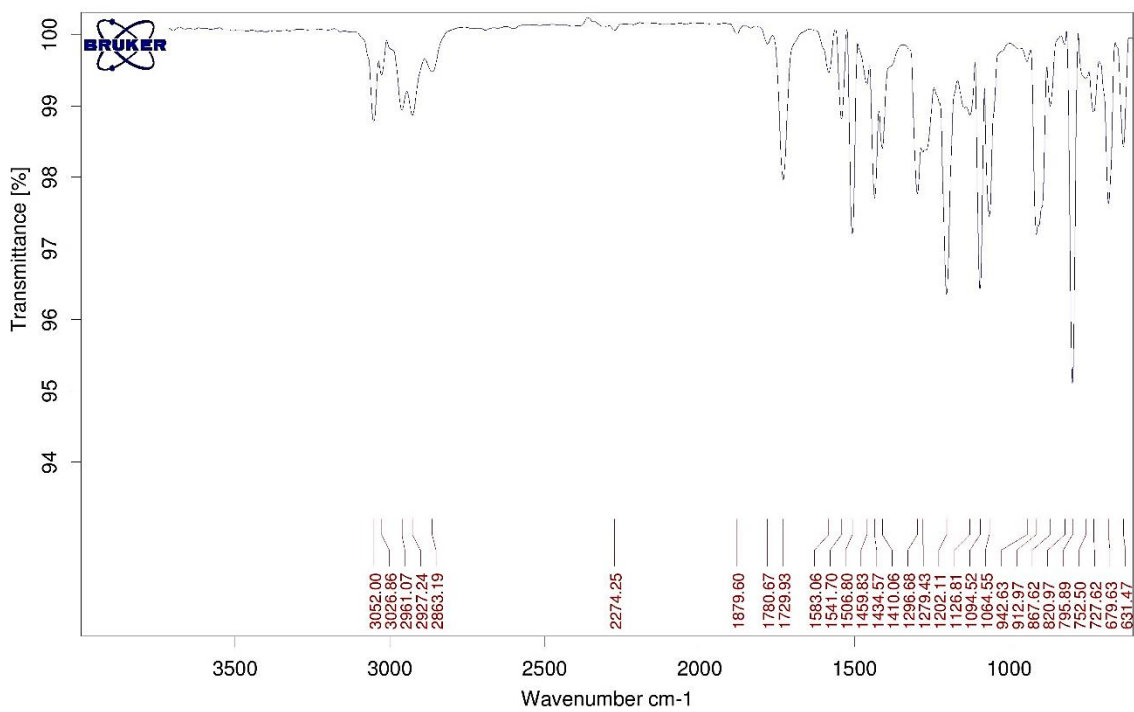


Figure A 24. IR spectrum of 14.

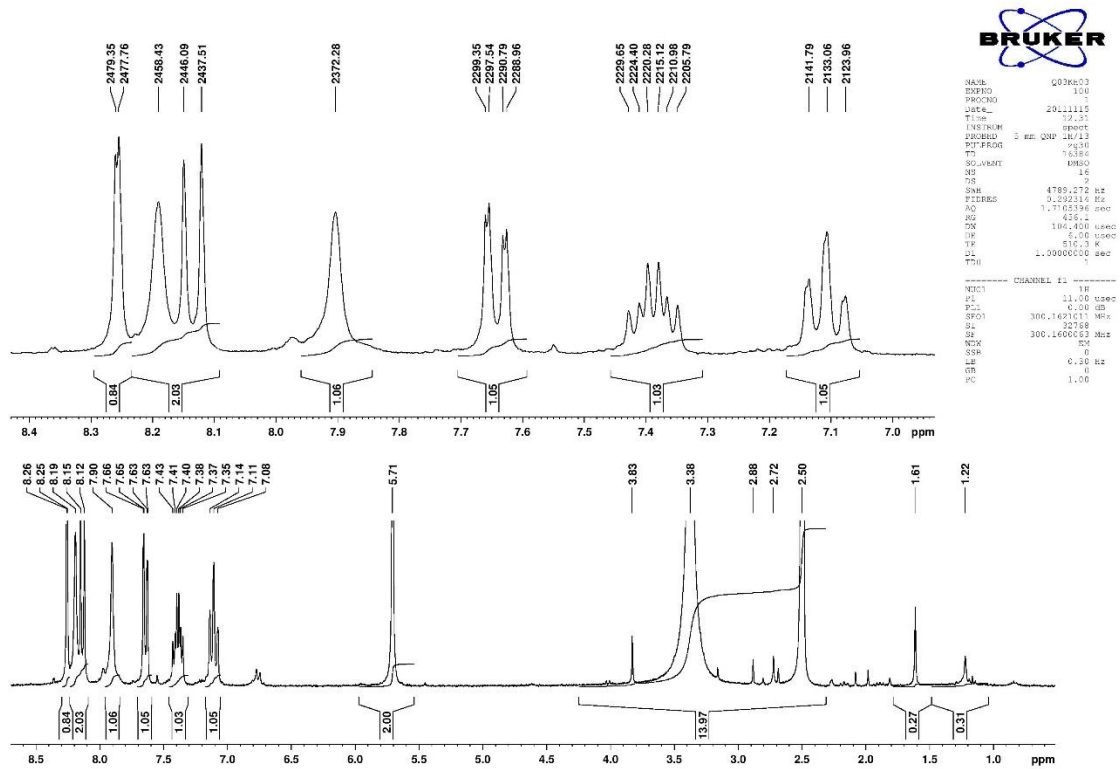


Figure A 25. <sup>1</sup>H NMR spectrum of 15.

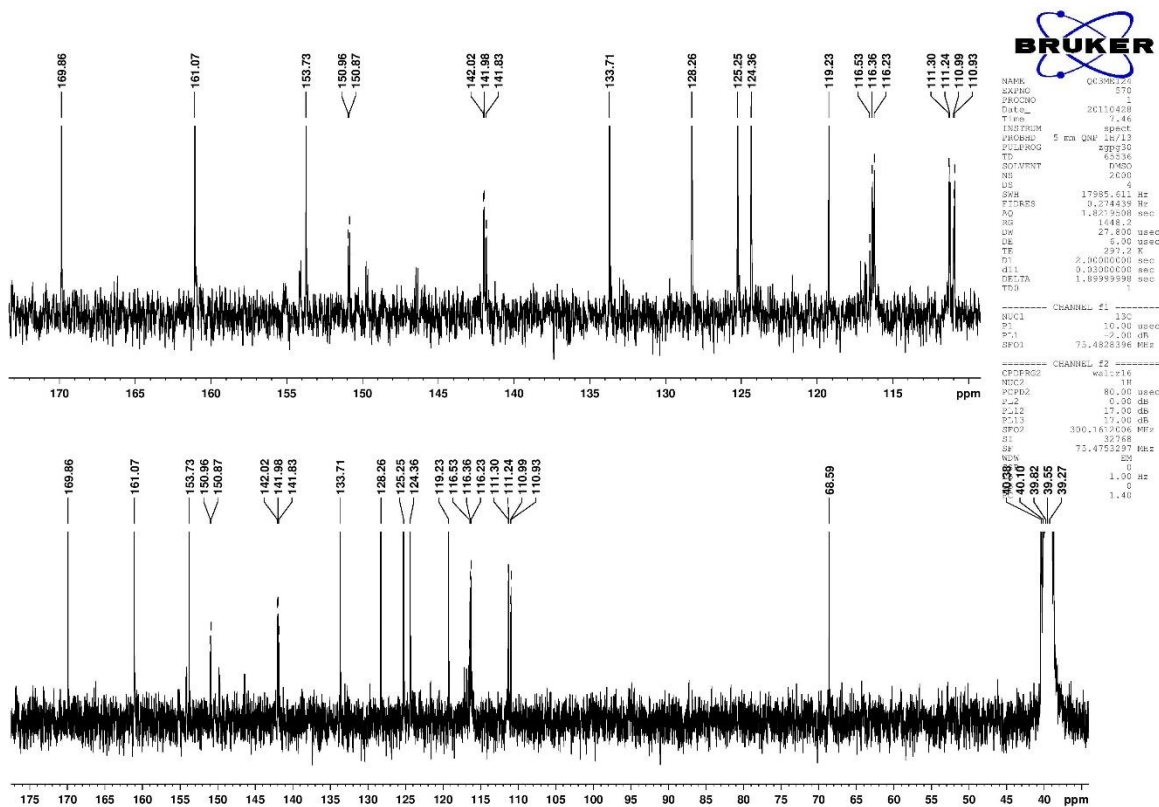


Figure A 26. <sup>13</sup>C NMR spectrum of 15.



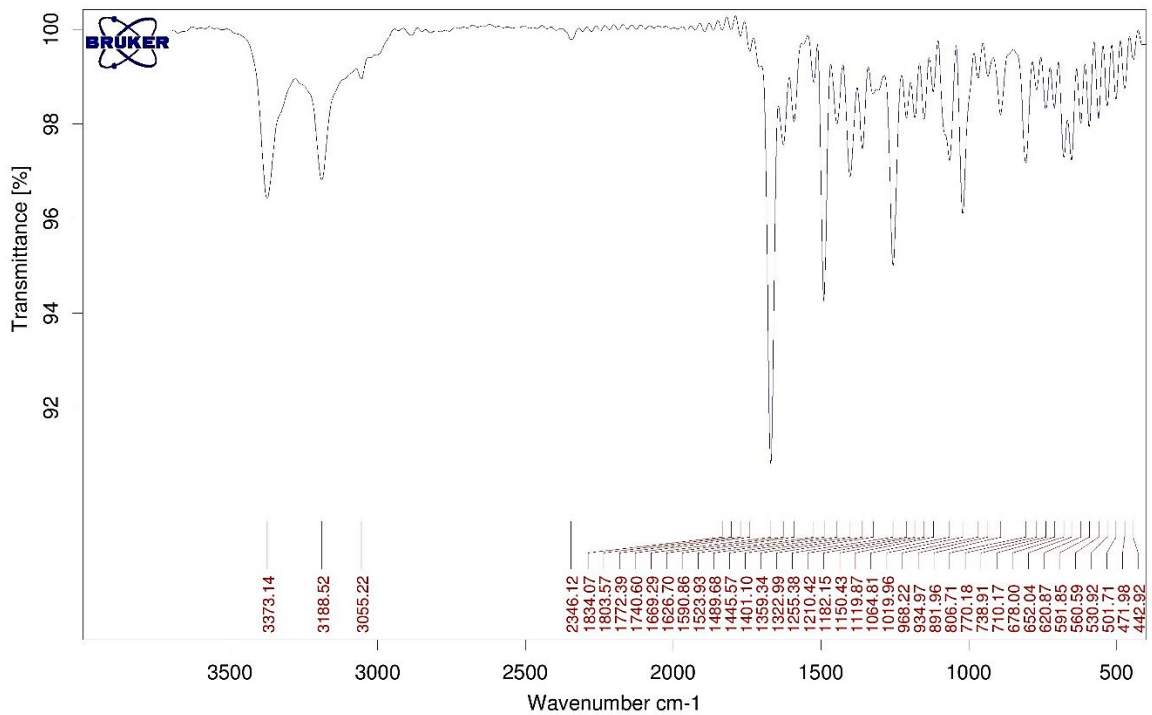


Figure A 27. IR spectrum of 15.

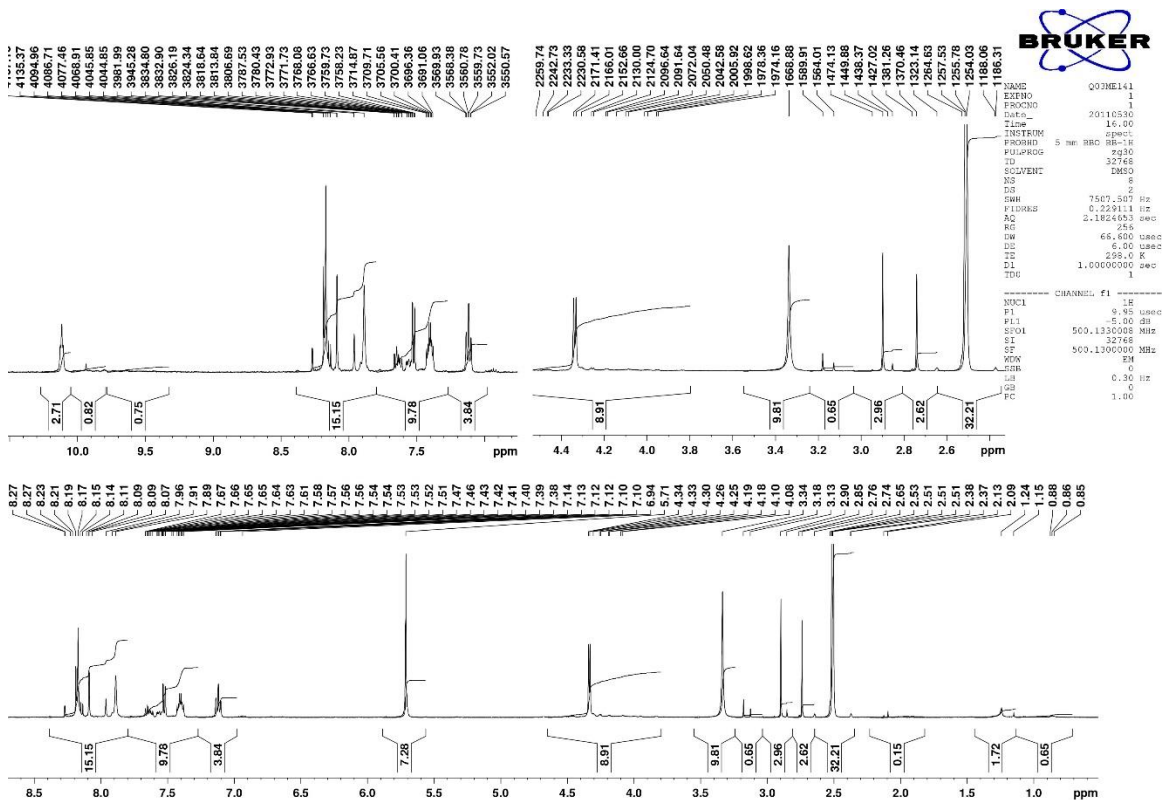


Figure A 28. <sup>1</sup>H NMR spectrum of 16.

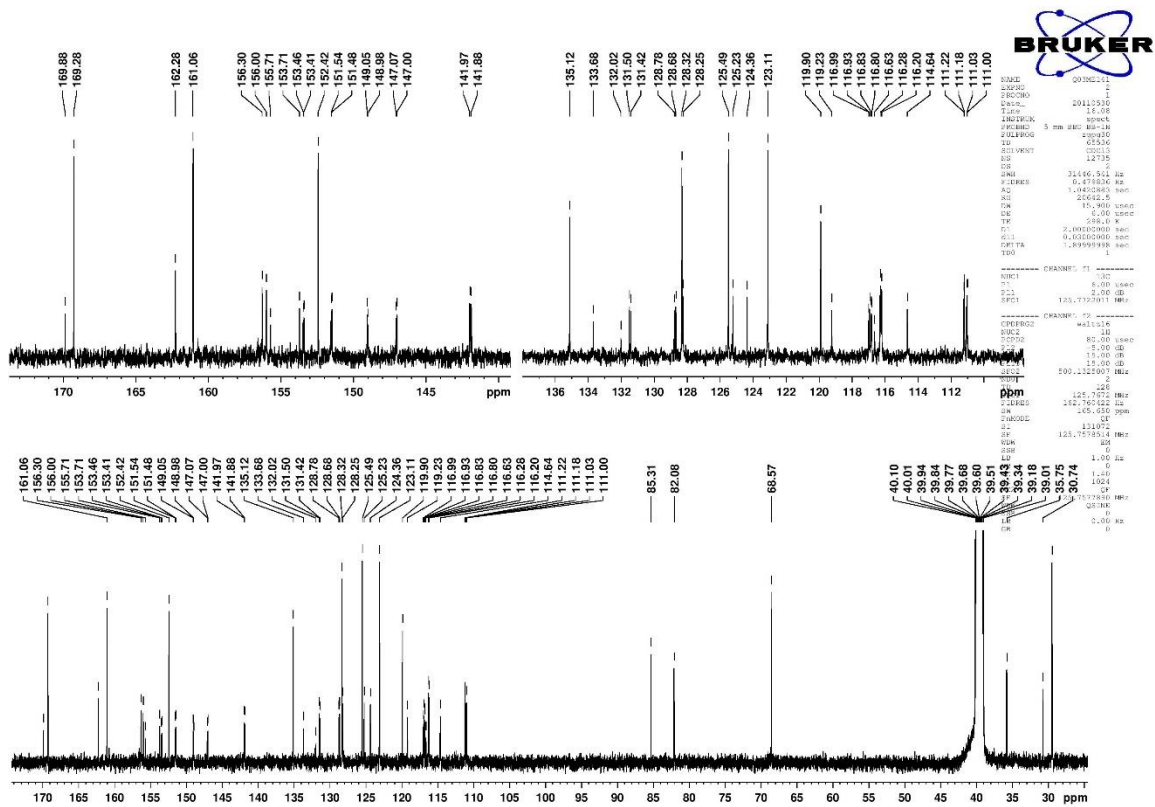


Figure A 29. <sup>13</sup>C NMR spectrum of 16.

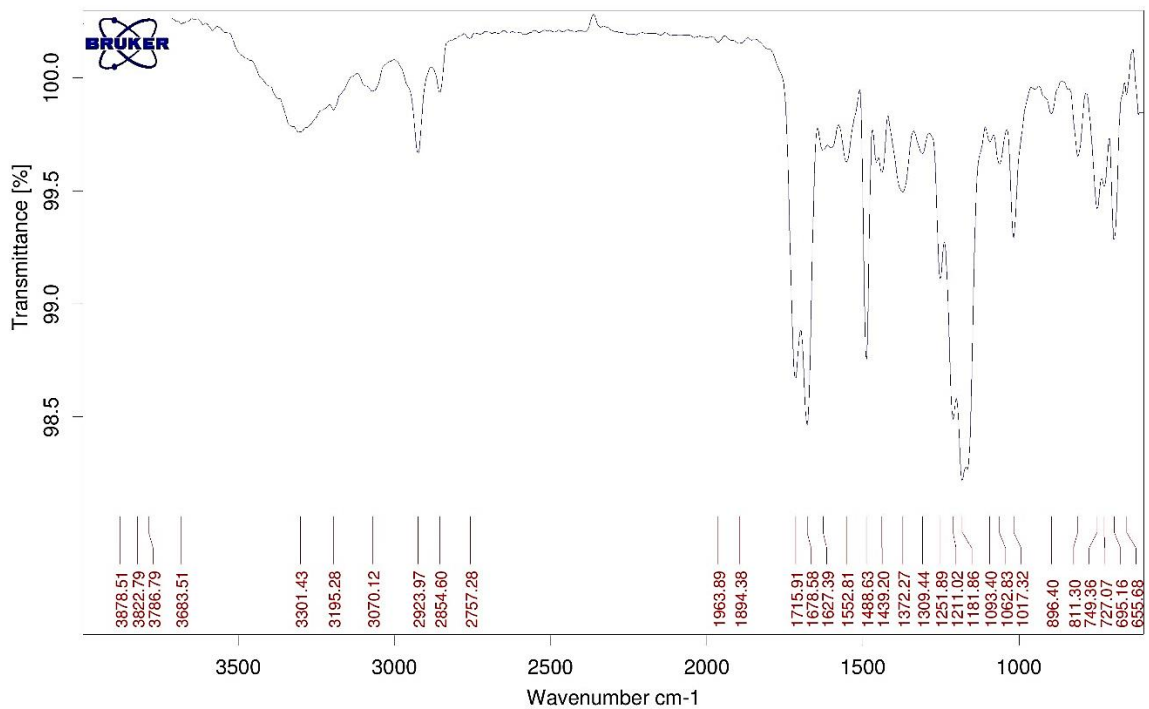


Figure A 30. IR spectrum of 16.





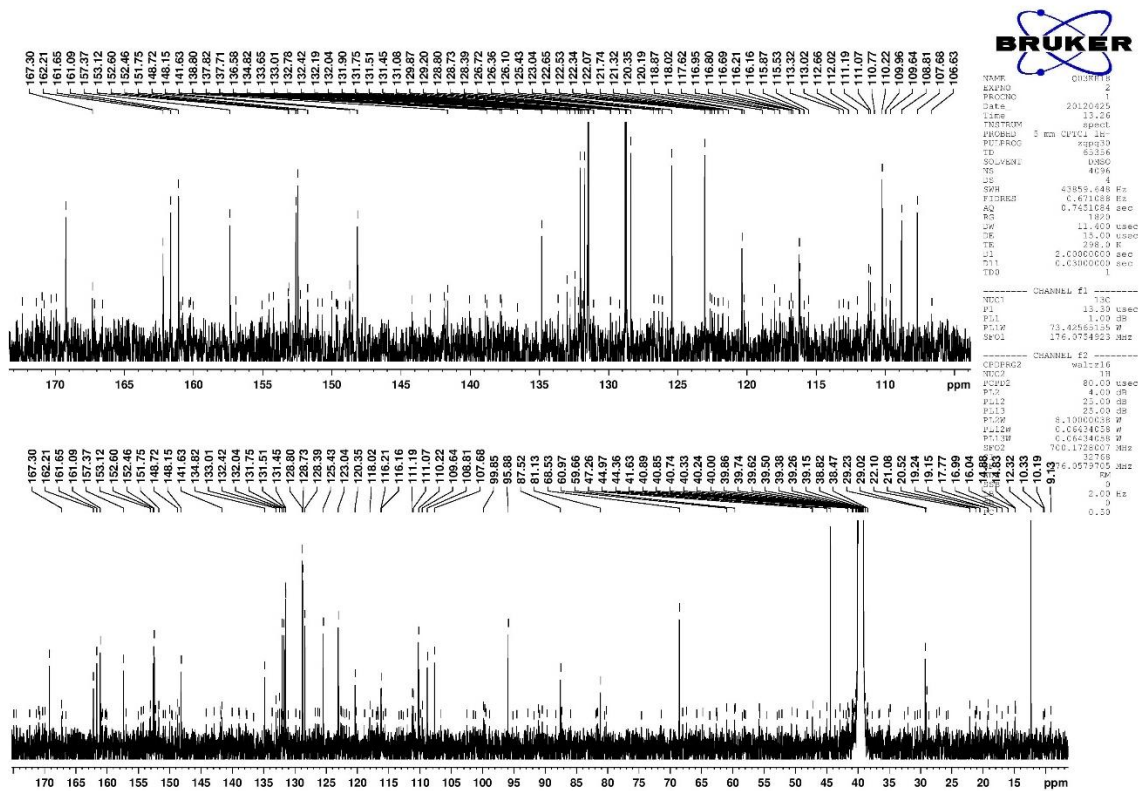


Figure A 35. <sup>13</sup>C NMR spectrum of 2b.

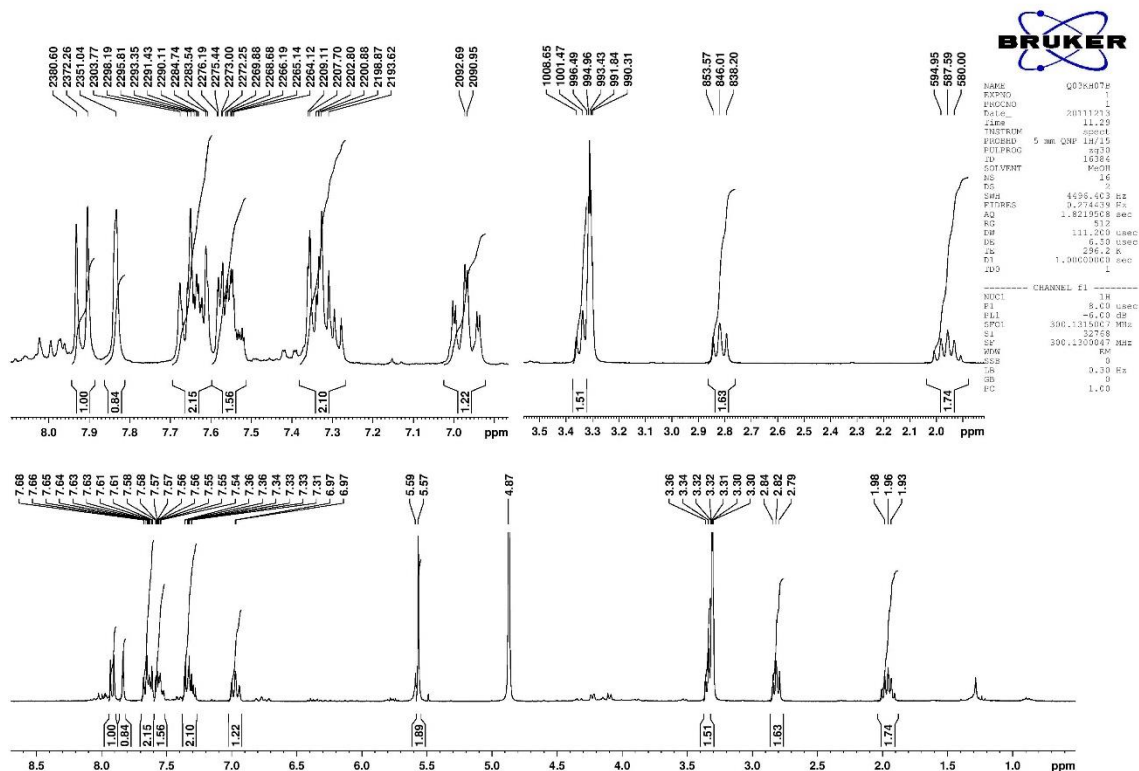


Figure A 36. <sup>1</sup>H NMR spectrum of 18.

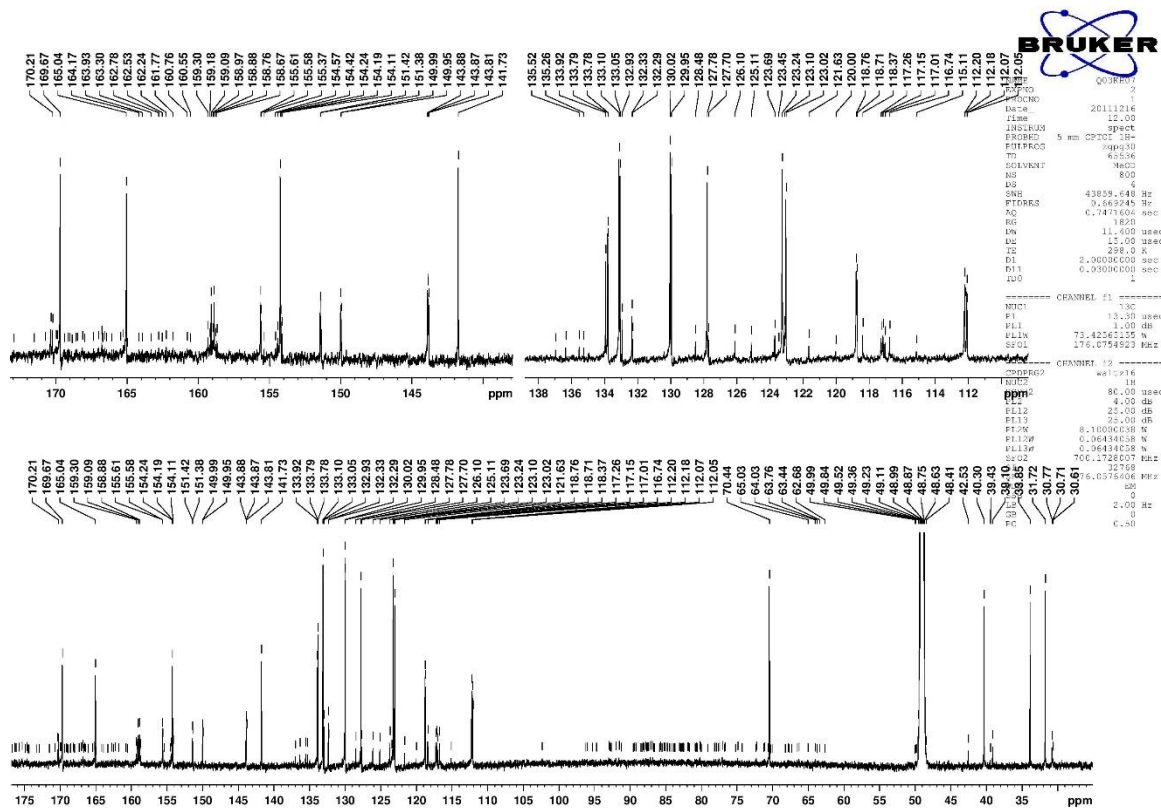


Figure A 37.  $^{13}\text{C}$  NMR spectrum of 18.

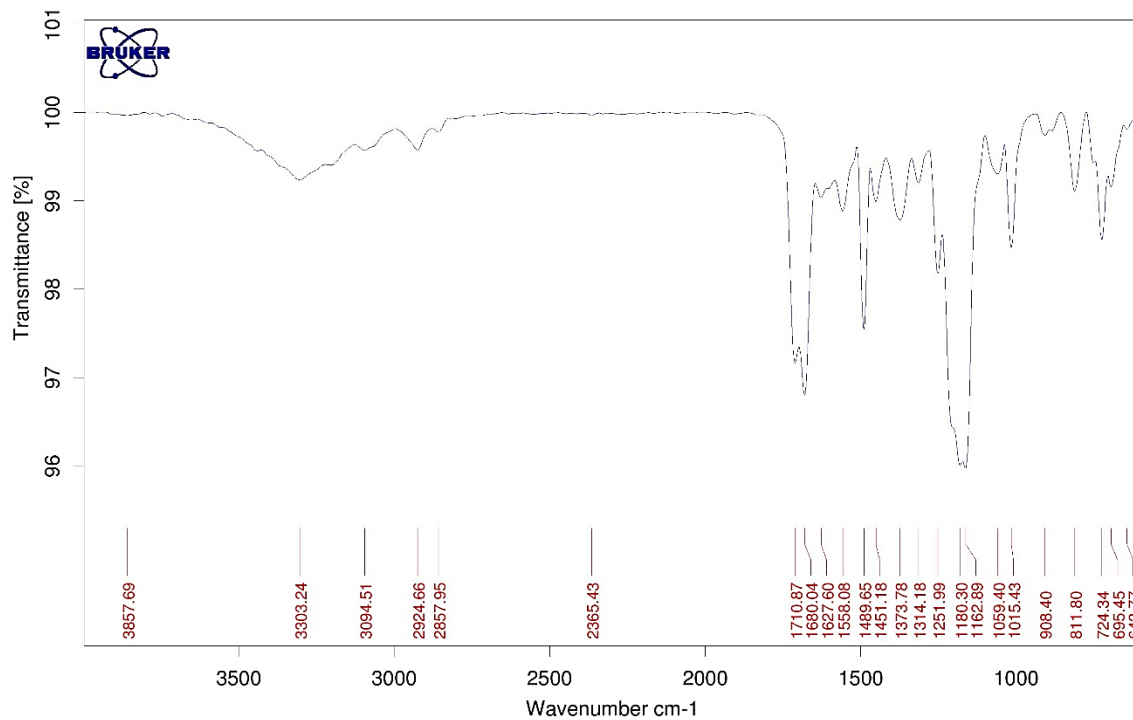


Figure A 38. IR spectrum of 18.

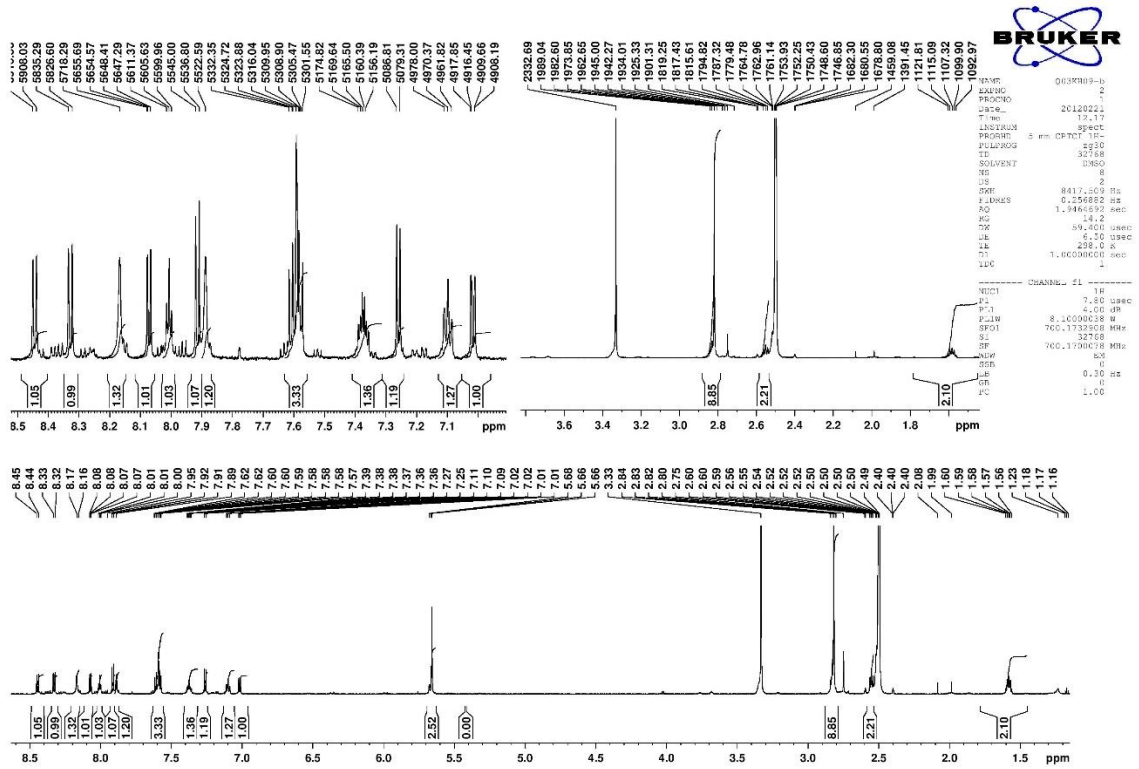


Figure A 39.  $^1\text{H}$  NMR spectrum of 3.

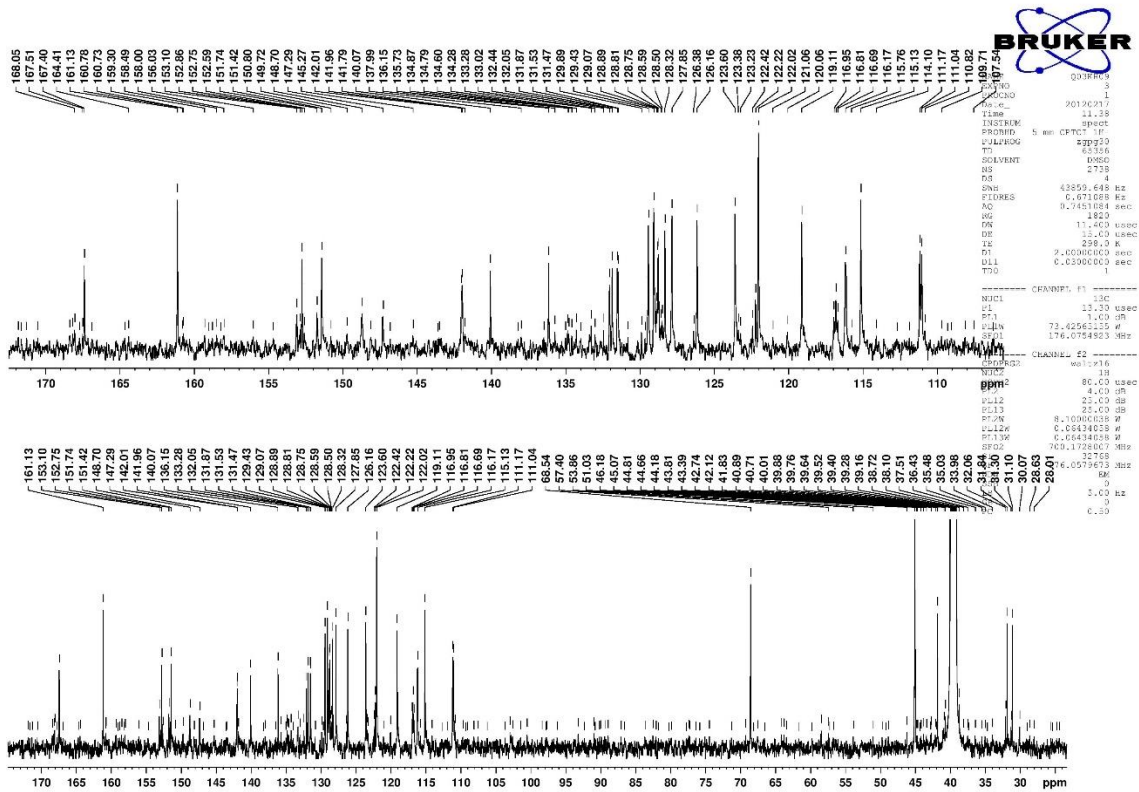


Figure A 40.  $^{13}\text{C}$  NMR spectrum of 3.

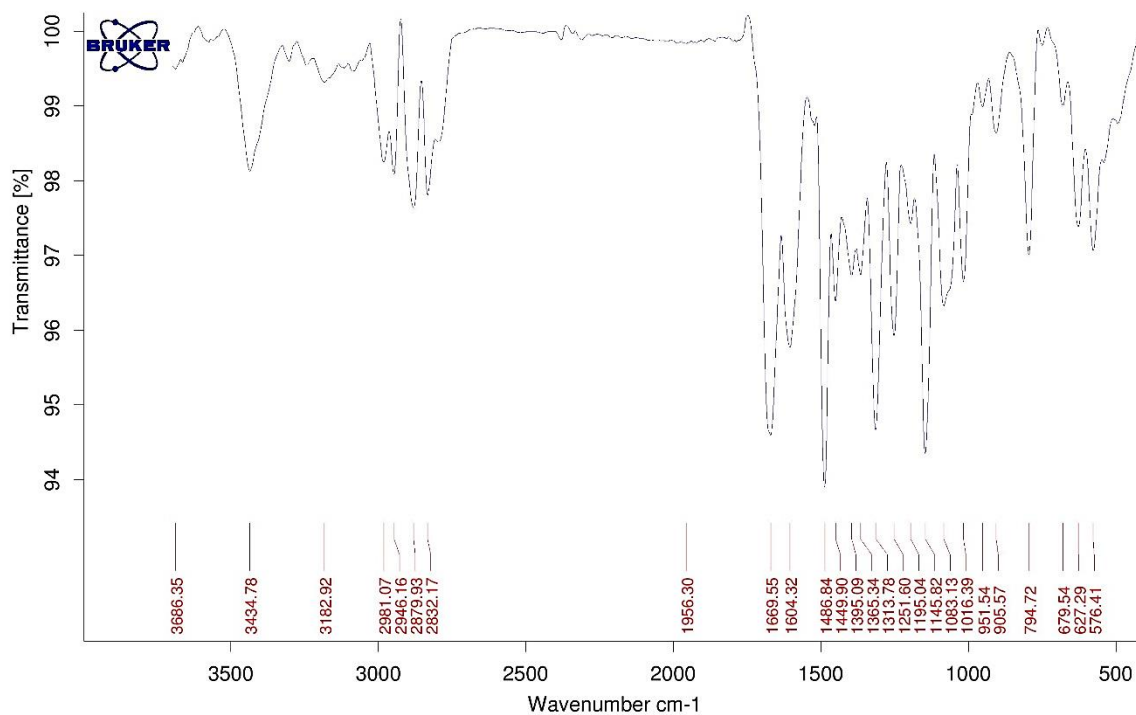


Figure A 41. IR spectrum of 3.

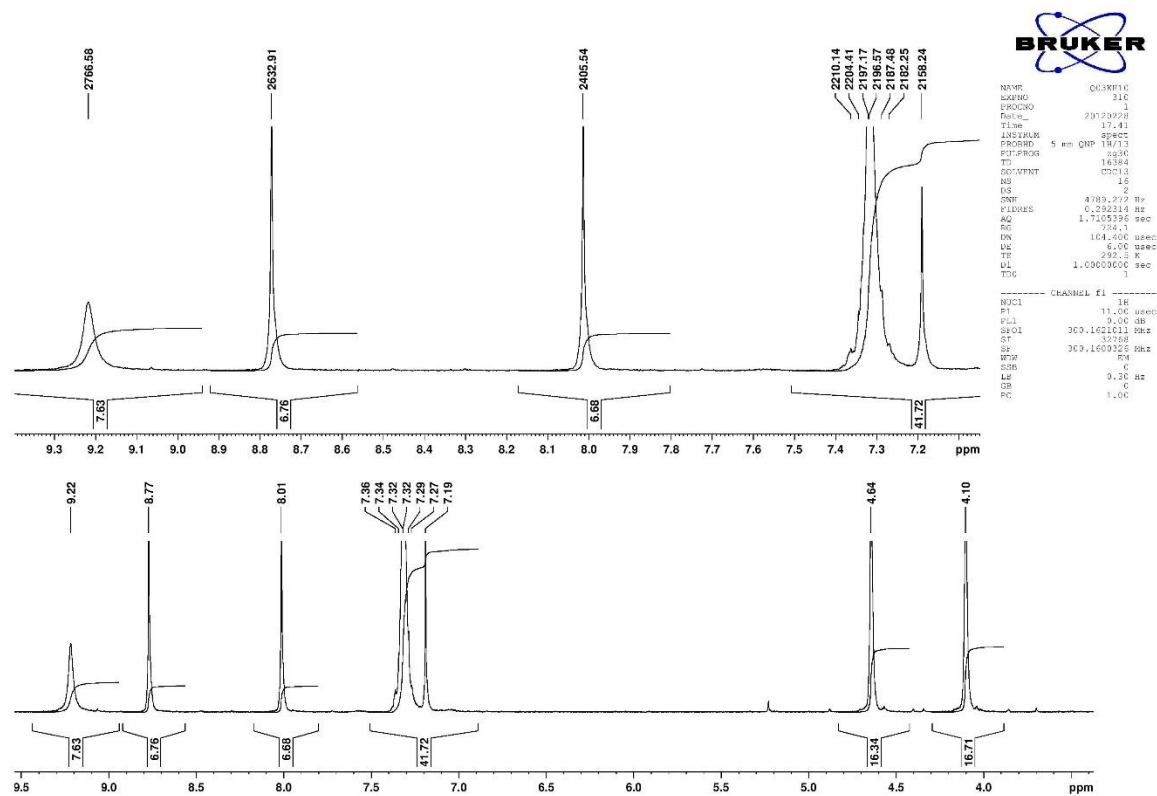


Figure A 42. <sup>1</sup>H NMR spectrum of 21.



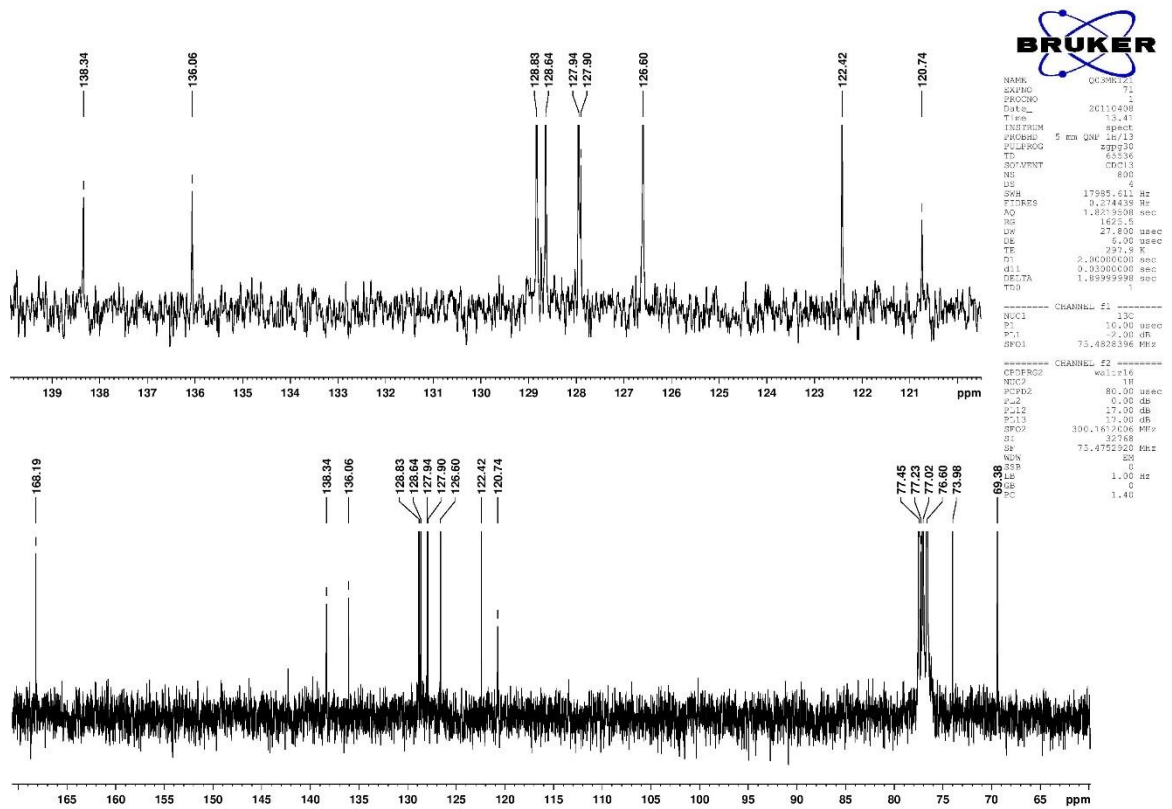


Figure A 43. <sup>13</sup>C NMR spectrum of 21.

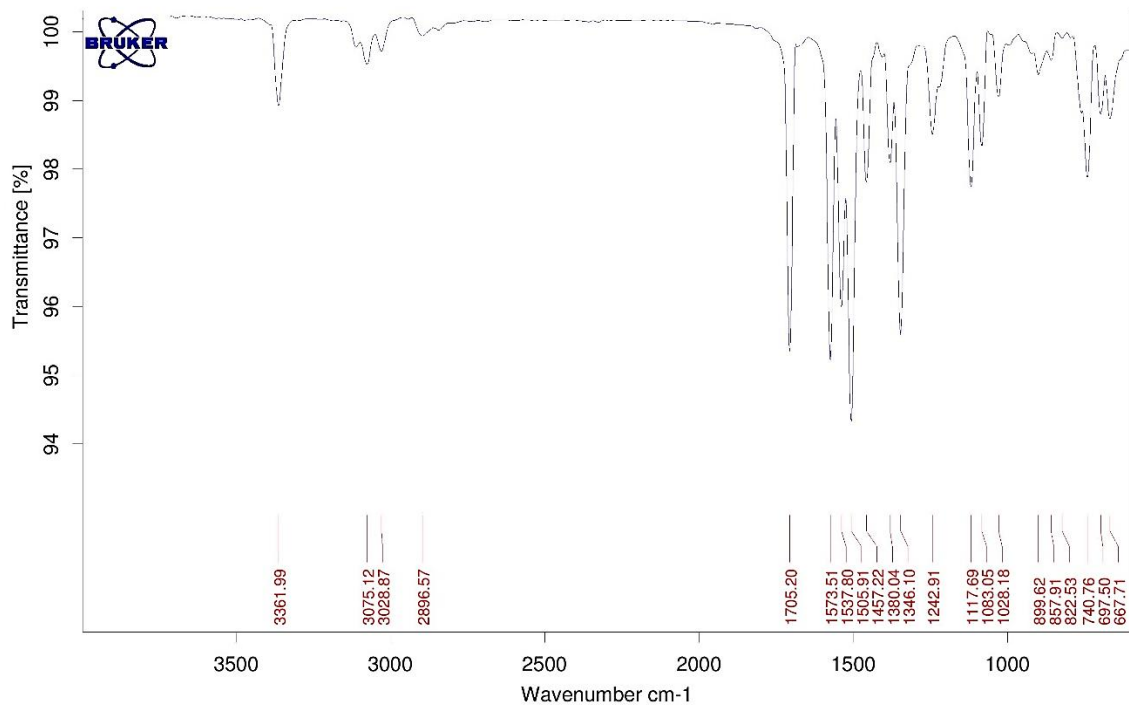


Figure A 44. IR spectrum of 21.

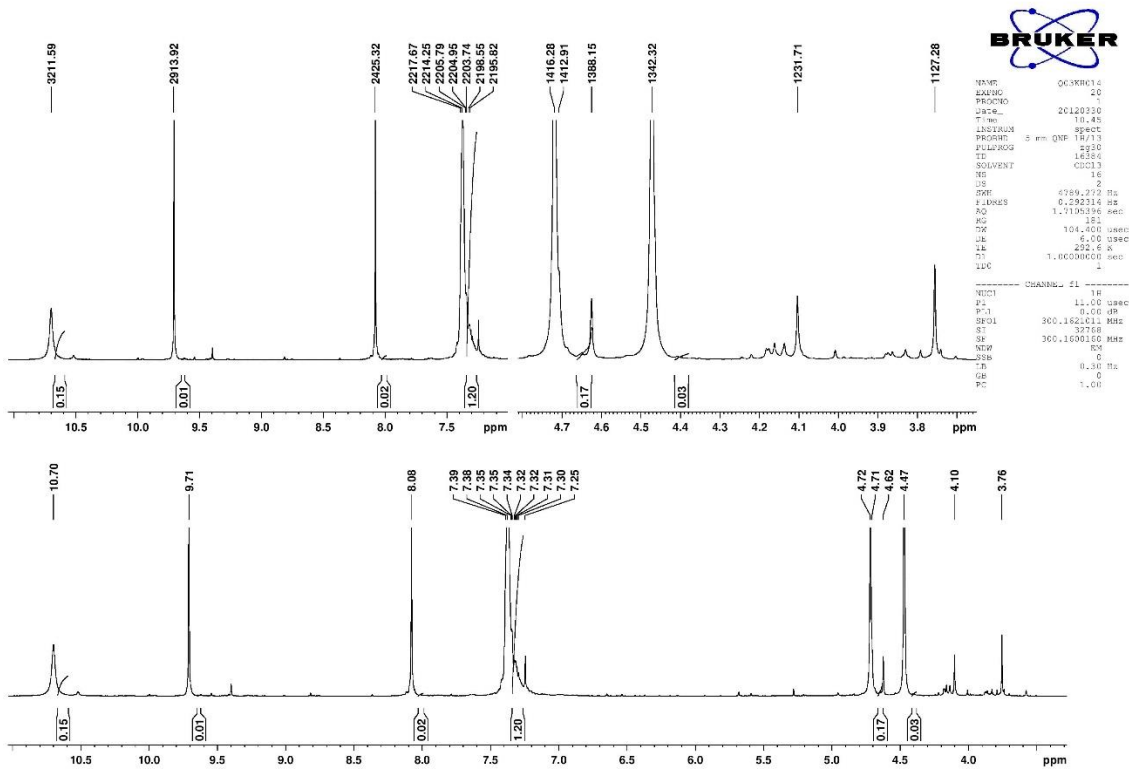


Figure A 45. <sup>1</sup>H NMR spectrum of 22.

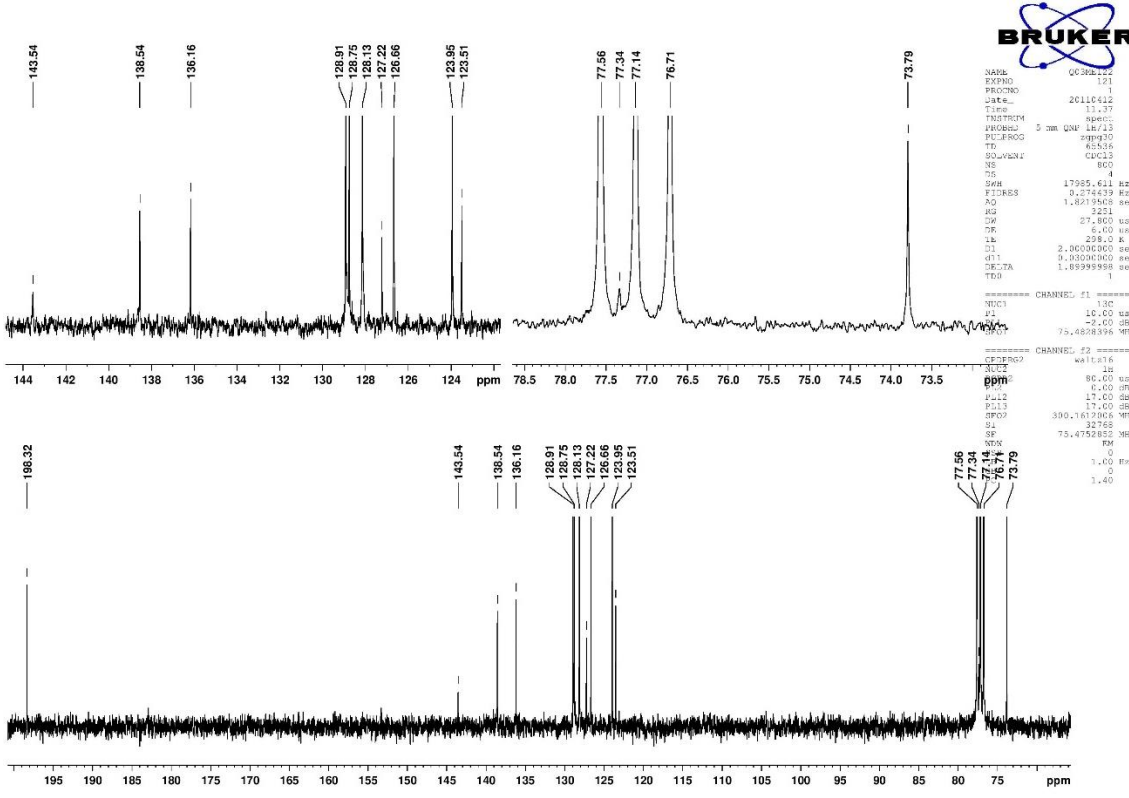


Figure A 46. <sup>13</sup>C NMR spectrum of 22.

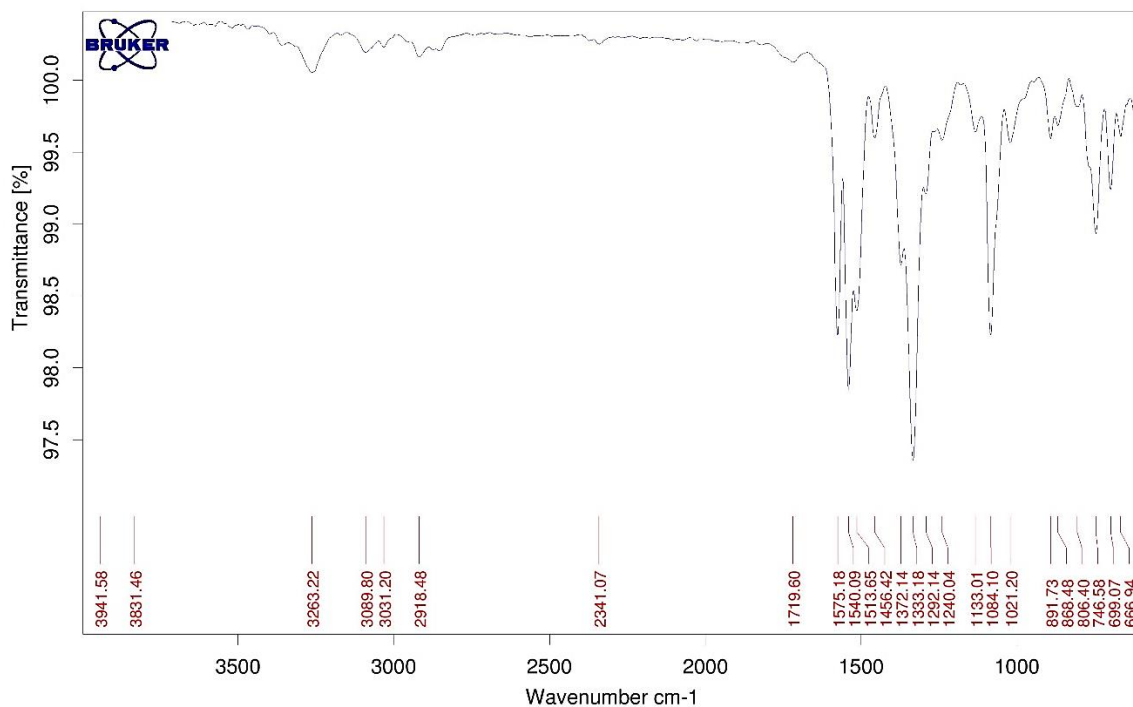


Figure A 47. IR spectrum of 22.

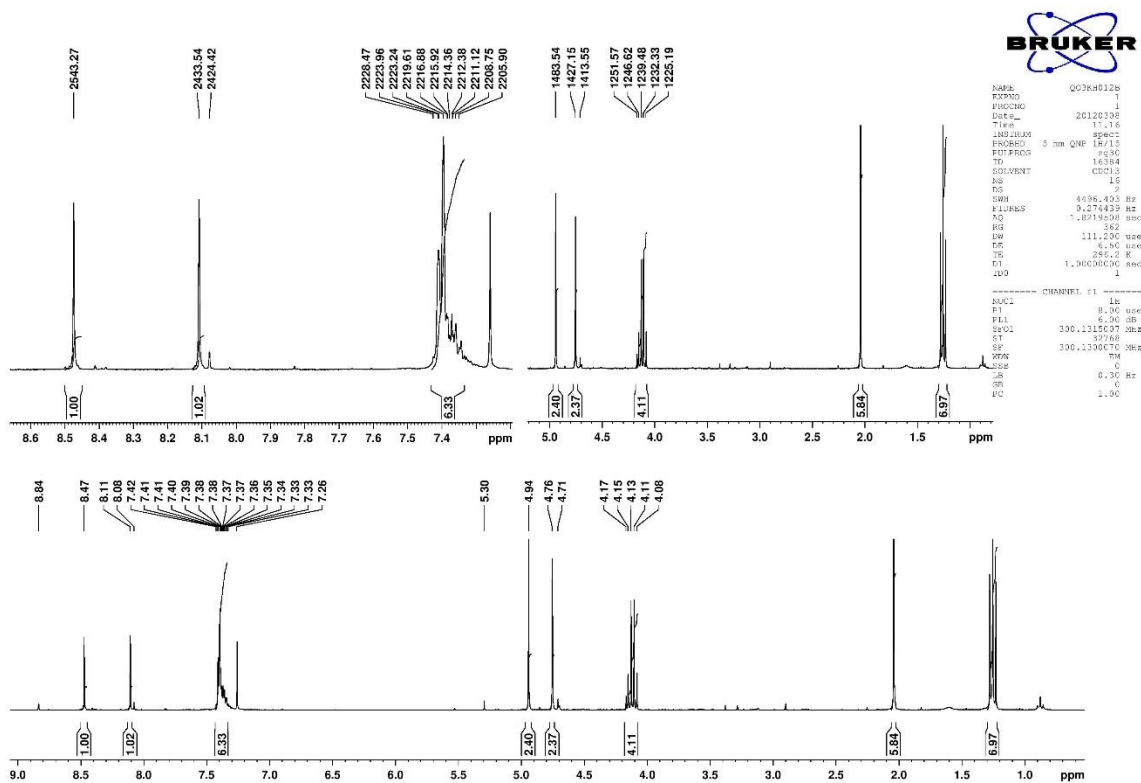


Figure A 48. <sup>1</sup>H NMR spectrum of 23.

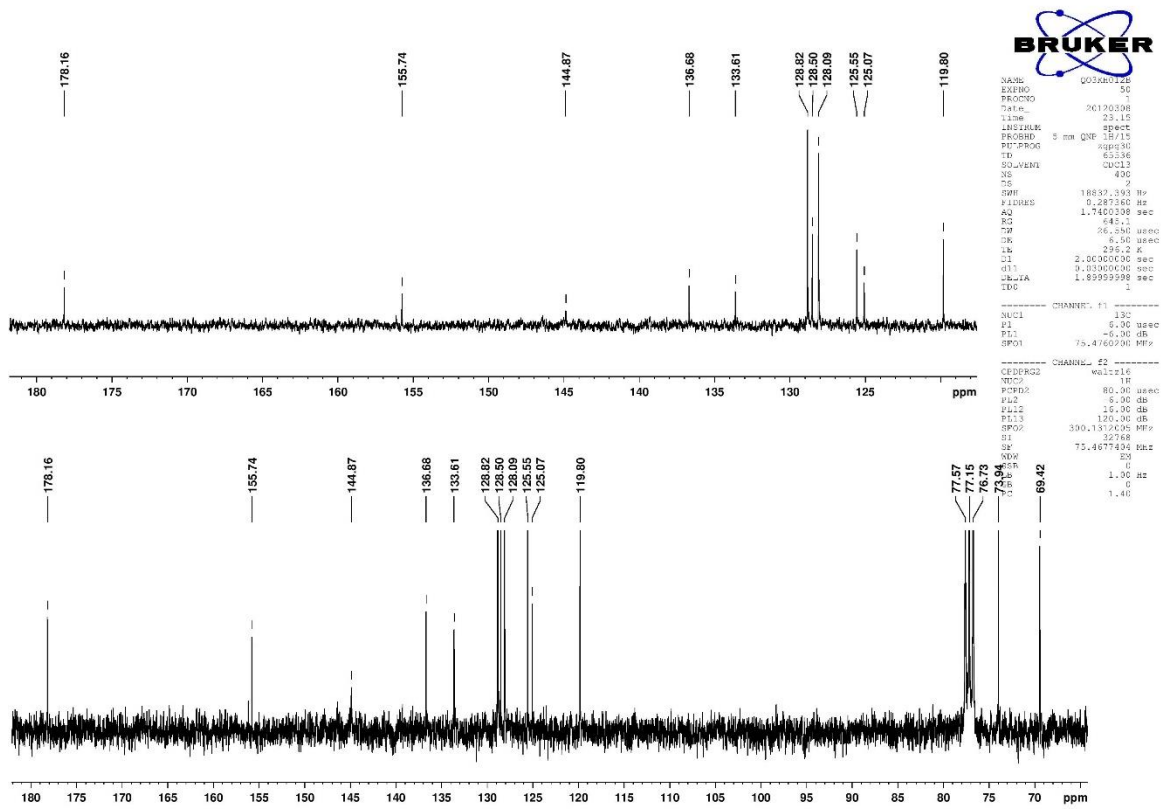


Figure A 49. <sup>13</sup>C NMR spectrum of 23.

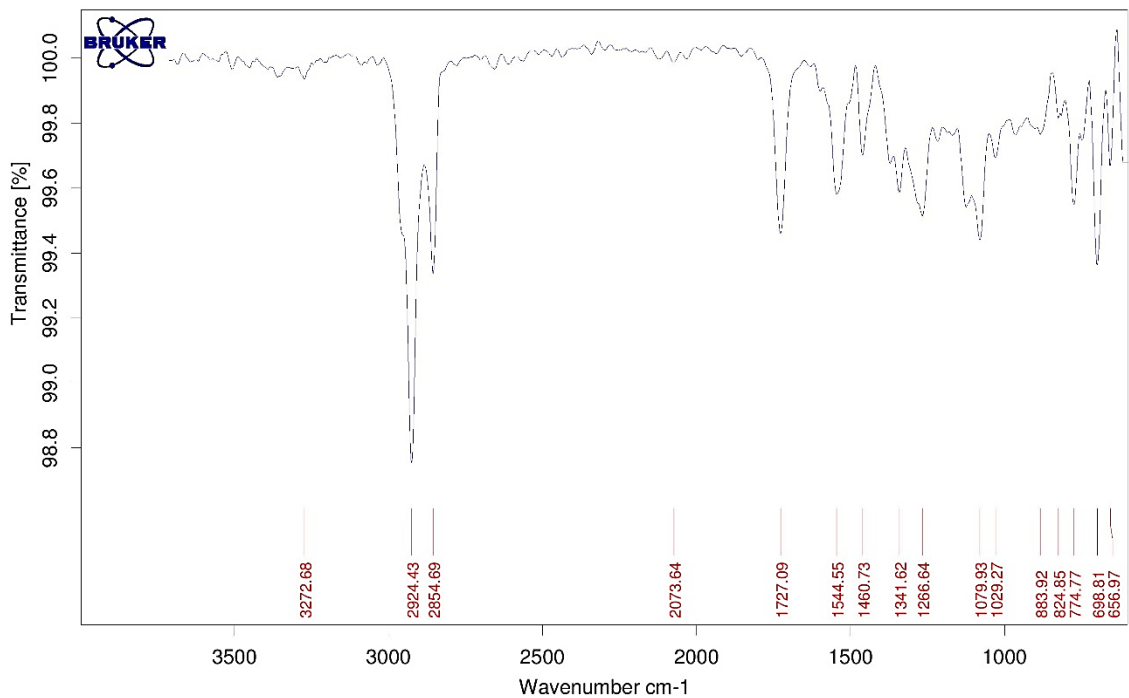


Figure A 50. IR spectrum of 23.